

Mutagenic studies into the catalytic versatility of soluble methane monooxygenase

NICHOL, Tim

Available from Sheffield Hallam University Research Archive (SHURA) at:

<http://shura.shu.ac.uk/16489/>

This document is the author deposited version. You are advised to consult the publisher's version if you wish to cite from it.

Published version

NICHOL, Tim (2011). Mutagenic studies into the catalytic versatility of soluble methane monooxygenase. Doctoral, Sheffield Hallam University.

Repository use policy

Copyright © and Moral Rights for the papers on this site are retained by the individual authors and/or other copyright owners. Users may download and/or print one copy of any article(s) in SHURA to facilitate their private study or for non-commercial research. You may not engage in further distribution of the material or use it for any profit-making activities or any commercial gain.

Sheffield Hallam University
Learning and Information Services
Adsetts Centre, City Campus
Sheffield S1 1WD

1 0 2 0 7 0 9 3 4 0

REFERENCE

**Mutagenic studies into the catalytic versatility of
soluble methane monooxygenase**

Tim Nichol

A thesis submitted in partial fulfilment of the requirements of
Sheffield Hallam University
for the degree of Doctor of Philosophy

July 2011

Table of contents	p.3
Statement	p. 16
Acknowledgements	p. 17
Abstract	p. 18
Chapter 1	p. 19
1.1 Methanotrophs and methane monooxygenase	p. 19
1.1.1) Methanotrophic bacteria	p. 19
1.1.2) Activity of methane monooxygenases	p.22
1.1.3) Copper dependent regulation of methane monooxygenases	p.23
1.1.4) Structure of particulate methane monooxygenase	p.25
1.1.5) Structure of soluble methane monooxygenase	p.27
1.1.6) The catalytic cycle of soluble methane monooxygenase	p.31
1.1.7) The substrate range of soluble methane monooxygenase	p.33
1.1.8) Site directed mutagenesis of soluble methane monooxygenase	p.34
1.2 Butane monooxygenase	p.36
1.2.1) Structure of butane monooxygenase	p.36
1.2.2) Site directed mutagenesis of butane monooxygenase active site residues to the sMMO counterparts	p.38

1.2.3) Activity of butane monooxygenase site directed mutants against small chain alkanes

1.2.4) Effect of mutations on inactivation of butane monooxygenase by propionate

1.2.5) Chloroethylene degradation by Butane monooxygenase site directed mutants

1.3 Toluene-4-monooxygenase

1.3.1) Structure of Toluene-4-monooxygenase

1.3.2) Site directed mutation of toluene-4-monooxygenase active site residues to sMMO counterparts

1.3.3) Regioselectivity of toluene-4-monooxygenase site directed mutants at positions T201 and G103

1.3.4) Identification of toluene-4-monooxygenase mutants for the increased production of pharmaceutical precursors

1.3.5) Regiospecific oxidation of naphthalene by toluene-4-monooxygenase mutants

1.3.6) Production of indigoid products by toluene-4-monooxygenase mutants

1.4 Toluene o/Tfro-monooxygenase

1.4.1) Structure of toluene-OAf/?o-monooxygenase

1.4.2) Directed evolution of toluene-orf/?o-monooxygenase towards increased naphthalene oxidation and chloroethylene degradation

1.4.3) Production of indigoid pigments by toluene-ortho- monooxygenase	p.50
1.5 Toluene/ o-xylene monooxygenase	p.51
1.5.1) Structure of toluene/o-xylene monooxygenase	p.51
1.5.2) Identification of toluene/o-xylene monooxygenase mutants for the increased production of pharmaceutical precursors	p.51
1.5.3) Directed evolution of toluene/o-xylene monooxygenase towards increased chloroethylene degradation	p.52
1.5.4) Investigation of toluene/o-xylene monooxygenase free radical intermediates using site directed mutagenesis	p.53
1.6 Toluene-3-monooxygenase	p. 111
1.6.1) Structure of toluene-3-monooxygenase	p.55
1.6.2) Site directed mutagenesis of toluene-3- monooxygenase	p.55
1.7 Deoxyhypusine hydroxylase	p.57
1.7.1) Structure of deoxyhypusine hydroxylase	p.57
1.7.2) Analysis of deoxyhypusine hydroxylase iron binding residues	p.57
1.7.3) Site directed mutagenesis of amino acid residues conserved among deoxyhypusine hydroxylase	p.58

1.7.4) Detection of a diiron site in deoxyhypusine hydroxylase using spectroscopic analysis	p.59
1.8 Ribonucleotide reductase	p.60
1.8.1) Structure of ribonucleotide reductase	p.60
1.8.2) Analysis of the radical pathway of ribonucleotide reductase using site directed mutagenesis	p.61
1.9 Stearoyl ACP desaturase	p.62
1.9.1) Activity of steaoryl ACP-desaturase	p.62
1.9.2) Site directed mutagenesis of stearoyl ACP- desaturase at position Thr 199	p.62
1.9.3) Creation of chimeric desaturase proteins	p.63
1.10 Scope of this thesis	p.64
Chapter 2: Materials and Methods	p.65
2.1 Bacterial strains and growth conditions	p.65
2.1.1) Bacterial strains	p.65
2.1.2) Growth of Bacterial Cultures	p.65
2.2 General DNA methods	p. 167
2.2.1) QIAprep spin plasmid miniprep protocol	p.67
2.2.2) Qiagen Maxiprep kit plasmid isolation protocol	p.68
2.2.3) Qiaquick gel extraction protocol	p.69
2.2.4) GeneClean III Protocol	p.69
2.2.5) Phenol/chloroform/Isoamyl alcohol extraction	p.70
2.2.6) Electrophoresis of DNA	p.70

2.2.7) Restriction digest	p.71
2.2.8) Phosphatase	p.71
2.2.9) End filling with T4 DNA polymerase	p.72
2.2.10) DNA ligase	p.72
2.3 Template preparation and amplification conditions for PCR	p.73
2.3.1) Culture template preparation	p.73
2.3.2) Colony template preparation	p.73
2.3.3) Genomic DNA isolation using Qiagen genomic tip kit	p.73
2.3.4) Standard PCR Protocol	p.74
2.3.5) Four primer overlap extension PCR	p.75
2.3.6) Error Prone PCR random mutagenesis	p.76
2.3.7) Genemorph random mutagenesis kit	p.76
2.4 Plasmids used in this study	p.77
2.4.1) Blue/White selection	p.77
2.5 Preparation of <i>E. coli</i> competent cells	p.78
2.5.1) CaCE cell preparation method	p.78
2.5.2) Transformation of CaCl ₂ competent cells	p.78
2.5.3) Preparation of electrocompetent cells	p.79
2.5.4) Electroporation of <i>E. coli</i>	p.79
2.5.5) Hanahan transformation method	p.80
2.6 Introduction of DNA into <i>M.trichosporium</i> by conjugation,	p.81
2.6.1) conjugation protocol	p.81
2.7 Protein quantification and visualisation	p.82
2.7.1) Protein estimation via the Bradford assay	p.82

2.7.2) SDS PAGE	p.82
2.8 Cell preparation and substrate oxidation assays	p.83
2.8.1) Whole cell assays	p.83
2.8.2) Soluble extract preparation	p.83
2.8.3) Colorimetric naphthalene oxidation assay	p.84
2.8.4) Semiquantitative colorimetric naphthalene oxidation assay	p.84
2.8.5) Product distribution of naphthols	p.85
2.8.6) Biphenyl oxidation assay	p.85
2.8.7) Mesitylene oxidation assay	p.86
2.8.8) Toluene oxidation assays	p.87
2.8.9) Ethyl Benzene oxidation assays	p.88
2.8.10) Butane oxidation assay	p.89
2.8.11) Pentane oxidation assay	p.89
2.8.12) Hexane oxidation assay	p.90
2.9) Data analysis	p.90
Chapter 3: Analysis of the role of Leu 110	p.91
3.1 Introduction	p.91
3.1.1) A proposed gating role for Leu 110	p.91
3.2) Comparison of Leu 110 with equivalent residues of related monooxygenases.	p.93
3.2.1) Mutagenesis of Val 106 from toluene <i>ortho</i> - monooxygenase	p.93

3.2.2) Mutagenesis studies of lie 100 from toluene 4-monooxygenase	p.93
3.2.3) Mutagenesis studies of lie 100 from toluene/o-xylene monooxygenase	p.94
3.2.4) Comparison to butane monooxygenase	p.95
3.3 Site directed mutagenesis studies of Leu 110 in sMMO	p.96
3.3.1) Mutagenesis of leucine gate residue produced mutants that gave an unusual naphthalene oxidation test result	p.96
3.3.2) The L110R and L110Y mutants of sMMO show inverted regioselectivity with naphthalene compared to the wild-type	p.99
3.3.3) The L110 mutants showed a relaxed regioselectivity and generated novel products with substituted monoaromatic substrates and biphenyl	p.100
3.3.4) Neither mutants nor wild-type oxidized triaromatic hydrocarbons	p. 104
3.4 Analysis of results	p.105
3.4.1) Regioselectivity of WT sMMO	p.105
3.4.2) Mutants showed relaxed regioselectivity but showed no activity towards triaromatic substrates	p.105

3.5) Summary	p.106
Chapter 4: Mutagenesis based upon butane monooxygenase	p. 108
4.1 Introduction	p. 108
4.1.1) Comparative analysis of sMMO	p.108
4.1.2) Comparison to butane monooxygenase	p.108
4.1.3) Comparison of a highly conserved hydrophobic pocket near the active site of BMO and sMMO	p. 109
4.2 Construction and expression of mutants	p. 112
4.2.1) Expression of mutants in <i>Ms. trichosporium</i> SMDM	p.112
4.2.2) Analysis of F282L soluble extract.	p. 113
4.2.3) The M184V mutant is an unstable enzyme	p.114
4.3 Oxidation of butane and naphthalene by the mutants showed no change in regioselectivity or activity compared to wild type sMMO	p.115
4.3.1) Oxidation of butane by BMO inspired site directed mutants	p.115
4.3.2) Oxidation of naphthalene by BMO inspired site directed mutants	p.116

4.4 Oxidation of Toluene, Biphenyl and Hexane by BMO inspired mutants shows relaxed regiospecificity compared to the wild type enzyme	p.119
4.4.1) Oxidation of toluene by BMO inspired mutants	p.119
4.4.2) Oxidation of Biphenyl by BMO inspired mutants	p.120
4.4.3) Oxidation of hexane by BMO inspired mutants	p.121
4.5 Oxidation of mesitylene by the M184V mutant shows novel oxidation products.	p.123
4.5.1) A novel substrate for studying monooxygenase activity	p.123
4.5.2) Mesitylene oxidation assays over 24 h and 72 h showed no monohydroxylated products	p.123
4.5.3) Mesitylene oxidation assays over 1 h showed monohydroxylated products	p.124
4.6 Summary of results	p.126
Chapter 5: Random mutagenesis of <i>mmoX</i>	p.127
5.1 Introduction	p.127
5.1.1) A mutagenesis approach to studying sMMO	

substrate specificity	p. 127
5.1.2 Mutagenesis studies of related monooxygenases	p. 127
5.1.3) Directed evolution studies of aromatic monooxygenases	p. 128
5.1.4) Directed evolution of alkene monooxygenase	p. 129
5.2 Development of a random mutagenesis method using <i>Taq</i> polymerase	p. 131
5.2.1) Use of <i>Taq</i> polymerase for error prone PCR	p. 131
5.2.2) Creation the random mutant libraries	p. 132
5.2.3) Transformation of <i>E. coli</i> S17-1	p. 133
5.3 Development of a colorimetric method for detecting oxidation of triaromatic compounds	p. 134
5.4 Use of Genemorph random mutagenesis kit to create random mutant libraries	p. 135
5.4.1) A new method for mutagenesis with reduced mutational bias and more controllable error rate	p. 135
5.5 Summary	p. 137
5.5.1) The colorimetric detection of triaromatic oxidation	p. 137
5.5.2) <i>E. coli</i> strain S17-1 is difficult to transform	p. 137

5.5.3) Difficulties encounter during the cloning stages	p. 138
Chapter 6: Construction of a new expression vector pT2ML	p. 139
6.1 Introduction	p.139
6.1.1) Cloning using the pTJS140/pTJS175 expression system	p. 139
6.2 Construction of new expression vector: pT2ML	p141
6.2.1) Modification of pTJS140 to remove <i>Bam</i> YW and <i>Nde</i> I sites	p. 141
6.2.2) Removal of <i>A</i> /cfel and first <i>Bam</i> HI site from pTJS175	p.141
6.2.3) Removal of final <i>Bam</i> HI site	p. 143
6.2.4) Deletion of 516bp fragment from <i>m m o X</i>	p. 144
6.2.5) Subcloning the modified sMMO operon into pTN1	p.145
6.3 Assessing the efficiency of pT2ML	p. 147
6.3.1) Expression of recombinant wild-type sMMO in pT2ML	p.149
6.3.2) Comparison of wild type OB3b and pT2ML.WT1A activities towards naphthalene	p. 150
6.4 Summary of the new expression vector pT2ML	p. 152
Chapter 7: Mutation studies using the new expression vector pT2ML	p. 153

7.1) Introduction	p.153
7.1.1 Role of Phe 188 as a substrate gating residue in sMMO	p.153
7.1.2 The Gly 113 mutant of butane monooxygenase	p. 154
7.1.3) Designing new sMMO mutants F188A and N116G	p.155
7.2 Construction of mutants N116G and F188A using pT2ML expression vector	p. 157
7.3 N116G and F188A show reduced rate with aromatic substrates but little or no change in regioselectivity	p. 160
7.3.1 Oxidation of Naphthalene by N116G and F188A	p.160
7.3.2 Oxidation of ethylbenzene by N116G and F188A	p. 162
7.3.3 Oxidation of mesitylene by N116G and F188A	p. 164
7.3.4 Oxidation of biphenyl by N116G and F188A	p.166
7.3.5 Oxidation of toluene by N116G	p.167
7.4 Kinetic data for toluene oxidation by wild type OB3b and N116G	p.168
7.5 The mutants showed no measurable activity towards alkanes or tri-aromatic substrates	p. 170
7.6 Summary	p.170
Chapter 8: Discussions	p.172
8.1) Leu 110 is not the limiting factor preventing oxidation of	

triaromatic compounds by wild-type sMMO	p. 172
8.2 Leucine 110 is an important residue in determining the regioselectivity of sMMO	p. 174
8.3 The presence of other enzymes in the methanotroph cells affects product distribution	p. 177
8.4 Different expression levels between batches affects rate analysis	p.180
8.5 Site directed mutations based upon BMO do not confer “BMO-like” regioselectivity.	p. 181
8.6 Single Mutations of sMMO active site residues to BMO counterparts are not sufficient to confer a BMO-like activity	p. 184
8.7 The M184V mutant is an unstable enzyme	p. 186
8.8 Evidence of substrate trafficking via hydrophobic cavities 1,2 and 3	p.188
8.9 Summary	p.191
References	p. 193
Appendix 1 media preparation	p.216
Appendix 2 Buffer preparation	p.219
Appendix 3 SDS PAGE reagents and protocol	p.221

Papers

Statement

The work carried out in this thesis was undertaken to study the soluble methane monooxygenase enzyme using mutagenic methods. The work contained in this thesis is the result of original research undertaken by myself under the supervision of Prof. T. J. Smith, Sheffield Hallam University and Prof J.C. Murrell, University of Warwick excepting the following:

(A) Creation of mutants L110C, L110G, L110Y, L110R (Chapter 3) and M184V, C151T, F282L (Chapter 4) by Dr E. Borodina, University of Warwick.

(B) Creation of plasmid PT2ML by Dr Malcolm Lock, Sheffield Hallam University

All sources of information have been referenced

None of the work contained in this thesis has been submitted previously for a research degree.

Tim Nichol

June 2011

Acknowledgements

First and foremost I would like to thank my supervisor Professor Thomas J. Smith (Sheffield Hallam University) for all the advice and support he has given me over the years, without his encouragement this thesis would not have been possible. I would also like to thank my collaborator Professor J. Colin Murrell (University of Warwick) who has given me lots of advice and support throughout my time working on sMMO; and thanks to my second supervisor Professor P. Strong who also given me advice on writing this thesis and taken time to help go through this work.

I would also like to thank Professor Nicola Woodroffe and the BMRC (Sheffield Hallam University) for funding and allowing me to carry out this PhD.

Thanks to Dr Elena Borodina (University of Bristol) for her help in creating the Leu110 mutants and to Dr Malcolm Lock (Sheffield Hallam University) for his help with the creation of the pT2ML expression vector and to all other members of the microbiology laboratory both past and present for your continued support.

I would also like to thank the technical staff here at Sheffield Hallam University, particularly Joan Hague, Mike Cox and Dan Kinsman for help with the GC and GCMS.

Outside of the laboratory I would like to thank my family and particularly my wife Caroline who has put up with me working on this PhD as long as I have known her and has shown complete patience and understanding at all times It's finally done!!!

Abstract

Soluble methane monooxygenase (sMMO) is a multicomponent bacterial enzyme that catalyzes the oxidation of methane to methanol, as well as oxidizing many other adventitious substrates. A number of mutagenic studies were carried out on the sMMO enzyme of *Methylosinus trichosporium* OB3b in order to gain insight into sMMO and probe how structural aspects relate to function of the enzyme.

Leu110 within the hydroxylase α -subunit of sMMO has been proposed as a possible gating residue, controlling access of substrate to the active site (Rosenzweig *et al.* 1997). A range of site directed mutants were created at the 110 position and screened for activity with a number of aromatic substrates. All mutants showed relaxed regioselectivity with all substrates assayed. However no evidence of a gating residue was found, indicating that Leu110 is more important in determining regioselectivity than substrate access to the active site.

Comparison to the highly similar butane monooxygenase led to the creation of three site directed mutants: M184V F282L and C151T. M184V and C151T showed small changes in regioselectivity and reduced activity with most substrates. The M184V mutant showed relaxed regioselectivity and a novel oxidation product with the substrate mesitylene which may have implications for substrate trafficking. The F282L mutant produced a stable enzyme which had no activity with any of the substrates tested, showing Phe282 is important for the enzyme function.

A random mutagenesis experiment was devised and a colorimetric screen for the oxidation of triaromatic compounds was used to screen mutant libraries for activity towards anthracene and phenanthrene. However no activity towards triaromatic compounds was detected. In order to improve the cloning strategies and to make creation of mutant libraries easier, a novel expression vector pT2ML was created. The pT2ML vector reduces the number of cloning steps required to make soluble methane monooxygenase mutants. This expression system was used to make a site directed mutants F188A and N116G in order to complement previous site directed mutant studies, as well as a recombinant wild type mutant in order to assess the activity of the new expression system which is comparable to the wild type enzyme.

Chapter 1: Introduction

1.1 Methanotrophs and methane monooxygenase

1.1.1) Methanotrophic bacteria

Methanotrophs are aerobic Gram negative organisms that utilize methane as their sole source of carbon and energy. These organisms oxidize methane via methanol to formaldehyde, which is then assimilated into cellular biomass via one of two distinct pathways (Fig. 1.1). Methanotrophic bacteria are highly prevalent in the environment and have been isolated from numerous diverse sources including wetlands, agricultural soils, marine sediments (Hanson and Hanson, 1996) as well as more extreme environments such as hot springs (Bodrossy *et al.* 1995) and alkaline soda lakes (Khmelenina *et al.* 1997). Symbiotic methanotrophs have also been identified such as those living in the gills of deep sea mussels and gutless tube-dwelling worms around hydrothermal vents (Cavanaugh *et al.* 1987; Schmaljohan, 1991). Methanotrophic bacteria are broadly divided into two groups based originally on the arrangement of their intracytoplasmic membranes (ICM) (Table 1.1). Type I methanotrophs contain bundles of vesicle discs throughout the cell and are grouped in the gamma proteobacteria subdivision. Type II methanotrophs have paired peripheral layers of intracytoplasmic membranes and are grouped in the alpha proteobacteria subdivision (Davies and Whittenbury 1970, Whittenbury *et al.* 1970). The type I methanotrophs, including the genera *Methylomonas*, *Methylobacter*, *Methylomicrobium* and *Methylococcus* assimilate formaldehyde into cellular biomass via the ribulose monophosphate pathway (RuMP), whereas the type II methanotrophs, including the genera *Methylosinus* and *Methylocystis* assimilate formaldehyde into cellular biomass via the serine pathway (Anthony 1992; Hanson and Hanson, 1996) (Fig. 1.1) In recent years a number of isolates have been discovered that extend this initial classification of methanotrophs. Filamentous bacteria of the *Clonothrix* and *Crenothrix* genera have been identified as methanotrophs. These have been identified as ICM type I belonging to the gamma proteobacteria phylum and contain particulate methane monooxygenase (Stoeker *et al.* 2006; Vigliotta *et al.* 2007). A number of methanotrophs of the acidophilic

Methylocapsa genus have been isolated and appear to belong to a new intracellular membrane classification type. The cells contain a well developed intracytoplasmic membrane system packed in parallel on one side of the membrane and have been termed type III (Dedysh *et al.* 2003; Dunfield *et al.* 2010). Three separate thermoacidophilic methanotrophs: *Methyloacidiphilium*, *Acidimethylosilex* and *Methyloacida* belonging to the Verrucomicrobia phylum have been identified (Pol *et al.* 2007; Hou *et al.* 2008; Islam *et al.* 2008; Khadem *et al.* 2010). These methanotrophs do not appear to have distinct intracytoplasmic membranes however the presence of polyhedral organelles in these organisms may represent a novel ICM type IV. These organelles are similar in appearance to carboxysomes involved in CO₂ function. The presence of these organelles as well as the detection of genes involved in the serine pathway, tetrahydrofolate pathway and Calvin cycle pathway led Birkeland and co-workers to suggest these organisms may assimilate carbon compounds via a unique mechanism (Islam *et al.* 2008).

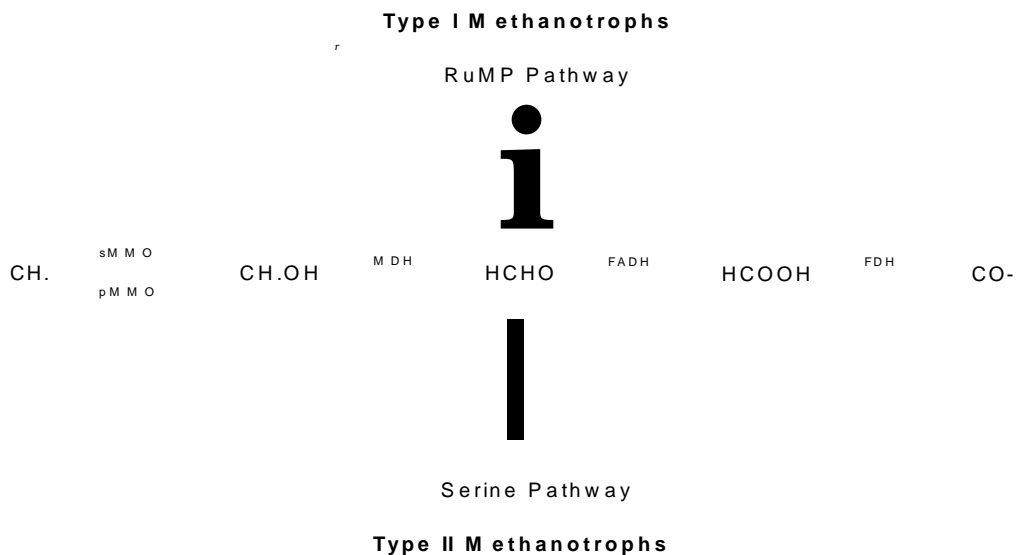


Fig. 1.1) Pathways for the oxidation of methane and assimilation of formaldehyde. Abbreviations: sMMO soluble methane monooxygenase, pMMO particulate monooxygenase, MDH methanol dehydrogenase, FADH formaldehyde dehydrogenase, FDH formate dehydrogenase (Anthony, 1992; Hanson and Hanson, 1996).

Table 1.1 Classification of methanotroph genera

Genus name	Phylogeny	MMO type	Ci assimilation	ICM type1	n2 fixation	G+C (mol %)	Major PLFA 2	Trophic niche
<i>Methylobacter</i>	<i>y Proteobacteria</i>	pMMO	RuMP	type I	No	49-54	16:1	some psychrophilic
<i>Methylosoma</i>	<i>y Proteobacteria</i>	pMMO	not known	type I	Yes	49.9	16:1	not extreme
<i>Methylomicrobium</i>	<i>y Proteobacteria</i>	pMMO +/- sMMO	RuMP	type I	No	49-60	16:1	Halotolerant; alkaliphilic
<i>Methylomonas</i>	<i>Y Proteobacteria</i>	pMMO +/- sMMO	RuMP	type I	some	51-59	16:1	some psychrophilic
<i>Methylosarcina</i>	<i>Y Proteobacteria</i>	pMMO	RuMP	type I	No	54	16:1	not extreme
<i>Methylosphaera</i>	<i>Y Proteobacteria</i>	pMMO	RuMP	ND3	Yes	43-46	16:1	psychrophilic
<i>Methylococcus</i>	<i>Y Proteobacteria</i>	pMMO + sMMO	RuMP/Serine	type I	Yes	59-66	16:1	thermophilic
<i>Methylocaldum</i>	<i>Y Proteobacteria</i>	pMMO	RuMP/Serine	type I	No	57	16:1	thermophilic
<i>Methylothermus</i>	<i>Y Proteobacteria</i>	pMMO	RuMP	type I	No	62.5	18:1/16:0	thermophilic
<i>Methylohalobius</i>	<i>Y Proteobacteria</i>	pMMO	RuMP	type I	No	58.7	18:1	halophilic
<i>Methylocystis</i>	<i>a Proteobacteria</i>	pMMO +/- sMMO	Serine	type II	Yes	62-67	18:1	some acidophilic
<i>Methylosinus</i>	<i>a Proteobacteria</i>	pMMO + sMMO	Serine	type II	Yes	63-67	18:1	not extreme
<i>Methylocella</i>	<i>a Proteobacteria</i>	sMMO	Serine	NA4	yes	60-61	18:1	acidophilic
<i>Methylocapsa</i>	<i>a Proteobacteria</i>	pMMO	Serine	type III	Yes	63.1	18:1	acidophilic
<i>Methyloferula</i>	<i>a Proteobacteria</i>	sMMO	Serine	NA4	Yes	56-58	18:1	acidophilic
<i>Crenothrix</i>	<i>Y Proteobacteria</i>	pMMO		type I				not extreme
<i>Clonotrix</i>	<i>Y Proteobacteria</i>	pMMO		type I				not extreme
<i>Methyloacidiphilium</i> ;	<i>Verrucomicrobia</i>	pMMO	Serine, RuMP?	type	No?		C18:0	acidophilic
<i>Acidimethylosilex</i> ;	<i>Verrucomicrobia</i>	pMMO	Serine, RuMP?	IV?				
<i>Methyloacida</i>	<i>Verrucomicrobia</i>	pMMO						

ICM, intracellular membrane; PLFA, phospholipid fatty acid; ND, not determined; NA, not applicable because ICMs are very limited in this genus

(adapted from Smith and Murrell, 2009)

1.1.2) Activity of methane monooxygenases

The methane monooxygenases are an enzyme which catalyze the first step in the methane metabolism pathway of methanotrophic bacteria. Methanotrophs oxidize methane via methanol to formaldehyde, which is then assimilated into cellular biomass (Hanson and Hanson, 1996). The methane monooxygenase enzymes catalyze the first step in this reaction, the oxidation of methane to methanol:



The ability of methane monooxygenases to convert methane to methanol has made them of great interest for several reasons. The ability to produce methanol with high turnover at ambient temperatures at 1 atm using dioxygen as the only oxidant makes it attractive to industrial applications. The C-H bond of methane is very unreactive requiring >100 kcal mol⁻¹ to abstract the first hydrogen. Presently the chemical synthesis of methanol requires high temperatures and pressure as well as expensive catalysts and multiple stages (Gesser *et al.* 1985). The ability to convert methane gas into an easily transportable form of energy also makes this enzyme of interest to industry. Another reason for such an interest in methane monooxygenases and methanotrophs is the vital role that they play in the global methane cycle (Reeburgh *et al.* 1993). In recent years the regulation of greenhouse gases has become a focus of much scientific research and methane has been shown to be 25 times more effective as a greenhouse gas than CO₂. Although CO₂ is the most abundant greenhouse gas, methane is the most abundant organic gas in the atmosphere and is a major factor in global warming (IPCC Fourth assessment report: Climate Change 2007: 2.10.2).

1.1.3) Copper dependent regulation of methane monoxygenases

Two forms of methane monooxygenase are known to exist; a membrane associated particulate monooxygenase (pMMO) and a soluble form (sMMO). The activity of these enzymes is copper dependent with the copper-containing pMMO being active at high copper-biomass ratios (>2.5 pmol g⁻¹ cell) and active sMMO only being expressed during low copper to biomass ratios (Stanley *et al.* 1983). It has also been shown that regulation of MMO expression by copper ions takes place at the transcription level with the sMMO operon only being transcribed at low copper-biomass concentrations (Nielsen *et al.* 1996, 1997). In comparison the *pmoA* gene of particulate methane monooxygenase has been shown to be constitutively expressed even in the absence of copper and that expression increases with increasing copper concentrations (Choi *et al.* 2003). The genes important in the transcription of sMMO were identified as *mmoR* (encoding σ^{54} -transcriptional regulator: MmoR), *mmoG* (encoding a GroEL like homologue: MmoG) and *rpoN* (encoding the transcription initiation factor σ^{54}). Inactivation of any of these genes was shown to halt sMMO transcription (Stafford *et al.* 2003). Using a construct containing a green fluorescent protein reporter gene found downstream of the start of *mmoX* it was shown that deletions to the 417bp region between *mmoG* and *mmoX* containing the σ^{54} promoter region also abolished transcription of the sMMO operon. Gel shift experiments suggest that both MmoR and MmoG are required for effective binding of MmoR to the promoter region (Scanlan *et al.* 2009). Although the exact mechanism is unclear it is proposed that *mmoR* and *mmoG* are expressed under low copper conditions and that MmoR facilitates transcription of sMMO structural genes by forming a complex with σ^{54} . It has also been suggested that in the presence of copper, MmoR is inactivated so that it does not bind σ^{54} and so inhibits transcription of the sMMO operon (Fig. 1.2). The requirement of MmoG for effective transcription of sMMO and the evidence that MmoG is probably required for effective binding of MmoR to the DNA activator sequence suggest that MmoG may be an MmoR specific chaperone required for expression of functionally active MmoR. Although much less is known about the genes controlling expression of pMMO, transcription is known to start from a σ^{70} (transcription initiation factor) dependant promoter in many

methanotrophs and thought to be facilitated by a copper binding regulatory protein (Gilbert *et al.* 2000, Stolyar *et al.* 2001, Ukaegbu *et al.* 2006)

m m o R m m o G m m o X m m o Y m m o B m m o Z m m o D m m o C

m m o R m m o G m m o X m m o Y m m o B m m o Z m m o D m m o C

Fig. 1.2) Proposed mechanism for the regulation of sMMO expression by copper. Under low copper conditions (<0.89 pmol/g cell; Hanson and Hanson 1996) functionally inactive mmoR (yellow) is expressed and binds a₅₄ to form the functionally active MmoR (green). MmoG (blue) associates with the functionally active MmoR and assists in binding to the a₅₄ promoter (P a₅₄) and initiating transcription of sMMO structural genes (black). Under high copper conditions MmoR cannot associate with a₅₄ and so functional MmoR cannot initiate expression of sMMO

Many methanotrophs such as *Methylomonas methanica* and *Methylomicrobium album* BG8 produce only the membrane bound pMMO. Others such as *Methylosinus trichosporium* OB3b and *Methylococcus capsulatus* Bath produce the pMMO and sMMO forms of the enzyme (Hanson and Hanson 1996). To date *Methylocella* and *Methyloferula* are the only methanotroph genera isolated which possesses only the soluble methane monooxygenase (Dunfield *et al.* 2003; Vorobev *et al.* 2010).

1.1.4) Structure of particulate methane monooxygenase

Fig. 1.3) Structure of pMMO from *M. capsulatus* (Bath). The 49, 27 and 22 kDa subunits, encoded by *pmoB*, A and C, are coloured lilac, yellow and green, respectively. Metal atoms in the protein are shown as spheres, copper red and zinc orange, (a) (af3y)₃ enzyme complex with the predominantly alpha-helical presumed membrane-spanning region uppermost; (b) view looking down on (a) from above; (c) one a(3y) protomer showing the mononuclear and dinuclear copper centres associated with each a (PmoB) subunit and the zinc within the membrane-spanning region (mononuclear copper in *M. trichosporium* OB3b). (PDB accession code 1YEW)

The crystal structure of pMMO for *Methylococcus capsulatus* (Bath) has been determined, showing that the enzyme is a trimer with an a₃p₃y₃ structure. The three subunits are encoded by *pmoABC* with masses of 49 kDa, 27 kDa and 22 kDa respectively (Leiberman and Rosenzweig, 2005; Fig. 1.3). Three separate metal containing sites were also detected in this structure. A dinuclear and a mononuclear copper centre were detected within the PMO a-subunit and a third zinc-containing centre co-ordinated by both the p and y subunits. Metal analysis by inductively coupled plasma atomic emission spectroscopy showed only 0.2 mol zinc per 100 kDa suggesting that zinc is probably taken up from the crystallisation buffer and so this site is more likely to be occupied by copper or iron in the active enzyme (Leiberman and Rosenzweig, 2005; Balasubramanian *et al.* 2010). The crystal structure of pMMO from *Methylosinus trichosporium* OB3B showed only two metal containing sites (Hakemian *et al.* 2008). The dinuclear copper centre was detected in the a-subunit however no mononuclear copper was detected. In the membrane spanning region, the site occupied by zinc in pMMO of *M. capsulatus* Bath was occupied by a mononuclear copper site adding further evidence to the hypothesis

that this is a metal labile site. Oxidation of methane at the mononuclear site is considered least likely due to the absence of this site in OB3b and the lack of conservation among PMO sequences from other methanotrophs (Hakemian *et al.* 2007, 2008). A number of models have been proposed for the oxidation of methane at the other two metal containing sites. Rosenzweig and co-workers have proposed a model for pMMO based on the crystal structures of *Ms. trichosporium* OB3B and *M. capsulatus* Bath (Leiberman and Rosenzweig, 2005; Hakemian *et al.* 2008). In this hypothesis the dinuclear copper centre is suggested as the site of methane oxidation, although oxidation of methane has not been ruled out at the site containing zinc or copper. The second functional model for pMMO is proposed by Chan and co-workers and proposes the existence of 12 - 15 copper ions per 100 kDa protomer arranged in trinuclear copper clusters based on electron parametric resonance (EPR) data and inductively coupled plasma mass spectrometry (ICP-MS) analysis. These trinuclear clusters although not seen in the crystal structures, have been proposed as being involved in both oxidation (C-clusters) and electron transfer (E-clusters) (Nguyen *et al.* 1994, 1998; Chan *et al.* 2004, 2007). The third functional model for pMMO oxidation has been proposed by both the Dispirito group and the Dalton group. In this model the presence of two copper ions and two iron ions per 100 kDa protomer has been proposed based on ICP-MS metal analysis and EPR studies (Zahn and Dispirito 1996; Basu *et al.* 2003; Choi *et al.* 2003; Kitmotto *et al.* 2005; Myronova *et al.* 2006; Martinho *et al.* 2007) The presence of a diiron site in the metal centre occupied by zinc/copper in the crystal structures, that is important in the oxidation of methane has led to the suggestion that pMMO can be regarded as a hydroxylase component of a larger 'supercomplex'. Dalton and coworkers have suggested that the methanol dehydrogenase enzyme acts as a reductase component in this supercomplex (Myronova *et al.* 2006). Whereas Dispirito and co-workers have suggested that methane oxidation by pMMO is coupled to the cytochrome bci complex possibly via ubiquinol. In this proposal the pMMO enzyme is coordinated with copper bound binding protein methanobactin (Zahn and Dispirito, 1996; Choi *et al.* 2005; Martinho *et al.* 2007).

1.1.5) Structure of soluble methane monooxygenase

Fig. 1.4) Structure of the hydroxylase component of sMMO. The α , β and γ subunits, encoded by the *mmoX*, *Y* and *Z* genes, are coloured blue, green and yellow, respectively. The iron atoms of the binuclear iron centres are shown as orange spheres. Figure was constructed using X-ray crystallographic data (PDB accession code 1MMO).

The structure of the sMMO enzyme and the function of the active site has been much more extensively categorized compared to that of pMMO. The sMMO enzyme is comprised of three components, a 39 kDa NADH reductase component encoded by *mmoC*, a 16 kDa effector protein component known as protein B encoded by *mmoB* and a hydroxylase component with an $\alpha_2\beta_2\gamma_2$ structure encoded by *mmoX*, *mmoY* and *mmoZ* with molecular masses of 61 kDa, 45 kDa and 20 kDa respectively (Colby and Dalton, 1978; Green *et al.* 1985; Green and Dalton, 1985; Cardy *et al.* 1991; Buzy *et al.*, 1998). Within the sMMO operon there are also genes *mmoG* and *mmoR* encoding a GroEL homologue and a σ^{54} -dependant transcriptional regulator as well as a protein of unknown function encoded by *mmoD* (Csaki *et al.* 2003; Scanlan *et al.* 2009; Fig. 1.2). The α subunits of the hydroxylase component each

contain a (μ-hydroxo)bridged binuclear iron active site which is co-ordinated by four glutamate and three histidine residues within a four-helix bundle (Woodland *et al.* 1986; Ericson *et al.* 1988; DeWitt *et al.* 1991). From the crystal structures of the sMMO hydroxylase component from both *Methylococcus canslatn.c* Rath and *Methylosinus trichosporium* OB3b have shown that these subunits are predominantly α-helical in shape with the diiron active site residing within a hydrophobic cavity designated cavity 1 (Rosenzweig *et al.* 1997, Elango *et al.* 1997). A number of other hydrophobic pockets have been identified and co-crystallization of the hydroxylase component with substrate analogues have implicated these cavities in being involved in access of substrate to the active site (Sazinsky *et al.* 2005; Fig. 1.5).

Fig. 1.5) The α-subunit of sMMO Hydroxylase depicting the hydrophobic cavities. The diiron centre is shown as orange spheres one of which is visible. Cavities 1-3 (purple, grey, turquoise respectively), helices A, E, and F, and the N and C termini are labelled (Taken from Sazinsky *et al.* (2004).

The use of mutagenic techniques in study of the relationship between the structure and the function of enzymes and the complex chemistry involved in their catalytic cycle is vital in understanding how these enzymes work. This chapter will focus on what is currently known about the catalytic cycle of sMMO and review mutagenic studies of sMMO and related members of the soluble diiron monooxygenase (SDIMO) family (Table 1.2)

Enzyme	Source organism	Genetic organisation	Reference(s)
soluble methane monooxygenase	<i>Methylosinus trichosporium</i> QB3b	'VtvoR >vtvoG rv'VoX rv<voV <vtvod v?>vcZrvtv oD (Vtv oC	1, 2, 3
butane monooxygenase	<i>Thauera butanivorans</i>	btvoX cvot otvod bmoZ cvcD crvoC	
toluene-4-monooxygenase	<i>Pseudomonas mendocina</i> KR1	tmoA Trvod Ttvoc fmoD tmcE ttvor	5, 6
toluene-ortho-monooxygenase	<i>Burkholderia cepacia</i> G4	iQtvA torvB totvC tomD iorvc :c"vr	
toluene / o-xylene monooxygenase	<i>Pseudomonas stutzeri</i> OX1	touA ICu'B IQi'C IQiD foti'E touF	
toluene-3-monooxygenase	<i>Ralstonia pickettii</i> PKOI	TCuAl tcud icu3 'ouV tbi:A2 ibuC	9, 10
ribonucleotide reductase	<i>Escherichia coli</i> K-12	nrctA 'irc,'3	11
deoxyhypusine hydroxylase	<i>Homo sapien</i>	DCdr!	12, 13, 14
stearoyl-ACP-desaturase	<i>Ricinis communis</i>	RCOM ±238359	14

Table 1.2: Genetic organisation of soluble diiron monooxygenases and related diiron enzymes

References

- | | |
|--------------------------------|-----------------------------------|
| 1. Stafford <i>et al.</i> 2003 | 9. Olsen <i>et al.</i> 1994 |
| 2. Scanlan <i>et al.</i> 2009 | 10. Byrne <i>et al.</i> 1995 |
| 3. Stein <i>et al.</i> 2010 | 11. Carlson <i>et al.</i> 1984 |
| 4. Sluis <i>et al.</i> 2002 | 12. Park <i>et al.</i> 2006 |
| 5. Yen <i>et al.</i> 1991 | 13. Kim <i>et al.</i> 2006 |
| 6. Yen and Karl 1992 | 14. Abbruzzese <i>et al.</i> 1986 |
| 7. Newman and Wackett, 1995 | 15' Shanklin and Somerville, 1991 |
| 8. Bertoni <i>et al.</i> 1998 | |

1.1.6) The catalytic cycle of soluble methane monooxygenase

The catalytic cycle of sMMO (Fig. 1.6) has been well characterized using a variety of spectroscopic techniques including UV/Vis, Mossbauer and EPR. In its resting state the diiron centre is in its diferric (Fe_2) form which is reduced to the diferrous (Fe_2) form to bind dioxygen (Woodland *et al.* 1986, Liu *et al.* 1995). The two electrons required for this reduction are provided by NAD(P)H via the FAD and $\text{Fe}_2\text{-S}_2$ sites of the reductase which acts as a transmembrane passing electrons singly to the active site (Lund and Dalton 1985). The non-covalent bonding of dioxygen to the active site is known as compound O, this is followed by compound P^* where dioxygen is covalently bound to the diiron site via an unprotonated peroxo bridge (Liu *et al.* 1995). The diiron site of compound P^* has been shown to be in a diferric (Fe_2) state (Brazeau and Lipscomb, 2000; Kopp and Lippard, 2002; Tinberg and Lippard, 2009). The protonation of the peroxo-bridge forms compound P that decays spontaneously cleaving the O-O bond. This leads to the formation of compound Q which is the kinetically active form of the diiron site that reacts with methane to produce methanol and has an Fe_2V "diamond core" structure. The presence of product in the diiron site has been shown with the chromogenic substrate nitrobenzene and the enzyme-product complex has been termed compound T (Lee *et al.* 1993). The exact mechanism of C-H bond breaking and substrate oxygenation are not fully understood but three possible mechanisms have been put forward. Either cleavage of the bond is homolytic and proceeds via a radical mechanism; cleavage is heterolytic whereby the carbanion is stabilized by binding to the iron atoms or the methane-Fe and oxygen species may react via a concerted mechanism of bond breakage and formation.

Fig. 1.6) Diagram showing the conformation of the diiron centre during the catalytic cycle of sMMO. Intermediates Hox, Hred, O, P*, P, Q, Q* and T are labeled. (adapted from: Smith and Dalton, 2004 to include intermediate Q*)

In the absence of substrate, compound Q decays back to the resting diferric (Fe_2) via another intermediate termed compound Q* (Tinberg and Lippard, 2009). Compound Q* was detected using stopped flow optical spectroscopy in the presence of $> 540\text{nM}$ methane to suppress the dominating absorbance signal due to compound Q and showed an absorbance band at 420nm . The authors showed that the rate of decay of Q* was not affected by the presence of methane and suggest that the mechanism of Q decay in the absence of substrate arises from the acquisition of two protons and two electrons either two stepwise electron transfer event from proximal amino acids or by receiving electrons from a diiron (Fe_2) centre present in the neighbouring hydroxylase protomer. From analysis of the optical spectra the authors suggest that Q* may be an $\text{Fe}^{\text{IV}}/\text{Fe}^{\text{V}}$ centre and a protein based radical or a combination of an $\text{Fe}^{\text{IV}}/\text{Fe}^{\text{V}}$ and an $\text{Fe}^{\text{IV}}/\text{Fe}^{\text{V}}$ species.

1.1.7) The substrate range of soluble methane monooxygenase

As well as oxidizing methane, sMMO has been shown to co-oxidize a range of adventitious substrates; however the resultant oxidation products are unable to provide a nutrient source for the methanotrophic bacteria (Colby *et al.* 1977; Burrows *et al.* 1984; Green and Dalton, 1989). As well as aliphatic hydrocarbons such as alkanes and alkenes, sMMO has also been shown to co-oxidize a wide range of monoaromatic, diaromatic and halogenated compounds leading to much interest in the use of soluble methane monooxygenase for biocatalysis and bioremediation applications. In the majority of reactions between sMMO and multi-carbon substrates, where a number of sites can be oxidised, a mixture of products is observed. Many halogenated compounds such as trichloroethylene and chloroform are considered to be major groundwater pollutants. These halogenated compounds do not seem to act as carbon and energy sources for bacteria and persist as pollutants for many years (Hanson and Hanson, 1996). Research has been carried out by a number of groups into the oxidation of trichloroethylene by soluble methane monooxygenase and the use of methanotrophs within consortia of bacteria able to metabolize the oxidation products of trichloroethylene have been shown to completely degrade trichloroethylene (Little *et al.* 1988; Tsien *et al.* 1989; Fox *et al.* 1990; Jahng *et al.* 1996; Lee *et al.* 2006; Hazen *et al.* 2009) To investigate the affect of specific amino acid changes on the substrate range and product distribution of sMMO has been one of the principal areas of research pursued.

1.1.8) Site directed mutagenesis of soluble methane monooxygenase

To date few site directed mutagenesis studies have been carried out on sMMO due to the lack of an adequate expression system. The inability to produce functional enzyme within *Escherichia coli* led to the development of a homologous expression system within an sMMO negative host and allowed the first site directed mutagenesis studies of sMMO (Smith *et al.* 2002). Two residues C151 and T213 were chosen as candidates for site directed mutagenesis due to the close proximity of these protonated side chains to the active site. The C151 position within the active site of sMMO is also analogous to the Y122 position within the R2 subunit of ribonucleotide reductase, where the generation of a tyrosyl radical by a diiron site is essential for initiating the ribonucleotide reductase catalytic cycle. The C151E mutant showed slight activity towards the diaromatic substrate naphthalene strongly suggesting that C151 was not involved in radical chemistry (Table 1.3). The activity of T213A and T213S towards naphthalene showed that this residue was also not essential for catalytic activity of sMMO. The instability of soluble cell extract preparations of the T213A mutant and the stability and activity of T213S mutant led to the suggestion of the importance of an OH group at this position for stability of the enzyme. However the activity of the T213S mutant within soluble cell extract preparation led to the first purification of a stable site directed mutant of sMMO (Table 1.4).

	activity with naphthalene	inhibition by acetylene		Activity (nmol min ⁻¹ mg ⁻¹);		
				Methane ^A	Propene ^B	Toluene ^B
wild type	Yes	Yes	Wild type	235 ± 22	244 ± 7	7.8 ± 0.83
C151E	Yes	Yes	T213S	169 ± 27	43 ± 3	5.6 ± 0.49
C151Y	No	N/A				
T213A	diminished	Yes				
T213S	Yes	Yes				

Table 1.3: Properties of sMMO site directed mutants
N/A = not applicable

Table 1.4: Activity of T213S mutant towards methane, propane and toluene.

^A Derived from oxygen uptake measurements
^B Derived from GC detection of oxidation products

The soluble methane monooxygenase enzyme is part of the soluble diiron monooxygenase (SDIMO) family of enzymes (Leahy *et al.* 2003). These enzymes including butane monooxygenase (BMO), toluene-4-monooxygenase (T4MO), toluene *-ortho-*monooxygenase (TOM) toluene / *o*-xylene monooxygenase (ToMO) and deoxyhypusine hydroxylase (DOHH) are homologous to sMMO and all have a diiron site with conserved His-Glu ligands (Table 1.2). The presence of similar iron binding motifs are also found in other diiron containing enzymes such as acyl carrier protein (ACP) desaturases (Shanklin and Somerville 1991) and the R2 subunit of Class Ia ribonucleotide reductase from *E. coli* (Carleson *et al.* 1984). Below are described a number of these SDIMOs and enzymes structurally related to soluble methane monooxygenase along with examples of how creation and expression of mutants has led to major breakthroughs and insights into the workings of these complex proteins.

1.2 Butane Monooxygenase

1.2.1) Structure of butane monooxygenase

The butane monooxygenase of *Thauera butanivorans* (formerly *Pseudomonas butanovora*) is one of the most closely related enzymes to soluble methane monooxygenase of *Ms. trichosporium* OB3b. This enzyme catalyses the conversion of butane to 1-butanol and is the first step in the butane metabolic pathway of *T.butanivorans*. The butane monooxygenase enzyme is made up of a 45 kDa oxidoreductase component encoded by *bmoC* a 22 kDa regulatory protein encoded by *bmoB* and a hydroxylase component (BMOH) made up of three subunits of 54, 43 and 25 kDa encoded by *bmoXYZ*. The hydroxylase component of BMO has an $\alpha_2\beta_2\gamma_2$ quaternary structure and like sMMO the non heme diiron active site is located in the α subunit encoded by *bmoX* (Sluis *et al.* 2002; Table 1). Analysis of the sequence of BmoX shows 63% sequence identity at the amino acid level to the α -subunit of sMMO. Comparison to the crystal structure of MmoH suggested the presence of a 19 residue hydrophobic pocket adjacent to the active site of BMO which may be involved in substrate binding. Fourteen of these putative substrate-binding residues were found to be conserved between BMO and sMMO (Fig. 1.7, Fig. 1.8). The iron-binding residue of sMMO are perfectly conserved suggesting a very similar diiron centre in both enzymes.

Fig 1.7) sMMO Hydroxylase α -subunit showing residues corresponding to those chosen for mutation in BMO by Halsey *et al.* (2006) The diiron centre is shown as orange spheres, residues are coloured as follows: N116 (RED), C151 (green), L279 (yellow), K323 (Magenta) and Y324(cyan). Picture is compiled from x-ray crystallography data of sMMO hydroxylase (1MTY)

Fig 1.8) BMOH α -subunit with showing residues chosen for mutation by Halsey *et al.* (2006) Residues are coloured as follows G113 (RED), T148 (green), L279 (yellow), Q320 (Magenta) and F321(cyan). Picture is compiled from structural data and based upon x-ray crystal structure of sMMOH α chain (1MTY)

1.2.2) Site directed mutagenesis of butane monooxygenase active site residues to the sMMO counterparts

The BMO enzyme has been shown to co-oxidize a number of alkanes and alkenes, although its substrate profile is much narrower than that of sMMO and it has very low activity towards methane. A number of site directed mutagenesis studies have been carried out on the BMOH a subunit by mutating specific amino acids to the counterpart residues within the hydroxylase α -subunit of sMMO in order to probe the differences in these two enzymes. Three distinct regions have been the focus of site directed mutagenesis studies to study how the differences between these two enzymes may give rise to the differences in their catalytic activity. These mutations have been made in the hydrophobic region adjacent to the active site, a nearby hydrophobic cavity termed cavity 2 and the putative binding site for the regulatory BMOB protein (Halsey *et al.* 2006). Below are described a number of studies carried out with these BMO mutants against some short chain alkane substrates, analysis of inactivation of some of these mutants by propionate and analysis of the degradation of a number of chloroethylenes.

1.2.3) Activity of butane monooxygenase site directed mutants against small chain alkanes

Five BMO mutants were created: G113N, T148C near the active site, L279F in hydrophobic cavity 2 and Q320K and F321Y at the BMOB binding site (Fig. 1.7, Fig. 1.8). It was found that all of these mutants had a reduced specific activity towards butane. All mutant enzymes could support growth on butane, propane and ethane, with the exception of the G113N mutant enzyme which could not support growth on propane (Table 1.5). The G113N expressing cells had significantly longer generation times of 9.1 h for growth on butane compared to 3.6 h for the wild type butane monooxygenase and 13.1 h for growth on ethane compared to 4.5h for the wild type. Studies on the product distribution of these mutants identified the G113N and L279F mutants as showing large changes in regiospecificity compared to the wild type

enzyme. The L279F and G113N mutants showed a 5.5-fold and 278-fold increase in the production of 2-butanol respectively (Table 1.6). Wild type butane monooxygenase oxidizes alkanes almost exclusively at the terminal carbon and the relaxation of regiospecificity seems to show a phenotype closer to methane monooxygenase for these mutants. The G113N mutant also oxidized propane exclusively at the sub terminal carbon to yield 2-propanol which is further oxidized to acetone as a dead end product which cannot be utilized by the organism for growth and so accumulates in the cell. Another MMO-like phenotype for the G113N mutant was the reduced methanol inhibition during methane oxidation assays compared to the wild-type enzyme and the other mutants. Further kinetic analysis using purified protein showed that while the wild type enzyme had similar K_m values of 1100 pM for methane and 1250 pM for methanol, the G113N mutant had a much lower K_m value of 340 pM for methane compared to 750 pM methanol (Cooley *et al.* 2009). This indicates that methanol is a less effective competitive substrate for the G113N mutant compared to the wild type, which explains the observation that methane oxidation could continue for a longer period of time with G113N until the methanol concentration reached a high enough level to inhibit the enzyme.

	butane (h)	propane (h)	ethane (h)
WT	3.6 ±0.2	4.0 ±0.4	4.5 ±0.3
T148C	4.4 ±0.3	4.2 ±0.4	7.0 ±0.1
Q320K	4.1 ±0.3	3.9 ±0.1	5.9 ±0.1
F321Y	3.4 ±0.3	3.4 ±0.2	3.8 ±0.1
L279F	5.7 ±0.1	4.5 ±0.1	7.9 ±0.6
G113N	9.1 ±0.4	NA	13.1 ±0.5

Table 1.5: Generation times of butane monooxygenase mutants grown on short chain alkanes
Taken from Halsey *et al.* 2006.

	1-butanol accumulation (nmol min ⁻¹ mg protein ⁻¹)	2-butanol accumulation (nmol min ⁻¹ mg protein ⁻¹)	Ratio of 2-butanol to 1-butanol
WT	74.0 ±3.9	2.7 ±0.91	0.04
T148C	41.3 ± 4.0	6.14 ±0.89	0.15
Q320K	50.4 ±7.8	10.3 ±0.53	0.2
F321Y	102.4 ±5.7	ND	NA
L279F	47.0 ±7.1	10.45 ±4.2	0.22
G113N	1.77 ±0.06	19.67 ±2.4	11.1

Table 1.6: Oxidation of butane by BMO mutants: product formation rates and product distribution
Taken from Halsey *et al.* 2006.

1.2.4) Effect of mutations on inactivation of butane monooxygenase by propionate

The mechanism of action of propionate, another BMO inhibitor, was studied using these mutants. It was shown that both reversible inhibition and inactivation of BMO occurred with propionate because some but not all activity could be recovered by washing of the cells to remove the propionate (Doughty *et al.* 2007). Although reversible inhibition was seen with all mutants tested, only those mutants close to the active site had any effect on the irreversible inactivation of BMO by propionate. The G113N mutant showed no inactivation by propionate treatment and the T148C mutant showed an increased in propionate dependant inactivation of BMO. Because the reversible inhibition by propionate remained unaffected in the G113N mutant, yet there was no irreversible inactivation, this led the authors to conclude that reversible inhibition and irreversible inactivation of BMO occurred through separate mechanisms. The authors proposed that irreversible inactivation of the BMO enzyme by propionate may be via coordination of aliphatic tail of propionate to Fe ions at the active site, resulting in the uncoupling of O₂ activation from substrate oxidation and leading to the formation of H₂O₂, which damages the enzyme. Interestingly, sMMO is not inactivated by propionate and so this is another MMO-like phenotype displayed by the G113N mutant (Doughty *et al.* 2007).

1.2.5) Chloroethylene degradation by butane monooxygenase site directed mutants

The oxidation of a number of chloroethylenes by G113N, L279F and F321Y mutants of BMO was studied, and the rate of oxidation and amounts of chlorine released during the complete degradation of 1,1-dichloroethylene, 1,2-c/s-dichloroethylene and trichloroethylene was compared to the wild type enzyme (Halsey *et al.* 2007). The wild type BMO enzyme was shown to release almost 100 % chlorine from each substrate tested. The G113N mutant showed reduced oxidation rates and reduced amounts of chlorine released for all substrates compared to the wild type enzyme. The L279F mutant showed reduced rates for trichloroethylene degradation with almost 100 % chlorine release and only 40 % of the chlorine released from 1,2-c/s-dichloroethylene but at a rate comparable to the wild type enzyme. The F321Y mutant showed comparable rates of degradation to the wild type for all three substrates, however only 40 % of the chlorine was released from 1,2-c/s-DCE and TCE. This shows that in both the L279F and F321Y mutants a proportion of the chlorine from these substrates is not converted to free chloride. It was also shown that the G113N mutant was the only isoform unable to degrade the product 1,2-c/s-DCE epoxide. By monitoring lactate dependent O_2 uptake of these cells during the degradation of chloroethylene substrates it was shown that the turnover of these substrates had toxic effects upon the cell with lactate dependent respiration dropping to <10% for the wild type enzyme and most of the site directed mutants. However, G113N was the only mutant that maintained >75 % of cellular respiration during oxidation of the chloroethylenes. This led to the suggestion that by altering the regioselectivity of the enzyme the G113N mutant was able to utilize a chloroethylene oxidative pathway separate from the pathway used by the wild type enzyme. It was proposed that this pathway could be utilized for more sustainable bioremediation of CEs from the environment (Halsey *et al.* 2007). By utilizing a pathway which forms oxidation products with reduced toxicity towards bacterial cells, these products could then be further degraded by other bacteria more effectively.

1.3 Toluene-4-monooxygenase

1.3.1) Structure of toluene-4-monooxygenase

A number of toluene monooxygenases related to sMMO that oxidize their natural substrate toluene at specific positions have been identified and studied extensively using a variety of mutagenesis techniques. The toluene 4-monooxygenase (T4MO) from *Pseudomonas mendocina* KR1 is a four component monooxygenase consisting of a 33 kDa oxidoreductase component (encoded by *tmoF*), a 12.5 kDa Rieske-type ferredoxin component (encoded by *tmoC*), an 11.6 kDa regulatory protein (encoded by *tmoD*) and a diiron hydroxylase (encoded by *tmoAEB*) component with an $\alpha_2\beta_2\gamma_2$ quaternary structure (Yen *et al.* 1991; Yen and Karl, 1992). The coordination and location of the active site is similar to that of sMMO; the diiron active site is found within the T4MOH α -subunit (encoded by *tmoA*) and x-ray crystallography has shown that this is coordinated by four glutamate residues (G104, G134, G197, G231) and two histidine ligands (H137, H234) within a four helix bundle (Bailey *et al.* 2008).

1.3.2) Site directed mutation of toluene-4-monooxygenase active site residues to sMMO counterparts

The T4MO enzyme shows high degrees of regioselectivity catalysing the para-hydroxylation of toluene to produce the oxidation product p-cresol. A number of mutagenesis studies have been used to probe the mechanism of action for this enzyme as well as to try and understand what role particular residues play in controlling the regiospecificity. A number of mutants were created to study the difference between T4MO and sMMO (Pikus *et al.* 1997). Three mutants with residue changes to their homologous counterparts within sMMO were created: Q141C (C151 in sMMO), I180F (F192 in sMMO) and F205I (I217 in sMMO). These mutants were assayed for activity with the substrates toluene, m-xylene and p-xylene (Table 1.7, Table 1.8). The greatest change in regioselectivity in comparison to the wild type enzyme was seen with the Q141C and F205I mutants. The I180F mutant

showed very little change in regioselectivity with any of the substrates however both the Q141C and F205I mutants showed a shift away from the *para*-hydroxylation when toluene was the substrate. There was a slight shift towards side chain hydroxylation with m-xylene as the substrate and a major shift towards side chain hydroxylation when p-xylene was the oxidation product. The detection of activity with the Q141C and Q141V mutants led the authors to conclude that glutamine was not an essential amino acid at this position. The large change in regioselectivity with the Q141 and F205 mutants compared to the relatively small change in regioselectivity of the I180F mutant suggest a possible substrate binding site within this enzyme. By using sequence alignments and comparison to the crystal structure of MMO (Rosenzweig *et al.* 1995; Elango *et al.* 1997) the authors suggest that the Q141 and F208 residues are on one side of the hydrophobic cavity close to the iron atom FeA whereas the 1180 position is on the opposite side of the cavity closer to FeBatom. This has since been confirmed by determination of the crystal structure of the T4MO hydroxylase (Bailey *et al.* 2008). These results implicate this region of the hydrophobic cavity adjacent to the active site of T4MO in orientating substrate in a manner which favours *para*-hydroxylation.

Toluene oxidation

Enzyme	^{OH} p-cresol (%)	^{OH} m-cresol (%)	^{OH} o-cresol (%)	^{OH} Benzyl alcohol (%)
WT	96	2.8	0.4	0.8
Q141C	85	5	4	6
F205I	81	14.5	3.5	1
I180F	96.7	1.2	0.2	1.9

Table 1.7: Product distribution from the oxidation of toluene by T4MO site directed mutants (Pikus *et al.* 1997).



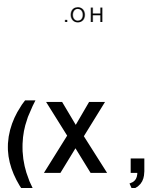

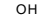
Enzyme	m-cresol oxidation (%)		p-xylene oxidation (%)		
					
	3,5-dimethylphenol	2,4-dimethylphenol	3-methylbenzyl alcohol	4-methylbenzyl alcohol	2,5-dimethylphenol
WT	0.3	97.4	2.2	82	18
Q141C	0.1	88.3	11.7	22	78
F205I	0.1	44.4	11.6	42	58
I180F	0.6	90.6	8.8	89	11

Table 1.8: Product distribution from the oxidation of m-cresol and p-xylene by T4MO site directed mutants (Pikus *et al.* 1997).

1.3.3) Regioselectivity of toluene-4-monooxygenase site directed mutants at positions T201 and G103

Fox and co-workers also adopted a saturation mutagenesis approach where all possible amino acid mutations were made at position T201, to probe whether or not this residue was essential for catalysis (Pikus *et al.* 2000). Comparisons of all bacterial diiron monooxygenases show that they have a threonine at a position equivalent to T201 in T4MO (T213 in sMMO) that possibly acts as a proton donor during O₂ activation by the enzyme. However by creating 5 mutants at this site, all of which had similar *k_{cat}* and *k_m* values, it was concluded that this site was not essential for catalysis. These results did, however, highlight the importance of this residue in the regioselectivity of the enzyme. The size of the sidechain dramatically affected the product distribution with toluene and p-xylene as substrates. The greatest relaxation of regioselectivity with toluene as substrate was seen with the T201F mutant with a large increase in oxidation at the *ortho* position. When p-xylene was the substrate the largest change in regioselectivity from sidechain to ring hydroxylation was seen

with the T201G mutant. These large shifts in regioselectivity led the authors to conclude that it was the size and volume of the sidechain that occupied this site that led to the alterations in the regiospecificity of T4MO. However it is notable that mutation to the much smaller glycine residue had little effect on regioselectivity with toluene as the substrate and similarly mutation to the much larger phenylalanine residue had little effect on the regioselectivity when p-xylene was the substrate.

The G103L mutant of T4MO was designed after sequence analysis of toluene monooxygenase alongside related phenol hydroxylase and alkene monooxygenase enzymes which have Leu at this position. The substitution of the *tm oD* effector protein with the T3buV effector protein of a toluene 3-monooxygenase showed little change in the regioselectivity of the enzyme and but did show a reduced turnover rate with toluene as the substrate. However enhanced regioselectivity towards *ortho* hydroxylation was seen with the mutant G103L for toluene, methoxybenzene and chlorobenzene oxidation further highlighting the importance that these active site residues have on regioselectivity (Mitchell *et al.* 2002).

1.3.4) Identification of toluene-4-monooxygenase mutants for the increased production of pharmaceutical precursors

The identification of G103 as an important residue for controlling regiospecificity of T4MO led to this residue being chosen as one of the sites for saturation mutagenesis studies (Tao *et al.* 2004). This site was chosen to investigate the synthesis of novel compounds along with sites A107 and 1100. These sites were also identified as being important in determining regioselectivity due to a previous study where a directed evolution approach led to creation of mutants of toluene-*ortho* monooxygenase with increased 1-naphthol synthesis activity (mentioned later in this chapter). Wild type T4MO was shown to oxidize o-cresol to the dihydroxylated product 3-methylcatechol and methylhydroquinone and to oxidize o-methoxyphenol to 4-methoxyresorcinol, 3-methylcatechol and methoxyhydroquinone. Using o-cresol, and o-methoxyphenol as substrates, mutants were screened for increased production of 3-methoxycatechol, methoxyhydroquinone and methylhydroquinone all

useful precursors for pharmaceuticals. A number of mutants were identified with increased production of these precursors compared to the wild type enzyme as well as a shift in the product distribution of these products, which led the authors of the work to argue that this enzyme could be engineered using mutagenesis to optimise the production of specific products by controlling regioselectivity (Tao *et al.* 2004).

1.3.5) Regiospecific oxidation of naphthalene by toluene-4-monoxygenase mutants

The G103, A107 and 1100 saturation mutagenesis libraries mentioned above were also screened for the production of 1-naphthol and 2-naphthol using naphthalene as the substrate (Tao *et al.* 2004b). Wild type T4MO oxidized naphthalene at a rate of 7.7nmol/min/mg protein to almost equimolar amounts of 1-naphthol (52%) and 2-naphthol (48%). The mutants I100A, I100S and I100G showed similar rates of naphthalene oxidation to that of the wild type but with 88-95 % 2-naphthol as the major oxidation product. The rates of naphthalene oxidation by mutants G103A and G103S were only slightly less than the wild type enzyme (5.6 and 5.9 nmol/min/mg respectively) but with 81 and 83 % 1-naphthol as the major oxidation product and a double mutant G103S/A107G producing > 99 % 1-naphthol was also identified (Table 1.9).

	Naphthalene oxidation		
	Rate (nmol/min/mg)	%1 naphthol	%2 naphthol
WTT4MO	7.7 ± 0.5	52	48
I100A	7.0 ± 0.5	8	92
I100S	5.5 ± 1.6	5	95
I100G	7.6 ± 0.5	12	88
I100L	3.2 ± 1.5	83	17
G103S/A107G	0.5 ± 0.1	99	1
G103A	5.6 ± 1.5	81	19
G103S/A107G	5.9 ± 0.1	83	17

Table 1.9: Activity and product distribution from the oxidation of naphthalene by T4MO site directed mutants (Tao *et al.* 2004b).

1.3.6) Production of indigoid products by toluene-4-monoxygenase mutants

Using the same sites 1100 G103, A107 and another site F196, Steffan and co-workers used site directed mutagenesis to create a number of mutants that produced novel pigmented products from the oxidation of indole (McCloy *et al.* 2005). These authors suggest that the alteration of regiospecificity of this enzyme could lead to a greener alternative to the formation of indigoid coloured products compared to current industrial synthesis and highlight a number of applications of these products in the textile industry as dyes as well as therapeutic applications of a number of these compounds. However the commercial viability of this approach compared to more well established chemical synthesis methods is unclear.

1.4 Toluene ortho-monooxygenase

1.4.1) Structure of toluene-ortho-monooxygenase

Similar mutagenesis experiments have been carried out with another monooxygenase from the toluene monooxygenase family: toluene ortho-monooxygenase (TOM) from *Burkholderia cepacia* G4. Like sMMO the toluene ortho-monooxygenase consists of three components: a 40 kDa oxidoreductase component (encoded by *tomAS*), a 10.4 kDa regulatory component (encoded by *tomA2*) and a 211 kDa hydroxylase component with an $\alpha_2\beta_2$ quaternary structure (encoded by *tomA1A3A4*) where the diiron site is located within the hydroxylase α -subunit encoded by *tomA* (Shields *et al.* 1995).

1.4.2) Directed evolution of toluene-ortho-monooxygenase towards increased naphthalene oxidation and chloroethylene degradation

The natural substrate for TOM is toluene and the enzyme shows a high degree of regiospecificity for hydroxylation at the *ortho* position to form *o*-cresol almost exclusively. One of the major successes in the mutagenesis studies of soluble diiron monooxygenases utilized a directed evolution approach to identify a mutant with increased naphthalene oxidation and increased chloroethylene degradation (Canada *et al.*, 2002). By using a DNA shuffling technique, a random mutant library was screened for naphthalene oxidation using the colorimetric naphthalene oxidation test and a mutant was identified with a six fold increase in activity towards naphthalene with no change in regiospecificity. Sequencing of the mutant identified it as having a mutation at the V106 position (L110 in sMMO 1100 inT4MO and ToMO). This V106A mutant (designated TOM-green) also showed increase degradation of 1,1-dichloroethylene and 1,2-trans-dichloroethylene and increased oxidation of triaromatic compounds phenanthrene and anthracene compared to the wild type enzyme. This supported the hypothesis that this residue was acting as a substrate gate and that mutation to a residue with a smaller side chain allowed greater access

of substrates to the active site. This gave experimental evidence supporting the hypothesis that L110 in sMMO also had a gating role controlling substrate access to the active site (Rosenzweig *et al.*, 1997). To further increase the production of 1-naphthol synthesis, a saturation mutagenesis approach at the 106 position of this TOM-green mutant enzyme was used and the resulting mutant library screened for increased naphthol synthesis (Rui *et al.*, 2004). An A106E mutant was identified that had a two fold increase in 1-naphthol synthesis with no change in regioselectivity. This enzyme showed 63% increase in toluene oxidation activity and had a large change in regioselectivity compared to the wild type with o-cresol (50%) m-cresol (25%) and p-cresol (25%) compared with 98 % o-cresol being produced by the wild type enzyme. Another mutant identified as A106F had a 62 % increased activity for toluene oxidation and also showed relaxed regiospecificity with o-cresol (28%) *tri-cresol* (18%) and p-cresol being produced (Table 1.10).

	toluene oxidation			naphthalene oxidation	
	% o-cresol	% <i>tri-cresol</i>	% p-cresol	rate of 1-naphthol (nmol min ⁻¹ mg protein ⁻¹)	% 1-naphthol
WT TOM	>98	0	0	0.80 ± 0.06	98
V106A	50	33	17	3.6 ± 0.4	97
A106E	50	25	25	7.4 ± 0.4	98
A106F	28	18	54	7.4 ± 0.4	99

Table 1.10: Product distribution from the oxidation of toluene and naphthalene by toluene *ortho*-monooxygenase site directed mutants (Rui *et al.*, 2004).

1.4.3) Production of indigoid pigments by toluene-ortho-monoxygenase

DNA shuffling and random mutagenesis were used to study the production of novel pigments from oxidation of indole by TOM, (Rui *et al.* 2004) in a similar experiment to that mentioned above by Steffan and co-workers using T4MO. Mutant libraries were screened on complex media and a mutant was identified with a distinct blue pigmentation in its colonies. The sequencing of this mutant identified three amino acid changes compared to the wild type enzyme at D14, A113 and F465. The D14 and A113 sites along with another site V106 identified as influencing regioselectivity in TOM (Canada *et al.* 2002) were chosen for saturation mutagenesis and a variety of mutants were created that oxidized indole to wide range of novel pigmented products. This led the authors to suggest that TOM mutants could also be created with altered regioselectivity to produce commercially viable products. However, as in the previous experiment with T4MO the question still remains about the commercial viability compared to conventional chemical synthesis methods.

1.5 Toluene/o-xylene monooxygenase

1.5.1) Structure of toluene/o-xylene monooxygenase

The toluene-o-xylene monooxygenase (ToMO) of *Pseudomonas stutzeri* 0X1 is a four component monooxygenase consisting of a oxidoreductase component (encoded by *touF*) an effector protein (encoded by *touD*) a Rieske type ferredoxin component (encoded by *touC*) and a hydroxylase component (encoded by *touABE*). The hydroxylase has an $\alpha_2\beta_2\gamma_2$ quaternary structure where the diiron centre is found within the hydroxylase α -subunit encoded by *touA* (Bertoni *et al.* 1998).

1.5.2) Identification of toluene/o-xylene monooxygenase mutants for the increased production of pharmaceutical precursors

ToMO hydroxylates toluene in the *ortho*, *meta*, and *para* positions, hydroxylates o-xylene in both the *meta* and *para* positions and also co-oxidizes a number of other aromatic substrates. Wood and co-workers have used both random mutagenesis using DNA shuffling and saturation mutagenesis approaches to study this enzyme in detail. Saturation mutagenesis at positions 1100 Q141 T201 and F205 identified a number of mutants including I100Q and F205G capable of producing novel oxidation products and important pharmaceutical precursors 4-methylresorcinol and methylhydroquinone (Vardar and Wood, 2004) in an experiment similar to that carried out in the same laboratory with T4MO mentioned above (Tao *et al.* 2004). Another M180T/E284G mutant identified from the DNA shuffling mutagenesis library was also able to form the novel oxidation product methylhydroquinone (Vardar and Wood, 2004). Nitrobenzene oxidation was also used to screen the DNA shuffling mutant libraries and saturation mutagenesis mutant libraries and yielded another residue E214 that was shown to affect regioselectivity of the enzyme and yielded a number of mutants with increased production of 3-nitrocatechol, 4-nitrocatechol and nitrohydroquinone.

1.5.3) Directed evolution of toluene/o-xylene monooxygenase towards increased chloroethylene degradation

A DNA shuffling random mutant library and a saturation mutagenesis (at positions 1100 Q141 T201 F205 and E214) library were used to screen for enhanced chloroethylene degradation where I100Q was shown to have a 2.8 fold increase in TCE degradation compared to the wild type ToMO enzyme. Another mutant identified from the DNA shuffling library E214G/D312N/M399V with increased degradation of 1,2-c/s-dichloroethylene (Vardar and Wood, 2005 b; Table 1.11). The authors also showed that mutants T201G T201S and A107T/E214A had significantly altered regiospecificity in the oxidation of naphthalene and o-xylene. In depth study of the M180 and E214 positions using saturation mutagenesis approach was also carried out (Vardar and Wood, 2005b; Table 1.12). The authors showed that M180 has a much more pronounced effect on regiospecificity with a number of aromatic compounds and that E214 has much less of an effect on the regiospecificity of the enzyme but does effect the rate of the reaction. These results lead to the hypothesis that M180 is another residue involved in gating access of the substrate to the active site.

	TCE degradation (nmole min ⁻¹ mg protein ⁻¹)	DCE degradation (nmole min ⁻¹ mg protein ⁻¹)
WT ToMO	0.41 ±0.02	2.7 ±0.05
I100Q	0.85 ±0.01	3.8
K160N	0.53 ±0.01	NM
E214G/D312N/M399V	NM	5.3

Table 1.11: Degradation rates for ToMO mutants against trichloroethylene and dichloroethylene (Vardar and Wood, 2005)

Enzyme	toluene regioselectivity (%)			o-xylene regioselectivity (%)		naphthalene regioselectivity (%)	
	O-cresol	m-cresol	p-cresol	3,4-DMP	2,3-DMP	1-Naphthol	2-Naphthol
	WT ToMO	32	21	47	82	18	88
I100Q	22	44	34	76	24	89	11
A107T/E214A	2	5	93	97	3	64	36
K160N	30	23	47	82	18	89	11
M180T/E284G	32	26	42	88	12	88	12
T201S	31	18	51	65	35	96	4
T201G	53	12	35	100	0	>99	<1
E214G/D312N/M399V	35	22	43	81	19	89	11
E214G	32	20	48	83	17	89	11

Table 1.12: Product distribution from the oxidation of toluene, o-xylene and naphthalene by ToMO site directed mutants (Vardar and Wood. 2005b).

1.5.4) Investigation of toluene/o-xylene monooxygenase free radical intermediates using site directed mutagenesis

Site directed mutagenesis was used to create mutants I100Y, I100W, F205W and L208F with the intention of creating a mutant with a large side chain that blocked the hydrophobic channel (Murray *et al.* 2007; Fig. 1.9). This allowed the accumulation of intermediates in the ToMO reactive cycle that had not previously been detected. In the I100W mutant the formation and decay of reactive species was characterized by rapid freeze-quench EPR, Mossbauer and ENDOR spectroscopy and the authors reported the detection of an EPR silent, optically transparent diiron (Fe^{II}) intermediate that was able to oxidize the nearby W100 residue to form a mixed valent diiron ($\text{Fe}^{\text{II}}/\text{Fe}^{\text{IV}}$) centre coupled to a tryptophanyl radical that displayed an absorption band at 500 nm. This species was shown to subsequently decay to the resting diiron (Fe^{II}) state. The detection of these intermediates led to the proposal of a scheme where dioxygen activation proceeds via the one electron reduction of a peroxodiiron (III) intermediate to form the mixed valent centre and led to comparisons with ribonucleotide reductase where a peroxodiiron centre has been shown to react in a similar manner (Krebs *et al.* 2000).

Fig 1.9) View of the active site pocket of ToMOH from the substrate access channel. The diiron atoms are shown as orange spheres. The opening to the pocket is bordered by residues 1100, T201, F205, and F196.

(Taken from Murray *et al.* (2007))

1.6 Toluene-3-monoxygenase

1.6.1) Structure of toluene-3-monoxygenase

The toluene-3-monoxygenase (T3MO) of *Ralstonia pickettii* PKO-1 is a four component monoxygenase consisting of a oxidoreductase component (encoded by *tbuC*) an effector protein (encoded by *tbuV*) a Rieske type ferridoxin component (encoded by *tbuB*) and a hydroxylase component (encoded by *tbuA1A2U*) with an $\alpha_2\beta_2\gamma_2$ quaternary structure where the diiron centre is found within the hydroxylase α -subunit encoded by *tbuA1* (Olsen *et al.* 1994; Olsen *et al.* 1995).

1.6.2) Site directed mutagenesis of toluene-3-monoxygenase

By comparison of mutagenesis experiments of related aromatic monoxygenases three amino acid positions were chosen for site directed mutagenesis of T3MO (Fishman *et al.*, 2004). The positions 1100, G103 and A107 were chosen based on the work of Woods and co-workers on analogous positions of T4MO mentioned earlier (Tao *et al.*, 2004) as well as mutagenesis experiments on analogous positions within TOM also mentioned above (Mitchell *et al.* 2002), (Rui *et al.*, 2005). Mutant libraries were created and expressed in *E. coli* and screened for activity against a number of substituted benzenes and phenols. Activity of the mutants was assessed by the formation of catechol derivatives from the oxidation of these substrates which auto-oxidize to form a red - brown colour. The wild type T3MO enzyme shows a preference for oxidation at the *para* position with 88% p-cresol being produced from oxidation of toluene. The authors identified a number of mutants with significantly altered regioselectivity towards oxidation at both the *ortho* and *meta* positions. The A107G mutant showed 80% o-cresol production when toluene was the substrate and 88% o-methoxyphenol produced when methoxybenzene was the substrate, compared to 100% p-methoxyphenol produced by the wild type enzyme. Two mutants I100S and G103S were shown to have an increase in hydroxylation activity at the *meta* position with 33% and 29% m-cresol being produced respectively when toluene was the oxidation product compared to 10% for the wild type enzyme. This led the authors to create the double mutant I100S/G103S which produced 75% *m*-

cresol when toluene was the substrate and 100% *m*-nitrophenol when nitrobenzene was the substrate compared to 100% *p*-nitrobenzene with the wild type (Fishman *et al.*, 2004). These results showed how the authors could use mutagenesis experiments of related monooxygenases to guide their choice of sites for mutagenesis to alter the regioselectivity of this enzyme.

1.7 Deoxyhypusine hydroxylase

1.7.1) Structure of deoxyhypusine hydroxylase

The human deoxyhypusine hydroxylase (DOHH) enzyme has also recently been shown to be a non haem diiron monooxygenase, however there is very little sequence similarity to the other monooxygenases mentioned here (Vu *et al.* 2009). Hypusine is an unusual amino acid present in the eukaryotic translational initiation factor eIF5A which is required for cell proliferation (Park *et al.* 1997, Chen and Liu, 1997, Caraglia *et al.* 2001). Deoxyhypusine hydroxylase works in conjunction with a second enzyme deoxyhypusine synthase to form the hypusine amino acid from a lysine residue on an eIF5A precursor.

1.7.2) Analysis of deoxyhypusine hydroxylase iron binding residues

The human deoxyhypusine hydroxylase enzyme contains the His-Glu iron binding ligands present in all bacterial diiron monooxygenases. A number of mutagenesis approaches were used to probe the activity of these glutamate and histidine iron ligands Site directed mutagenesis was used to show that by substituting an alanine residue into any of the glutamate or histidine residues within the four His-Glu binding motifs resulted in a loss of enzymatic activity (Kim *et al.* 2007). Wild type and site directed DOHH mutants were created as GST-fusion proteins by sub cloning into the pGEX-4T-3 expression vector and over expressing within *E. coli* strain BL21(DE3). By measuring the metal content of these mutants using ICP-MS it was shown that there was a significant reduction in the iron content of six out of the eight single site directed mutants compared to the wild type enzymes. The two mutants E57A and E208A showed normal iron content but had no detectable activity. This provided strong evidence that these His-Glu motifs were involved in iron binding at two separate iron coordination sites.

1.7.3) Site directed mutagenesis of amino acid residues conserved among deoxyhypusine hydroxylase

A study of 36 amino acid sites that were highly conserved among eukaryotic deoxyhypusine hydroxylases was carried out including those of His-Glu motifs mentioned above and alanine substitutions at each site were created using the same expression system described above (Kang *et al.* 2007). Affinity chromatography with GSH-sepharose beads was used to study substrate binding of these mutants. It was shown that four mutants E57A, E208A, E90A and E241A all exhibited significantly less substrate binding than the wild type enzyme. As described previously these mutants showed no enzyme activity but E57A and E208A showed a iron content comparable to the wild type enzyme highlighting the role of these residues in substrate binding. The poor binding efficiency of E90A and E241A indicated that these residues were involved in both iron coordination and substrate binding. The histidine to alanine substitutions within the His-Glu motifs all showed substrate binding activity comparable to the wild type enzyme. As these mutants were shown to have very little iron content, this shows that the substrate binding of the enzyme is not dependant on the presence of iron although it is necessary for activity. The remaining alanine substituted mutants all retained activity but less than that of the wild type enzyme. Of these mutants G63A and G214A showed reduced substrate binding which possibly accounts for the reduction in activity. Another mutant Met237 also showed a weak holoenzyme band on a non-denaturing native gel, leading the authors to suggest that this too may be involved in iron binding. Further site directed mutagenesis to create substitutions of alanine, asparagine and glutamine at E57 and E208 sites showed that only asparagine substitutions at these sites retained any enzyme or substrate binding activity. This provided strong evidence that it was the interaction of the carboxylate side chain that was required for activity. The M237A mutant showed a faint band on a native gel corresponding to the holoenzyme, leading the author to suggest this too may be involved in iron binding. However there is insufficient evidence to confirm this as it is possible that the reduced iron centre may be due to instability of the enzyme and not due to altered iron binding.

1.7.4) Detection of a diiron site in deoxyhypusine hydroxylase using spectroscopic analysis

The presence of a diiron centre suggested by the mutagenesis studies mentioned above was confirmed using a combination of various spectroscopic approaches including EPR, Mossbauer and RAMAN spectroscopy (Vu *et al.* 2009). The detection of a diiron centre in this enzyme, the fact enzyme activity is O₂ dependent and evidence of a η^2 -peroxo-diiron (Fem) intermediate detected by Raman spectroscopy led the authors to suggest a monooxygenase like reaction for this enzyme. Although to date the source of electrons for the reduction of the diiron site is still unknown.

1.8 Ribonucleotide reductase

1.8.1) Structure of ribonucleotide reductase

Ribonucleotide reductases play a central role in DNA biosynthesis catalysing the reduction of ribonucleotides to the corresponding deoxyribonucleotides. There are three classes of ribonucleotide reductases, the class 1 enzymes contain a diiron site homologous to sMMO, the class 2 enzymes contain a cobalt containing cofactor and the class 3 enzymes contain a [4Fe-3S] cluster. The Class 1A enzyme of *E. coli*, while not a monooxygenase, contains a diiron site homologous to sMMO which interacts with dioxygen via a well established radical chemistry pathway which was one of the functions that led to the suggestion of radical chemistry in sMMO. The enzyme has an $\alpha_2\beta_2$ structure with the α subunit containing the active site and the β subunit containing the diiron site. In *E. coli* the α -subunit is designated R1 and is encoded by *nrdA*. The diiron containing β subunit is encoded by *nrdB* and is designated R2 (Carlson *et al.* 1984). The diiron site within R2 is housed within a four helix bundle similar to that in the SDIMOs and is coordinated by a three glutamate (G115, G204, G238) and two histidine residues (H118, H241) as well as one aspartate residue (D84) (Nordlund and Ecklund, 1993). The diiron centre forms a stable catalytic tyrosyl radical at position Y122 which is essential for activity of the enzyme (Sjoberg *et al.* 1978) and occupies an equivalent position in the structure to C151 in sMMO (Elango *et al.* 2007). The tyrosyl radical is transferred to a cysteine within the active site of R1 via a conserved array of hydrogen bonded amino acids to produce a thiyl radical which removes the hydroxyl group from the ribonucleotide (Uhlin and Ecklund 1994; Sjoberg 1997; Eckberg *et al.* 1998; Stubbe *et al.* 2003)

1.8.2) Analysis of the radical pathway of ribonucleotide reductase using site directed mutagenesis

A number of site directed mutants have been created to closely study the radical transport from the R2 subunit to the active site. Extensive studies on mutations of Y122, W48, D237 and Y356 have identified these amino acids as being involved in the transfer of the radical from the R2 diiron site to the R1 subunit (Bollinger Jr. *et al.* 1994; Climentefa/. 1992; Sahlin *et al.* 1994; Eckberg *et al.* 1998; Krebs *et al.* 2000).

Other mutagenesis studies have focussed on the intermediates in the activation of Y122 by the diiron site. The iron ligand D84 has also been the subject of much investigation by mutagenesis. The creation of a ribonucleotide reductase R2 W48F/D84E double mutant allowed the characterization of a peroxo-diiron intermediate similar to that detected in the sMMO enzyme (Baldwin *et al.* 2001), which was followed by the self hydroxylation of residue F208. This is not seen in the wild type activity of the R2 subunit of ribonucleotide reductase where the natural reaction is the one electron oxidation of tyrosine to a tyrosyl radical. This showed that by altering the iron ligands and disrupting the electron transport chain an MMO like activity could be conferred upon the R2 subunit. The double mutant F208A/Y122F mutant created a larger hydrophobic pocket around the active site which allowed the binding of azide to the diiron site (Andersson *et al.* 1999). The azide was able to mimic the interaction of oxygen to the active site since it is able to bind the iron without oxidizing it. This allowed Nordlund and coworkers to carry out analysis on the crystal structure of this mutant and observe a carboxylate shift of the E238 iron ligand, a phenomenon also seen within the catalytic cycle of sMMO (Whittington *et al.* 2001).

1.9 Stearoyl ACP desaturase

1.9.1) Activity of steaoryl ACP-desaturase

The acyl-carrier protein (ACP) desaturases are a family of proteins which catalyse the first step in the synthesis of unsaturated fatty acids in plants. These enzymes catalyse a dehydrogenation reaction at specific locations along the fatty acid chain and insertion of a double bond in saturated fatty acids. One of the most common of these enzymes is the soluble A9-stearoyl-ACP (18:0) desaturase which catalyses the synthesis of oleoyl-ACP (18:1) from stearoyl-ACP by abstracting a hydrogen from the A9 position and inserting a double bond between C9 and C10 of this 18-carbon fatty acid chain. To carry out this reaction the enzyme uses an active site diiron centre to activate oxygen in order to carry out the abstraction of hydrogen (Lindqvist *et al.* 1996). This is another example of an enzyme that while not strictly a monooxygenase is related to sMMO and has a similar mechanism of action that has been studied using site directed mutagenesis.

1.9.2) Site directed mutagenesis of stearoyl ACP-desaturase at position

Thr199

The determination of the crystal structure for this enzyme has enabled structural comparisons which have been the basis of some site directed mutagenesis experiments. By comparing the active site to that of another related diiron containing peroxidase enzyme ruberythrin, the residue T199 was noted as possibly interacting with the diiron site and affecting the end product (Guy *et al.* 2006). This has given support to the theory that the four helix diiron protein family evolved from an ancient ancestral oxidase protein since such structural homology is seen despite a lack of sequence homology for these enzymes. The corresponding position within ruberythrin was occupied by a glutamate residue and so mutants T199D and T199E were created where the threonine sidechain was replaced by a carboxylate containing glutamate or aspartate residue. These mutants were expressed within *E.*

coli and purified before being assayed for desaturase activity using radiolabeled substrate and analysis by thin layer chromatography. The reduced (diferrous) form of the enzyme has been shown to have a slow rate of autooxidation in the absence of substrate compared to that of other diiron enzymes. Therefore the peroxide-dependent reoxidation of the reduced form of the enzyme was used as a basis for assaying peroxidase activity. Both enzymes had reduced desaturase activity compared to the wild type enzyme but the T199D had a >31-fold increase in peroxidase activity compared to the wild type enzyme.

1.9.3) Creation of chimeric desaturase proteins

Shanklin and coworkers have used the structures of a number of different ACP-desaturase enzymes as a basis for site directed mutagenesis experiments in order to study the product specificity of these enzymes. By creating chimeric proteins of the Δ^6 -16:0-ACP desaturase and the Δ^9 -18:0-ACP desaturase; a Δ^6 -16:0-ACP chimeric mutant was created which displayed Δ^6 and Δ^9 desaturase activities towards both 16:0-ACP and 18:0-ACP (Cahoon *et al.* 1997). This led to the identification of a group of 29 amino acids (residues 178 - 207 in stearyl acp desaturase corresponding to residues 226 - 256 in MmoX) which contained determinants of both chain length and double bond position specificity. The authors then used this knowledge as the basis for the rational design of a L118F/P179I Δ^9 -18:0-ACP desaturase double mutant with a 15-fold increase in specific activity towards 16:0-ACP. The creation of a triple mutant of Δ^9 -18:0-ACP desaturase designed to study the determination of regioselectivity of a Δ^4 -16:0-ACP desaturase produced a mutant which retained activity towards Δ^9 -18:0-ACP desaturation activity however the products were further metabolized to the corresponding trans-allylic alcohol and a conjugated linolenic acid isomer (Whittle *et al.* 2008). In both these studies, the alteration of the substrate binding site and in particular of a bend in the active site has led to the greatest change in regioselectivity suggesting that this structural feature is key in the regioselectivity of this enzyme.

1.10 Scope of this thesis

The mutagenesis studies described above have allowed substantial insight into the structural basis for many aspects of the activity of diiron monooxygenases and their related enzymes. These diverse previous studies have led to a number of hypotheses about the roles of specific residues in sMMO that can only reasonably be tested by site directed mutagenesis. The aim of this thesis is to use a combination of site directed and random mutagenesis to study the structural features that affect the regioselectivity and substrate access to the active site. Site directed mutagenesis will be used to probe the function of Leu110 within sMMO hydroxylase α -subunit. By selecting specific residues located within the active site of soluble methane monooxygenase and mutating them to the counterpart residues of related butane monooxygenase; the aim is to gain insight into the differences in catalytic activity between these two enzymes. The final objective of this thesis is to create a random mutant library and screen for activity against triaromatic compounds in order to understand more about the structural limitations of the soluble methane monooxygenase enzyme.

Chapter 2: Materials and Methods

2.1 Bacterial strains and growth conditions

2.1.1) Bacterial strains

The bacterial strains used in this project were *Methylosinus trichosporium* strains OB3b and the sMMO-negative strain SMDM obtained from the culture collection of Professor J.C.Murrell, University of Warwick. The commercially available competent *Escherichia coli* strains Solopack gold, XL-1 and XL-10 were supplied by Stratagene. The donor strain used for conjugation was *Escherichia coli* S17-1 (Simon *et al.* 1983)

2.1.2) Growth of bacterial cultures

E. coli strains were cultivated in LB or Nutrient broth No. 2 (Oxoid) liquid media or on agar plates (see Appendix 1). Inoculated agar plates were incubated at 37 °C overnight. Liquid cultures were incubated in flasks at 37 °C, shaking at 180 rpm overnight.

Ms. trichosporium strains were cultivated on nitrate mineral salts (NMS) medium (see Appendix 1) in Quikfit flasks, in 5 litre batch fermentor cultures and on NMS agar plates using methane as the sole carbon source. NMS agar plates were sealed in anaerobic jars containing 50% air/methane. Liquid cultures were cultivated in 250 ml Quickfit flasks with a Subaseal and 50 ml of the headspace replaced with methane. Cultures were incubated at 30 °C with methane being replaced every 3-5 days. Liquid cultures were incubated with shaking at 180 rpm. After 2-3 weeks growth, biomass was usually sufficient to produce a positive naphthalene test indicating expression of sMMO. Plates could be stored at 4 °C for more than 1 month before subculturing onto fresh NMS agar plates. Batch fermentor cultures were grown in a New Brunswick Bioflo 101 fermentor fitted with an additional rotameter to

allow simultaneous gassing with methane and air. The vessel of the fermentor had a working volume of 5 litres and contained NMS inoculated with 50-100 ml of liquid culture. The fermentor was kept at 30 °C and constantly supplied with air and methane at flow rates 750 ml min⁻¹ and 55 ml min⁻¹ respectively. The optical density was measured at 600 nm using a spectrophotometer at regular intervals to observe growth of the culture. Cells harvested from the fermentor were pelleted by centrifugation for 15 min at 12,000 x g, washed once with 25 mM MOPS (pH 7.0), 1 mM benzamidine 1 mM dithiothreitol (buffer B) and resuspended in a minimum amount of buffer B. The cell were frozen dropwise into liquid nitrogen and stored at -80 °C.

Where appropriate, antibiotics were used at the following working concentrations: ampicillin 50-100 µg ml⁻¹, streptomycin 20 µg ml⁻¹, spectinomycin 20 µg ml⁻¹ and gentamicin 5 µg ml⁻¹.

2.1.2) Growth of bacterial cultures

All chemical reagents were supplied by Sigma Aldrich and Melford Labs. Gases were supplied by BOC and Air liquide (formerly Scott gas).

2.2 General DNA methods

General methods for DNA purification, analysis and cloning with *E. coli* were performed according to Sambrook *et al.* (1989). Restriction enzymes were supplied by New England Biolabs and Promega; DNA ligase, phosphatase and T4 DNA polymerase enzymes were supplied by New England Biolabs and manufacturers' protocols were followed. For composition of all buffers used for DNA manipulation and analysis see Appendix 2. For extraction of smaller amounts of plasmid DNA (< 50 ng) the QIAprep spin miniprep kit (QIAGEN) was used following the manufacturers protocol. For larger concentrations of DNA (> 100 ng pi⁻¹) the plasmid maxi kit (QIAGEN) was used.

2.2.1) QIAprep spin plasmid miniprep protocol:

This is a modification of the alkaline lysis method of Birnboim and Doly (1979). LB medium (5 ml) plus appropriate antibiotics was inoculated with a single colony and grown overnight at 37 °C. 1.5 ml of the resulting culture was transferred to a fresh Eppendorf tube and centrifuged at maximum speed (16,100 * g) on a benchtop centrifuge for 30 s to pellet cells. The pellet was resuspended in 250 pi of P1 resuspension buffer and 250 pi of lysis buffer P2 was added. The lysate was mixed by inverting 6 times before 350 pi of neutralisation buffer N3 was added to stop lysis. The lysate was inverted again and the white precipitate containing SDS, denatured proteins and chromosomal DNA was pelleted out by centrifugation for 10 mins at maximum speed (16,100 * g) at 4 °C. The supernatant was applied to a minicolumn by centrifugation at maximum speed for 30 s at 4 °C and flow-through discarded. The column was washed by adding 0.5 ml binding buffer PB to the column, centrifuging at maximum speed and flow through discarded as above. The column was centrifuged for another minute at maximum speed to remove all traces of the PB buffer. The column was transferred to fresh Eppendorf tube and the DNA eluted by adding 30-50 pi sterile distilled water (sdFEO) or 10 mM Tris-HCl (pH8.5), allowed to

stand for 1 min and centrifuged for 1 min at 16,100 x g. The eluted DNA was then stored at -20 °C. Buffers P1, P2, N3 and PB were supplied in the Qiaprep spin miniprep kit.

2.2.2) Qiagen Maxiprep kit plasmid isolation protocol

A flask containing 500 ml of fresh LB media was inoculated with 5 ml overnight culture and incubated overnight at 37 °C, shaking at 200 rpm. The culture was centrifuged at 6,000 x g for 15 min at 4 °C and resuspended in 10 ml P1 buffer. An equal amount of P2 buffer was added; the contents of the tube were mixed by inverting 6 times and incubated for 5 mins at room temperature. The lysis was stopped by adding 10 ml pre-chilled neutralization buffer P3 and inverting to mix. The lysate was incubated on ice for 20 min and pelleted at > 20,000 x g for 30 min at 4 °C to remove the white precipitate containing SDS, denatured proteins and chromosomal DNA. The cleared lysate supernatant was centrifuged as above for a further 15 min in a fresh tube to remove any trace precipitate. A QIAGEN-tip 500 column was equilibrated by adding 10 ml equilibration buffer QBT and allowed to run through by gravity flow. The lysate was added applied to the column and the column washed twice with 30 ml buffer QC. The DNA was eluted from the column with 15 ml buffer QF and precipitated by adding 10.5 ml isopropanol at room temperature and centrifuging at > 20,000 x g for 30 min at 4 °C. The DNA pellet was washed with 5 ml 70% ethanol (v/v); air dried and resuspended in 1 ml 10 mM Tris-HCl (pH 8.5). Buffers P1, P2, P3, QBT QC and QF were all supplied in the Qiagen maxiprep kit.

To obtain pure DNA fragments for cloning and DNA sequencing, PCR fragments and digested plasmid DNA were run on a 1 % agarose gel and the desired bands excised and purified using a gel extraction kit. For DNA < 10 kb the Qiaquick gel extraction kit (Qiagen) was used, for DNA > 10 kb the GeneCleane III kit (BIO 101) was used.

2.2.3) Qiaquick gel extraction protocol

The desired DNA containing band was excised from an agarose gel using a scalpel and carefully weighed to estimate volume (1 mg = 1 μ l). The band was placed in an Eppendorf tube and 3 volumes of buffer QG were added. The sample was incubated in a heat block at 55 °C for 2-3 min till the agarose had dissolved and then 1 volume isopropanol was added. The sample was applied to a QIAquick spin column by centrifugation for 1 min at max speed in a benchtop centrifuge and the flow through discarded. The spin column was washed with 750 μ l elution buffer PE and centrifuged for a further minute to remove last traces of buffer. The DNA was eluted from the column by adding 30 -50 μ l elution buffer EB, standing for 1min and centrifuging at maximum speed for 1 min. Buffers QG and EB were supplied in the Qiaquick gel extraction kit.

2.2.4) GeneClean III Protocol

The desired band was excised from the agarose gel and weighed to estimate volume as above and 3 volumes of supplied NaI solution added. The mixture was heated at 55 °C for 5 min until the agarose had dissolved. 10 μ l of supplied glassmilk silica suspension was added to the tube and mixed by pipetting up and down. The sample was incubated at room temperature for 15 min, inverting every 2-3 min to resuspend the glassmilk. The glassmilk was pelleted by centrifugation at maximum speed for 5 s to pellet glassmilk, washed twice with the supplied NEW Wash buffer and pelleted as above. The pellet was heated at 55 °C for 2 min to remove last traces NEW Wash buffer, resuspended in 20 μ l sdH_2O , allowed to stand for 1 min then centrifuged for 30 s and the supernatant (containing the purified DNA) transferred to a fresh Eppendorf tube and stored at -20 °C.

2.2.5) Phenol/chloroform/Isoamyl alcohol extraction

An equal volume of buffer saturated phenol (Sigma) was added to the DNA-containing solution and vortexed to mix. If the total volume of the DNA-containing solution was less than 100 μ l then the solution was made up to 100 μ l with sterile distilled water (sdH₂O). The layers were separated by centrifugation at maximum speed in a benchtop centrifuge for 1 min and the upper aqueous phase removed to a separate Eppendorf tube. An equal volume of sdH₂O was added to the phenol solution and the upper aqueous phase retained as above. The aqueous phases were combined and an equal amount of CHCl₃/isoamyl alcohol (24:1 v/v) added. The sample was vortexed briefly to mix and centrifuged as above retaining the upper aqueous phase. A 0.1 volume of 3 M sodium acetate (pH 5.5) and 3 volumes ice cold ethanol were added to the aqueous phase. The solution was mixed carefully and incubated overnight at -20 °C or for 1 h at -70 °C. The sample was centrifuged at 4 °C at maximum speed using a bench top centrifuge for 30 min and the DNA pellet was washed with 50 μ l ice cold 70 % ethanol to remove excess salts. The tube was centrifuged at 4 °C at maximum speed for 15 min and the 70% ethanol was aspirated using a small pipette and discarded. The resulting DNA pellet was air dried for 15 min before being resuspended in either sdH₂O or 10 mM Tris-HCl (pH8.5) and stored at -20°C.

2.2.6) Electrophoresis of DNA

Where necessary, DNA was analysed and visualized by running on agarose gels in TAE buffer (40 mM Tris-acetate 10 mM EDTA) containing 0.5 μ g ml⁻¹ ethidium bromide run at 90-110 V for 30-50 min and viewed under a UV light. Separation of gel fragments < 500 bp was carried out using 1.5 % agarose gels (wt/vol), all other separations were carried out using 1 % agarose (wt/vol).

2.2.7) Restriction digest

Restriction digests were set up in a 50 μ l reaction volume containing DNA and the appropriate restriction enzymes (1-10 units), 1 \times enzyme buffer and 1 μ l BSA. The reaction was incubated for between 1 and 4 hours in a waterbath at the temperature recommended by the enzyme suppliers, usually 37 $^{\circ}$ C.

2.2.8) Phosphatase

The ends of digested vector DNA were de-phosphorylated using calf intestinal alkaline phosphatase (CIP) or Antarctic alkaline phosphatase (AP) (New England Biolabs) to prevent self-ligation. Digested DNA fragments were either heated to inactivate restriction enzymes and used directly or purified from a gel prior to dephosphorylation. 50 μ l reaction volumes were set up containing 1 unit (< 100 ng DNA) or 10 units (> 100 ng DNA) alkaline phosphatase and 1 \times phosphatase buffer. The reaction mix was incubated at 37 $^{\circ}$ C for 30 min. Where CIP was used the DNA was further purified by GeneClean III or Qiagen gel purification kit to remove the phosphatase. When AP was used the phosphatase was inactivated by heating at 65 $^{\circ}$ C for 5 min.

2.2.9) End filling with T4 DNA polymerase

Filling of DNA cohesive ends to create blunt ends was carried out using T4 DNA polymerase (Promega). The reaction was set up in 50 μ l volume containing < 2 μ g DNA, 1 x T4 polymerase buffer, 100 μ M dNTPS (25 μ M of each dNTP) (Invitrogen) and 5 units of T4 DNA polymerase. The reaction mix was incubated at 37 $^{\circ}$ C for 5 min and the reaction stopped by incubating at 75 $^{\circ}$ C for 10 min. T4 polymerase buffer was (10^{*}) was supplied by Promega and diluted according to the manufacturer's instructions.

2.2.10) DNA ligase

T4 DNA ligase was used to join cohesive ends of DNA. When inserting DNA into a digested plasmid vector, the ratio molar concentration of DNA was 1:1 or 3:1 (insert:vector). The reaction was carried out in a 50 μ l volume containing 1^{*} ligase buffer (containing ATP) and 1 μ l concentrated T4 ligase solution. The reaction was incubated for 60 - 90 min at 16 $^{\circ}$ C or incubated overnight at 4 $^{\circ}$ C. The enzyme was then inactivated by heating to 65 $^{\circ}$ C for 20 min. The T4 ligase buffer (10^{*}) was supplied by New England Biolabs and diluted according to the manufacturer's instructions.

2.3 Template preparation and amplification conditions for PCR

2.3.1) Culture template preparation

This is a method of extracting DNA from a culture of bacterial cells for use as a template for PCR amplification. An Eppendorf tube containing 1 - 1.5 ml liquid culture was centrifuged for 1 min at maximum speed in a benchtop centrifuge to pellet the cells. The pellet was washed once with 50 μ l sdH₂O, centrifuged for 1 min and resuspended in 30 μ l sdH₂O. The cell suspension was boiled at 100 °C for 10 min then centrifuged for 10 min at maximum speed and 1 - 5 μ l of the resulting supernatant was used as the DNA-containing template for PCR.

2.3.2) Colony template preparation

A small amount of cell biomass was removed from a colony of *E. coli* using a sterile toothpick, resuspended in 20 μ l sdH₂O and used as DNA template for PCR.

2.3.3) Genomic DNA isolation using Qiagen genomic tip kit

An Eppendorf tube containing 1 ml liquid culture (OD₆₀₀: 0.5 - 1) was centrifuged at 5000 \times *g* for 5 min to pellet cells. The pellet was resuspended in 1 ml buffer B1 by vortexing and 20 μ l lysozyme (100 mg ml⁻¹) and 45 μ l Proteinase K (20 mg ml⁻¹) added. The reaction mix was incubated at 37 °C for 30 min, 0.35 ml buffer B2 added and the mixture was incubated at 50 °C for 30 min. A genomic tip 20 column was equilibrated with 2 ml QBT buffer and allowed to flow through by gravity. The lysed cell-containing sample was added to the column and washed with 3 x 1 ml Qiagen QC buffer. The genomic DNA was eluted using 2 x 1 ml Qiagen QF buffer and precipitated by adding 1.4 ml isopropanol at room temperature and centrifuged at 8000 \times *g* for 20 min at 4 °C to pellet the DNA. The pellet was washed with 70 % Ethanol, centrifuged at 8000 \times *g* for 10 min at 4 °C and allowed to air dry for 10 min. The pellet was resuspended in 50 – 100 μ l 10 mM Tris-Cl, pH 8.5 and placed in shaker at 30 °C overnight to dissolve (or 55 °C for 1 - 2 h). Buffers B1, B2, QBT, QC

and QF were made according to the manufacturer's instructions (see Appendix). Proteinase K solution (20 mg ml⁻¹) was supplied by Qiagen.

2.3.4) Standard PCR Protocol

Taq polymerase (Invitrogen) or *Pfu* Turbo (Stratagene) proofreading polymerase was used for PCR reactions. Primer melting temperatures T_m were estimated using:

$T_m(^{\circ}\text{C}) = 2(\text{N}_a + \text{N}_t) + 4(\text{N}_g + \text{N}_c)$ where N_a , N_t , N_c and N_g are the number of adenosine, thymine, cytosine and guanine bases present respectively.

The reaction mix was incubated at 95 °C for 2 min to denature the DNA. The DNA was amplified by 30-35 cycles of: 95 °C for 30 s; ($T_m - 5$ °C) for 30 s; 72 °C for 1 min. The final amplification step was heating at 72 °C for 10 min and then the temperature held at 4 °C. For PCR reactions using colony template or culture template 35 cycles was used.

PCR Setup:

e	dNTPs (25 mM each dNTP)	0.5 pi
©	10 x buffer	5 pi
G	primer 1 (100-200 ng)	1 pi
Q	primer 2 (100-200 ng)	1 pi
G	DNA template	1 - 5 pi
©	<i>Taq</i> polymerase or <i>Pfu</i> turbo	1 pi
Q	50 mM MgCl ₂ (not added for <i>Pfu</i> Turbo)	2 pi
©	BSA (colony and culture template only)	1 pi
Q	sdH2Q	up to 50 pi

2.3.5) Four-primer overlap extension PCR

P 1

P 3

P 4

Fig. 2.1 Diagram showing the creation of site directed mutants by the four primer overlap PCR method (Ho *et al.* 1989). Primers P1 and P4 bind the external ends of the DNA sequence to be amplified. Internal primers P2 and P3 are complementary to each other and contain the desired mutation. DNA fragment AB upstream of the desired mutation is amplified using primers P1 and P2. DNA fragment CD downstream of the desired mutation is amplified using primers P3 and P4. Fragments AB and CD bind form a complete template which is amplified by primers P1 and P4.

This technique uses two internal complementary primers containing a desired mutation to create upstream and downstream DNA with complementary ends (Fig. 2.1). These bind and form the template DNA for subsequent amplification cycles. Upstream and downstream complementary DNA template fragments were amplified using standard PCR conditions as above and purified by gel extraction. The template fragments were mixed in equimolar amounts with the rest of the PCR components as above, omitting primers and polymerase. The reaction was heated to 96 °C for 2 min to allow DNA to denature and then cooled slowly to allow complementary ends to anneal. The polymerase was added, mixed and heated to 72 °C for 2 min. The external primers were added and PCR thermal cycling was continued under normal conditions for 30 cycles as above.

2.3.6) Error Prone PCR random mutagenesis

Taq polymerase was chosen for the error prone PCR technique due to its intrinsic high error rate (Tindall and Kunkel, 1988). The reaction conditions were set up below to favour low fidelity of the enzyme and incorporation of mismatches into amplification of the DNA template.

Error-prone PCR setup:

• DNA template (80ng/pl)	1pl
100 mM dCTP	0.5pl
100 mM dTTP	0.5pl
10 mM dATP	1pl
10 mM dGTP	1pl
• 10 x <i>Taq</i> polymerasebuffer	5pl
• primer 1 (100-200 ng)	1pl
• primer 2 (100-200 ng)	1pl
• <i>Taq</i> polymerase	1pl
• 50 mM MgCb	7pl
• 50 mM MnCb	0.5pl
BSA	1pl
• sdH20	up to 50pl

The reaction follows normal PCR conditions (section 2.3.4) for 30 cycles.

2.3.7) Genemorph random mutagenesis kit

Error prone PCR was also carried out using the Genemorph II random mutagenesis kit (Stratagene) with Mutazyme II polymerase enzyme. The error rate of the Mutazyme II is altered by different concentrations of target DNA. To maintain a low error rate 500-1000 ng target DNA was used with 1 x Mutazyme II buffer, dNTP's, primers and polymerase as in the *Pfu* turbo standard PCR setup (omitting additional MgCl₂) and amplified by 30 PCR cycles as above.

2.4 Plasmids used in this study:

Plasmid		Reference
pTJS140	Broad-host-range cloning vector, 7.5 kb; Mob, Apr Spr Smr <i>lacZ'</i>	Smith <i>et al.</i> 2002
pTJS175	Methanotroph expression vector, pTJS140 containing 10.1 kb insert including the sMMO operon. Apr Spr Smr	Smith <i>et al.</i> 2002
pTJS176	Cloning vector containing 10.1 kb <i>KpnI</i> insert including the sMMO operon Apr.	Smith <i>et al.</i> 2002
pTN1	pTJS140 with <i>A/cI</i> site and one BamHI site removed, Apr Spr Smr	This study
pTN2	pTJS140 with all BamHI and <i>NdeI</i> sites removed, Apr Spr Smr	This study
pT2ML	New methanotroph expression vector, pTN2 containing 9.6 kb <i>kpnI</i> insert including sMMO operon with 500 bp deletion of <i>mmoX</i> gene, Apr Spr Smr	This study

2.4.1) Blue/White selection

Cloning experiments using plasmids containing a unique restriction site within a functional *lacZ* gene were screened for successful ligations by blue/white selection. The *lacZ'* gene allows expression of p-galactosidase within an appropriate host strain. In the presence of the chromogenic substrate 5-bromo-4-chloro-3-indolyl-p-D-galactopyranoside (X-gal) and induced by isopropyl-1-thio-p-D-galactopyranoside (IPTG), p-galactosidase expressing colonies form the coloured product indigo. Successful cloning into the *lacZ* gene results in no p-galactosidase being produced and colonies are white in colour. The transformants were plated on LB agar containing 80 µg ml⁻¹ X-gal and 20 mM IPTG.

2.5 Preparation of *E. coli* competent cells

2.5.1) CaCl₂ cell preparation method

This method was adapted from that of Sambrook *et al.* (1989). LB (2 ml) was inoculated with a fresh single colony from an *E. coli* culture plate and incubated overnight at 37 °C. The culture was diluted 50 fold with LB + MgCl₂ [10 mM], MgSO₄ [10 mM] (up to 100 ml final volume) and incubated at 37 °C with shaking at 200 rpm until the culture reached an OD₆₀₀ of 0.5 - 0.6 (mid log phase). The cells were pelleted by centrifugation at 5000 x *g* for 10 min (4 °C), washed in 25 ml ice cold filter sterilized 0.1 M MgCl₂ and pelleted by centrifugation as above. The cells were washed in 5 ml filter sterilized CaCl₂, pelleted again and resuspended in 5 ml 0.1 M MOPS, 50 mM CaCl₂, 20 % glycerol. The cells were drop frozen in 200 μ l aliquots in liquid nitrogen and stored at -80 °C. Using this method cells can be stored for several years.

2.5.2) Transformation of CaCl₂ competent cells

An aliquot of 200 μ l of competent cells was thawed on ice and 1-5 μ l DNA was added. The cells were incubated on ice for 30 min then heat shocked in a waterbath at 42 °C for 90 s. The cells were incubated on ice for a further 2 min and LB or SOC media was added up to 1 ml. The cells were incubated at 37 °C with shaking at 200 rpm for 1 h and then plated on LB plates containing the appropriate antibiotic. When using commercially available competent cells such as Solopack gold ultracompetent cells (Stratagene) the suppliers' transformation protocols were used.

2.5.3) Preparation of electrocompetent cells

LB (5 ml) was inoculated with a fresh single colony of *E. coli* and incubated at 37 °C overnight. The culture was diluted 100-fold up to 500 ml with fresh LB medium and incubated at 37 °C with shaking at 220 rpm until the culture had reached an OD₆₀₀ of approximately 0.5-0.7. The culture was incubated on ice for 20 min, transferred to a pre chilled centrifuge bottle and centrifuged at 4000 x g for 15 min at 4 °C. The pellet was washed in 500 ml ice-cold 10 % (vol/vol) glycerol and pelleted as above. The pellet was further washed with 250 ml ice-cold 10 % glycerol, centrifuged as above and washed with 20 ml ice-cold 10 % glycerol. The cells were centrifuged again and the pellet resuspended in 1 ml 10 % glycerol and drop frozen in 50 µl aliquots in liquid nitrogen.

2.5.4) Electroporation of *E.coli*

All cells, DNA and electroporation cuvettes were kept on ice at all times. A 50 µl aliquot of electrocompetent *E. coli* was thawed on ice and 100 - 300 ng DNA added in < 5 µl volume. The cells and DNA were transferred to a Bio-Rad electroporation cuvette (0.1 cm gap width) and electroporated using a Bio-Rad Micropulser using program Ec 1 (1.8 kV). LB or SOC medium was added up to 1 ml, and then the cell suspension was transferred to an Eppendorf tube and incubated at 37 °C, with shaking at 220 rpm for 60 min. 100 µl of the cell suspension were spread on LB-agar plates containing the appropriate antibiotic and incubated at 37 °C overnight.

2.5.5) Hanahan transformation method

This method was adapted from that of Hanahan (1983). SOB medium (10 ml) was inoculated with a fresh single colony of *E. coli* and incubated at 37°C shaking at 180 rpm till an optical density at 550 nm (OD₅₅₀) of between 0.5 and 0.6 was reached. The culture was incubated on ice for 10 min then pelleted by centrifugation at 1000 x g (4°C) for 12 min. The pellet was resuspended in 3 ml of ice-cold TFB Buffer and incubated on ice for 10 min. The cell suspension was pelleted again by centrifugation at 1000 x g (4°C) for 12 min and resuspended in 800 µl ice cold TFB. 28 µl of DnD Solution was added and the cell suspension incubated on ice for 10 min. An additional 28 µl of DnD Solution was added and the cell suspension was incubated on ice for a further 15 min. A 200 µl aliquot of cell suspension was transferred to a pre-chilled 15 ml Falcon tube and 10 µl vector DNA (up to 100ng) was added. The cell suspension was incubated on ice for 20 min, heat shocked at 42°C for 90 s and incubated on ice for a further 2 min. SOC medium (800 µl) was added before incubation at 37°C for 1 h. LB broth containing ampicillin [50 µg/ml] was added up to 10 ml and culture was incubated overnight at 37°C. This overnight culture was then used for conjugation with *Ms. trichosporium* SMDM (see section 2.6.1)

2.6 Introduction of DNA into *Ms. trichosporium* by conjugation.

For expression of recombinant sMMO within a homologous host the expression vector was transformed into the conjugative *E. coli* strain S17-1 (Simon *et al.* 1983) and transferred to a mutant sMMO negative methanotroph recipient, SMDM (Borodina *et al.* 2006). The *Ms. trichosporium* SMDM strain has all the sMMO operon except 3' portion of *mmoC* deleted and replaced with a GentRcassette.

2.6.1) Conjugation protocol

A 10 ml overnight culture of *E. coli* S17-1 containing the desired plasmid was mixed with 50 ml *Ms. trichosporium* SMDM (OD₆₀₀ ~0.5) and pelleted by centrifugation at 5000 x *g* for 10 min. The cells were resuspended in 50 ml sterile NMS and collected onto a sterile nitrocellulose filter (0.2 µm pore size). The filter paper was transferred to NMS agar plates containing 0.02 % proteose peptone (w/v) and incubated at 30 °C for 24 h in a sealed container with 50 % air/methane. The filter paper was briefly vortexed with 10 ml NMS to resuspend the cells and centrifuged as above. The cells were resuspended in 1 ml NMS, plated in 100 µl aliquots onto NMS + streptomycin [20 µg ml⁻¹] and incubated at 30 °C in 50 % air/methane for 1.5-2 weeks until methanotroph colonies were clearly visible. Individual colonies were subcultured onto fresh NMS agar containing gentamicin, streptomycin, spectinomycin and nalidixic acid [20 µg ml⁻¹] until pure colonies free of *E. coli* growth were seen. Nalidixic acid was used because it inhibits the growth of the *E. coli*, gentamicin was used to maintain the antibiotic cassette within the SMDM chromosome, and streptomycin and spectinomycin were used to maintain the expression vector. Pure methanotroph colonies free of *E. coli* were assessed by plating onto nutrient agar.

2.7 Protein quantification and visualisation

2.7.1) Protein estimation via the Bradford assay

Protein standards were prepared by adding varying amounts of BSA to 1 ml MOPS [25 mM] (pH 7.0). 100 μ l of protein sample was added to 3 ml Bradford reagent at room temperature and incubated for 5 min. The increase in absorbance relative to a no-protein control was measured at 595 nm using a Jenway 6715 UV/Vis spectrophotometer and protein concentration estimated from comparison against a protein standard curve. When the $A_{595} > 1$, protein samples were diluted 1:10 or 1:20 to give reliable readings.

2.7.2) SDS PAGE

Composition of all gels buffers and solutions can be found in Appendix 3. A 10 ml 12 % acrylamide resolving gel mixture was prepared adding ammonium persulfate (APS) solution and tetramethylethylenediamine (TEMED) last and overlaying with 700 μ l ethanol or isopropanol. The gel was allowed to set for 30 min before the ethanol was washed off. The 5 % acrylamide stacking gel mixture was overlaid with comb inserted and allowed to set. An equal amount of sample buffer was added to each protein sample and boiled for 10 min. The samples were loaded onto the gel and run at 130 V for 1 h or until the dye front had reached the bottom of the gel. The gel was submerged in 0.1 % Coomassie stain solution, slowly shaking at room temperature for 40 min. The stain was washed off and gel submerged in destain solution (30 % methanol, 10 % glacial acetic acid) for 40 min to reveal protein bands.

2.8 Cell preparation and substrate oxidation assays

2.8.1) Whole cell assays

Drop frozen cells were resuspended in 25 mM MOPS buffer (pH 7.0) to an OD₆₀₀: 5-10. Sodium formate was added [5 mM] to provide an excess of reducing equivalents for the sMMO. Analysis of aromatic substrates was carried out using whole cells as these compounds do not serve as a substrate for the particulate methane monooxygenase. Aliphatic compounds can serve as a substrate for pMMO and so were assayed using cell free extract where the pMMO-containing cell membranes have been removed (see below).

2.8.2) Soluble extract preparation

Drop frozen cells were washed once with 25 mM MOPS buffer + 1 mM benzamidine, 1 mM dithiothreitol (DTT), 1 mM DNase and resuspended in a minimum volume of the same buffer. Once cells were thawed they were kept on ice at all times. The cells were broken either by 3 passages through a French cell press (Thermo) at 20,000 mPa or for smaller amounts (< 5 ml) using a Sonics vibracell VOX 750 sonicator on ice using 10 x 30 s bursts at 40% amplitude with 30 s on ice between each burst to allow cooling. The cells were centrifuged in pre-chilled Oakenridge tubes at 10,000 * g for 5 min to remove the majority of the cell debris. The supernatant was then transferred to ultracentrifuge tubes and centrifuged for 90 min at 50,000 x g at 4 °C. The soluble extract was aliquoted into pre chilled Eppendorf tubes before being drop frozen in liquid nitrogen and stored at -80 °C. For soluble extract assays, aliquots of soluble extract were thawed and used immediately.

2.8.3) Colorimetric naphthalene oxidation assay

The naphthalene oxidation assay was carried out in cell suspension and on plates. A few crystals of naphthalene were added either directly to the reaction mixture or on the lid of inverted freshly grown plates. The cells were incubated for 1 h at 30 °C and naphthol products visualized by adding tetrazotized o-dianisidine (TOD) reagent solution [0.5 mg ml⁻¹] which forms a pink - purple diazo dye complex upon contact with the hydroxylated products. For solid media assays the whole plate was flooded with TOD reagent solution and for liquid cultures 100 µl TOD reagent solution was added

2.8.4) Semiquantitative colorimetric naphthalene oxidation assay

Based on the method described by Wood and co-workers (Canada *et al.* 2002), 5 ml cell suspension was prepared as above. The cells were equilibrated in a 30 °C water bath for 2 min before addition of a crystal of naphthalene (~5 mg). Cells were incubated for 1 h at 30 °C shaking at 180 rpm. The reaction was stopped by transferring to ice and incubating for 5 min. Cell debris was removed by centrifugation for 1 min at 17,000 x g (4 °C) and 1 ml supernatant was transferred to a 1 ml cuvette. 50 µl 1 % TOD reagent was added and mixed by pipetting up and down. The reaction was halted after 15 s by addition of 120 µl glacial acetic acid to quench the dye complex formation and stabilize the colour. Quantification of naphthol formation was carried out by measuring the increase in absorbance at 540 nm using a Jenway 6715 UVA/vis spectrophotometer and comparing against a product standard curve of known 1-naphthol concentrations.

2.8.5) Product distribution of naphthols

5 ml assays were set up as above using naphthalene as the substrate and incubated for up to 48 h. Oxidation products were extracted into 1 ml ether and evaporated to < 50 pi under a laminar flow hood. 1 pi samples were analysed via GC-MS using a 5890 GC (Hewlett Packard) coupled to a Trio-1 mass spectrometer. The GC was fitted with a Hewlett Packard HP-5 column with a (5 % phenyl) methyl polysiloxane coating (50 m * 0.32 mm; coating thickness 0.25 pm) and operated with a carrier gas (nitrogen) flow rate of 1.5 ml min⁻¹. The separations were carried out without split and the column temperature was ramped from 80 °C to 126 °C at 10 °C min⁻¹, followed by 126 °C to 129 °C at 0.1 °C min⁻¹ and then 129 °C to 250 °C at 10 °C min⁻¹. Samples (2.5 pi) were also analysed via a Shimadzu GC2010 coupled to a flame ionisation detector. The GC was fitted with a Restek RTX-5 column with a 5 % diphenyl/95 % dimethyl polysiloxane coating (50 m x 0.32 mm; coating thickness 0.25 pm) and operated with a carrier gas (nitrogen) flow rate of 1.5 ml min⁻¹. The temperature was ramped from 100 - 200 °C at 10 °C min⁻¹, held at 200 °C for 1 min then ramped to 250 °C at 5 °C min⁻¹ and held at 250 °C for 15 min. The carrier gas flow rate was 30 ml min⁻¹ and the split ratio was 30:1.

2.8.6) Biphenyl oxidation assay

A 5 ml cell suspension was equilibrated for 1 min in a 30 °C water bath. A few crystals of biphenyl were added and the cells incubated at 30 °C shaking at 180 rpm for 30 min. Cells were transferred onto ice for 5 min to quench the reaction before extraction into 1 ml diethyl ether and evaporation to < 50 pi. The products of biphenyl oxidation were characterised using a Shimadzu GC2010 and RTX-5 column as above. The column temperature was ramped from 100 °C to 200 °C at 2°C min⁻¹ and held for 1 min. The column temperature was then increased to 250 °C at a rate of 15°C min⁻¹ and held for 15min. The carrier gas flow was 30 ml min⁻¹ and the split ratio was 30:1

2.8.7) Mesitylene oxidation assay

A 5 ml cell suspension containing sodium formate [5 mM] was incubated with 5 μ l mesitylene at 30 °C for between 1- 72 hours shaking at 180 rpm. An internal standard of 2 pmoles m-cresol was added and the hydroxylated products were extracted into 1 ml diethyl ether. The ether was then concentrated to <50 μ l by evaporation under a laminar flow hood and analysed by GC-MS via injection onto a 5890 Series II gas chromatograph (Hewlett Packard) coupled to 5917A mass selective detector (Hewlett Packard). The GC was fitted with a Hewlett Packard HP-5ms column with a (5 % phenyl) methyl polysiloxane coating (30 m x 0.32 mm; coating thickness 0.25 μ m) and operated with a carrier gas (helium) flow rate of 1 ml min⁻¹. The separations were carried out with a split ratio of 30:1 and the column temperature was held for 5 min at 50 °C then ramped from 50 °C to 118 °C at 10 °C min⁻¹, followed by 118 °C to 125 °C at 1 °C min⁻¹ and then 125 °C to 280 °C at 50 °C min⁻¹ and held for 2 min. The injection temperature was 260 °C and the detector temperature was 300 °C. The products of mesitylene oxidation were detected by monitoring the total ion count between 50 - 550 *m/z*.

2.8.8) Toluene oxidation assays

The whole cell suspensions were prepared as above. 5 ml was added to a 30 ml universal tube with sodium formate [5 mM] and equilibrated in a 30 °C water bath for 1 min. 5 μ l toluene was added and the tubes were incubated at 30 °C for up to 48 h shaking at 180 rpm. When an internal standard was required 2-phenyl ethanol was added and the hydroxylated products were extracted into 1 ml diethyl ether. The ether was then concentrated to < 50 μ l by evaporation under a laminar flow hood.

For GC-MS analysis a 1 μ l sample was injected onto a 5890 series II gas chromatograph coupled to a 5971A mass selective detector (Hewlett Packard) using the same parameters as for the analysis of mesitylene by GC-MS above. The products of toluene oxidation were detected by selected ion monitoring at 39.0, 50.0, 51.0, 53.0, 77.0, 78.0, 79.0, 80.0, 89.0, 90.0, 91.0, 107.0, 108.0, and 109.0 *m/z*. These represent the main mass ions present in the mass spectra of toluene oxidation products.

The products of toluene oxidation were also characterised by means of GC, using a 6890 GC apparatus (Hewlett Packard) fitted with a Stabilwax capillary column with a Carbowax PEG coating (50 m x 0.32 mm; coating thickness, 1 μ m) and coupled to a flame ionisation detector. The column temperature at the beginning of the separation was held at 100 °C for 5 min, whereafter it was ramped to 180 °C at 2 °C min⁻¹, followed by 15 min at 180 °C. The flow rate of carrier gas (nitrogen) was 1.5 ml min⁻¹ and the split ratio was 10:1. The injector temperature was 150 °C and the detector temperature was 220 °C.

For determination of specific activity with toluene as substrate a 2 ml cell suspension was incubated with 1 μ l toluene in a water bath for 5 min. The reaction was stopped by placing tubes on ice for 5 min. An internal standard of 2-phenylethanol was added as before extraction into ether and evaporation to < 50 μ l as above. The rate of formation of oxidation products was measured using a Shimadzu GC2010 connected

to a RTX-5 column (Restek) with flame ionisation detector. The temperature was ramped from 150 °C to 180 °C at 2 °C min⁻¹. The temperature increased to 220 °C at 200 °C min⁻¹ and was held for 15 min. The carrier gas flow rate was 30 ml min⁻¹ and the split ratio was 20:1. The injector temperature was 150 °C and the detector temperature was 250 °C.

The K_{m} and V_{max} data were measured by adding varying amounts of toluene saturated water with 750 μl cell suspension making up to 1 ml with 25 mM MOPS buffer (pH 7.0) and running on a Shimadzu GC2010 using conditions above. 2 ml toluene was vortexed for 1 min with 5 ml sdH₂O and 2 ml of the aqueous layer was removed to separate Eppendorf tubes and centrifuged at 17,000 x g for 1 min and used immediately as toluene saturated water. The amount of toluene dissolved in the water was measured by direct injection of 2.5 μl toluene saturated water onto a the GC column using the above conditions.

2.8.9) Ethyl benzene oxidation assay

The whole cell suspensions were prepared as described above. 5 ml cell suspension containing sodium formate [5mM] added to a 30 ml universal tube and equilibrated for 1 min at 30 °C. Ethyl benzene was added (50 μl) and the tubes were incubated at 30 °C for up to 48 h shaking at 180 rpm. The hydroxylated products were extracted into 1 ml diethyl ether. The ether was then concentrated to < 50 μl by evaporation under a laminar flow hood. The oxidation products were analysed via GC-MS using a 5890 GC (Hewlett Packard) coupled to a Trio-1 mass spectrometer. Here, the GC was fitted with a Hewlett Packard HP-5 column with a (5 % phenyl) methyl polysiloxane coating (50 m x 0.32 mm; coating thickness 0.25 μm) and operated with a carrier gas (nitrogen) flow rate of 1.5 ml min⁻¹. The split ratio was 30:1 and the column temperature was ramped from 80 °C to 250 °C at 4 °C min⁻¹, followed by 1 min at 250 °C. The injector temperature was 180 °C and the detector temperature was 250 °C.

2.8.10) Butane oxidation assay

Soluble extract was prepared as described above, 1.9 ml was sealed in 8 ml Teflon sealed GC vials (Agilent) and 3 ml butane added by syringe. The cells were equilibrated at 30 °C for 30 s and the reaction started by adding 100 μ l 100 mM NADH (ethanol free) prepared as described in Appendix 4. Cells were incubated for time intervals ranging between 1 and 30 min and reaction stopped by placing immediately on ice. The hydroxylated products were extracted into 500 μ l diethyl ether and concentrated by evaporation to < 50 μ l as above. The rate of formation of butane oxidation products was measured using a Shimadzu GC2010 connected to a RTX-5 column with flame ionisation detector. The temperature was held at 50 °C for 19 min then ramped to 250°C at 250°C min⁻¹ and was held for 25 min. The carrier gas flow rate was 12.6 ml min⁻¹ and the split ratio was 10:1. The injector temperature was 150 °C and the detector temperature was 250 °C.

2.8.11) Pentane oxidation assay

Soluble extract was prepared as described above, 1.9 ml was sealed in 8 ml Teflon sealed GC vials (Agilent) and 1 μ l pentane added. The cells were equilibrated at 30 °C for 30 s and the reaction started by adding 100 μ l 100 mM NADH (ethanol free). Cells were incubated for between 5 and 20 min and reaction stopped by placing immediately on ice. An internal standard of 2-phenylethanol was added and the oxidation products were extracted into 500 μ l diethyl ether and evaporated to < 50 μ l as above. The rate of formation of pentane oxidation products was measured using a Shimadzu GC2010 connected to a RTX-5 column with flame ionisation detector. The column temperature was held at 70°C for 25 min then ramped to 250 °C at 100 °C min⁻¹ and was held for 5 min. The carrier gas flow rate was 12.1 ml min⁻¹ and the split ratio was 30:1. The injector temperature was 150 °C and the detector temperature was 250 °C.

2.8.12) Hexane oxidation assay

Soluble extract was prepared as described above, 1.9 ml was sealed in 8 ml Teflon sealed GC vials (Agilent) and 1 μ l hexane added. The cells were equilibrated at 30 °C for 30 s and the reaction started by adding 100 μ l 100 mM NADH (ethanol free). Cells were incubated for between 5 and 20 min and reaction stopped by placing immediately on ice. An internal standard of 2-phenylethanol was added and the oxidation products were extracted into 500 μ l diethyl ether and evaporated to < 50 μ l as above. The rate of formation of hexane oxidation products was measured using a Shimadzu GC2010 connected to a RTX-5 column with flame ionisation detector using the same GC settings as above for the pentane oxidation assay (2.8.11). The temperature was held at 100 °C for 20 min then ramped to 250 °C at 100 °C min⁻¹ and was held for 5 min. The carrier gas flow rate was 27 ml min⁻¹ and the split ratio was 30:1. The injector temperature was 150 °C and the detector temperature was 250 °C.

2.9 Data analysis

2.9.1) Statistical analysis

Comparison of OB3b wild-type and sMMO mutant data was carried out using a two-tailed student T-Test. Data was seen as having a statistical significant difference if $P < 0.05$. All statistical analysis was carried out using Sigmaplot data analysis software (Systat software inc.)

Chapter 3: Analysis of the role of Leu 110

3.1 Introduction

3.1.1) A proposed gating role for Leu 110

The crystal structures of the sMMO hydroxylase components from *Methylosinus trichosporium* (OB3b) and *Methylococcus capsulatus* (Bath) indicate that the active site is deeply buried in the protein and hence the substrates and products must travel a substantial distance between the external solvent and the active centre. The crystal structures indicate that a chain of buried solvent-filled cavities that communicate between the active site and the solvent may be the route of substrate entry and product egress (Elango *et al.* 1997; Rosenzweig *et al.* 1997). At the end of this proposed substrate channel between the so-called cavity two and the active site lies the residue Leu 110 (Fig. 3.1). The oxidized and reduced crystal forms of the hydroxylase differ in the conformation of Leu 110 leading to this residue being proposed by Rosenzweig and co-workers as a gating residue (the "leucine gate"), regulating access of the substrate to the active site (Rosenzweig *et al.* 1997). In the crystal structure of oxidized hydroxylase protein, Leu 110 blocks the pathway between cavity two and the active site. However in the reduced form, a 2.6-Å diameter channel opens between the two cavities. It has been hypothesised that a larger conformational change, such as may be caused by interaction with the other components of the sMMO complex, could open this 'leucine gate' further, to allow passage of substrates and products.

Fig. 3.1) The active site of sMMO hydroxylase showing proposed substrate entry route from cavity 2 (blue) to cavity 1 (tan) adjacent to the active site. The binuclear iron centre is highlighted in orange and the proposed gating residue Leu 110 is highlighted in green. Figure was constructed using X-ray crystallographic data (PDB accession code 1MTY).

3.2 Comparison of Leu 110 with equivalent residues of related monooxygenases.

3.2.1) Mutagenesis of Val 106 from toluene ortho-monooxygenase

As mentioned in chapter 1, mutagenesis studies of homologous monooxygenases whose natural substrates are monoaromatic hydrocarbons have indicated that the equivalent position to Leu 110 is indeed important in the interaction between these enzymes and their substrates (Fig. 3.2). In a directed evolution study of toluene *ortho*-monooxygenase (TOM) of *Burkholderia cepacia* G4, a Val to Ala mutation at position 106, equivalent to Leu 110 in sMMO, gave increased naphthalene and phenanthrene oxidation but no change in regioselectivity with naphthalene (Canada *et al.* 2002). Both mutant and wild-type gave predominantly 1-naphthol as the product. This was consistent with the proposed gating role of this residue, i.e. the mutation affected the rate of oxidation of large substrates but did not greatly impact on regioselectivity.

3.2.2) Mutagenesis studies of Leu 100 from toluene 4-monooxygenase

A number of mutagenesis studies at the equivalent position Leu 100 of toluene-4-monooxygenase (T4MO) in *Pseudomonas mendocina* KR1 have also indicated that this residue may play an important role in access of substrate to the active site. A reduction in rate of indole formation from indole by the Ala, Cys and Val mutants of the equivalent Leu 100 in T4MO back up this hypothesis (McClay *et al.* 2005). Site directed mutagenesis studies carried out on this enzyme also identified that the L100L mutant showed a two-fold increase in the rate of oxidation of 2-methoxyphenol with only a modest loss of regiospecificity, however the mutant (like the wild-type) gave 3-methoxyresorcinol (3,5-dihydroxyanisole) as the major product. Similar results were observed with toluene as the substrate, where an increase in rate of

toluene oxidation was recorded but no change in regioselectivity (Tao *et al.* 2004). A further site directed mutagenesis study of this residue has highlighted a number of mutants with both altered rates of oxidation and enantioselectivity with aromatic sulphides as the substrate. The I100G mutant showed a 1.7 fold increase in the rate of oxidation of methylphenylsulfide and enantiomeric excess increased from 86% to 98% (pro S). Similarly the rate of oxidation of methyl *para*-tolyl sulphide by this mutant rose 11-fold compared to the wild type and an increase in enantiomeric excess from 41% pro-R to 77% pro-S was observed. These results coupled with *in-silico* homology modelling of T4MO and toluene *ortho*-monooxygenase have led to the I100 residue in T4MO being implicated not only in controlling access to the active site but also influencing the orientation of substrate within the active site (Feingersch *et al.* 2008).

3.2.3) Mutagenesis studies of lie 100 from toluene/*o*-xylene monooxygenase

Mutation studies of the equivalent residue in toluene/*o*-xylene monooxygenase of *Pseudomonas* sp strain OX1 (ToMO) have shown that the Ile 100 residue of this enzyme has an important role in both rate and regioselectivity of aromatic substrate oxidation. The oxidation of toluene and naphthalene by an I100A mutant of ToMO showed reduced oxidation rates and relaxed regioselectivity with both these substrates (Notomista *et al.* 2009). A change in the predominant product of phenol hydroxylation from catechol to hydroquinone (i.e. a shift in regioselectivity from the 2- to 4-position) in the I100Q mutant of ToMO also indicates that the equivalent site to Leu 110 may have a role in determining regioselectivity as well as substrate access (Vardar and Wood, 2004).

3.2.4) Comparison to butane monooxygenase

The equivalent residue to Leu 110 of sMMO is also a Leucine, Leu 107 in BMO of *Thauera butanivorans* (formerly *Pseudomonas butanovora*). Results from mutagenesis studies of the nearby Gly 113 have shown an important role for this residue in determining regioselectivity of this enzyme in the oxidation of short chain alkanes and chloroethylene derivatives which could be explained by a conformational change within the active site (Halsey *et al.* 2006).

mnoX	97	PRWGETMKVISNFLEVGEYNAIAASAMLWDSATAAEQKNGYLAQVLDEIR	146
touA	87	PGWVSTMQLHFGAIALEEYAASTAEARMARFAKAPGNRMATFGMMDENR	136
tmoA	87	PGWISTLKSHYGAIIVGEYAAVTGEGRMARFSKAPGNRMATFGMMDELRL	136

Fig. 3.2) Partial protein sequence alignment of hydroxylase α -subunit of sMMO (mnoX), toluene/*o*-xylene monooxygenase (touA), toluene 4-monooxygenase (tmoA), butane monooxygenase (bmoX) and toluene *ortho*-monooxygenase (tomA3). Leu 110 (mnoX) and analogous residues are highlighted yellow.

3.3 Site directed mutagenesis studies of Leu 110 in sMMO

In order to probe the role of Leu 110 in sMMO, a number of mutants with varying sized side chains were created by Dr Elena Borodina (University of Warwick) to study the effects this has on entry of larger substrates into the active site. Several mutants at position 110 in the α -subunit of the hydroxylase have been analysed using bulky aromatic substrates in order to evaluate the role of this residue in the sMMO system and to compare its function to that of the equivalent residues in the aromatic monooxygenases. These mutants have also been screened for triaromatic oxidation activity using the triaromatic compounds phenanthrene and anthracene, which are not oxidized by the wild type enzyme (Jenkins *et al.* 1994). Since wild type sMMO can accommodate the large diaromatic compound naphthalene, it was hypothesised that the mutations of Leu 110 to smaller residues Cys and Gly may allow access of these larger substrates to the active site. Conversely mutations to arginine and tyrosine at this position might reduce the substrate range of the enzyme.

3.3.1) Mutagenesis of leucine gate residue produced mutants that gave an unusual naphthalene oxidation test result

A number of mutants of the proposed gating residue Leu 110 were created with varying sized side chains, in order to probe how the size of the amino acid at this position affected the functionality of the enzyme. Four mutants L110G, L110C, L110R and L110Y were created, confirmed by DNA sequencing and expressed in the *Ms. trichosporium* SMDM homologous expression system as described in the Materials and Methods chapter using pTJS175 as the expression vector. When the four mutant strains were grown in liquid culture at a low copper-to-biomass ratio to induce expression of sMMO, all four gave positive naphthalene tests. This confirmed that all the mutant clones produced mutant enzymes that were active with naphthalene as the substrate. Observations of the purple diazo dye product formed with a positive naphthalene test differed between the four mutants. The L110G and

L110C mutants gave a purple product that was stable for over 10 min, similar to results observed for wild type sMMO. However the colour formed by the L110R and L110Y mutants was stable for less than 1 min and appeared pink compared to the purple seen with the wild-type.



Fig 3.3) Products of naphthalene oxidation by Leu 110 mutants showing percentage product distribution. Data are derived from three separate experiments from a single batch of drop frozen cells for each mutant and are shown in the form mean \pm SD

Fig. 3.4) GCMS trace from wild type sMMO naphthalene oxidation assay showing oxidation products 1-naphthol and 2-naphthol. Identity of peaks was confirmed by comparing retention times against authentic standards (not shown)

3.3.2) The L110R and L110Y mutants of sMMO show inverted regioselectivity with naphthalene compared to the wild-type

It was reasoned that the qualitative difference in stability of the naphthalene test colour among the mutant and wild-type enzymes was most likely due to an alteration in the position(s) of hydroxylation in the products of naphthalene oxidation by the L110R and L110Y mutants. GC-MS analysis confirmed that there were significant alterations in the distribution of mono-hydroxylated products from the mutant enzymes. Both the wild type enzyme and the L110C mutant gave a slight excess of 2-naphthol over 1-naphthol. This regioselectivity was reversed with the other three mutants, with a significantly smaller percentage of 2-naphthol being detected with the bulkier mutants L110R and L110Y ($P=0.02$ and 0.00003 respectively) (Figs 3.3, 3.4). No novel oxidation products such as dihydroxylated products were detected with any of the mutants. A separate experiment using 10 pM solutions of the two isomers of naphthol and the same concentration of tetrazotised o-dianisidine as used in the naphthalene test for sMMO activity revealed that the diazo dye produced by 1-naphthol forms more quickly and decays more quickly than that produced by 2-naphthol (Fig. 3.5). Thus the difference in regioselectivity of the mutants accounts for the difference in coloured product formation observed in their naphthalene tests.

OD 530 of 1 and 2 naphthol standards upon addition of Diazo reagent

1-naphthol
— 2naphthol

Fig 3.5) Change in absorbance of $10 \text{ } \mu\text{M}$ 1-naphthol and 2-naphthol solutions at 530 nm over a 20 min period. Data are derived from three separate experiments and are shown in the form mean + SD

3.3.3) The L110 mutants showed a relaxed regioselectivity and generated novel products with substituted monoaromatic substrates and biphenyl

Oxidation assays with a number of aromatic substrates were carried out over a 48 h period and analysed using GC and GC-MS as described in the Materials and Methods chapter. With the monoaromatic substrate toluene, the wild-type sMMO exhibits a mixture of side-chain hydroxylation and ring hydroxylation at the *p*-position, with ring hydroxylation predominating. When Leu 110 was mutated to the larger arginine and tyrosine residues, ring hydroxylation at the *p*-position predominated (as with wild type sMMO) with *p*-cresol being detected as the major oxidation product. However when Leu 110 was replaced by the smaller glycine and cysteine residues a shift in regioselectivity towards side-chain oxidation was observed with benzyl alcohol being detected as the major oxidation product. All the mutants at position 110 showed relaxed regioselectivity (Table 3.1), with the appearance of significant amounts of *m*-cresol, which is not seen with the wild-type. The activity of all the mutants was less than that of the wild type enzyme.

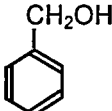
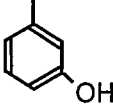
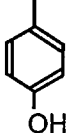
Enzyme	Products (molar %)			Molar ratio aromatic: benzylic hydroxylation	Relative total activity (%) ^a
	Benzyl alcohol 	<i>m</i> -cresol 	<i>p</i> -cresol 		
Wild-type	36.5 ± 8.7 ^b	0.0	63.5 ± 8.7	1.7	100
L110G	53.7 ± 12.5	14.6 ± 6.7	31.7 ± 9.7	0.86	12
L110C	59.4 ± 12.1	11.2 ± 7.7	29.4 ± 5.4	0.68	7.4
L110Y	34.9 ± 8.2	17.8 ± 7.4	47.3 ± 0.8	1.9	2.8
L110R	28.0 ± 6.5	14.0 ± 3.1	58.0 ± 9.7	2.6	2.5

Table 3.1: Products of toluene oxidation by Leu 110 mutants showing percentage product distribution, relative total activity and ring:side chain hydroxylation ratio. ^a Relative total activities with toluene as the substrate, which were corrected for differences in culture OD₆₀₀, are given as percentages of the increase in total product concentration with wild-type *Ms. trichosporium* OB3b, which was 12 μM h⁻¹. ^b Data are derived from three separate experiments from a single batch of drop frozen cells for each mutant and are shown in the form mean ± SD

When ethylbenzene was the substrate, the wild type enzyme showed predominantly side chain hydroxylation with 1-phenylethanol being the major oxidation product. All the mutants showed a very large shift from sidechain to ring hydroxylation and at least one new product (2-ethylphenol) was observed with each mutant (Table 3.2, Fig. 3.6). In these experiments 3-ethylphenol and 4-ethylphenol were not resolved and so it is not clear whether the product 3-ethylphenol was produced. However the use of single ion recognition to scan for the mass ion 122 (the mass of hydroxylated ethyl benzene) showed a shoulder peak with the arginine mutant which correlated to the retention time of a standard of 3-ethylphenol suggesting this as another possible novel oxidation product. No 2-phenylethanol or dihydroxylated products were detected with either the wild type enzyme or any of the mutants.

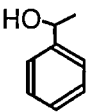
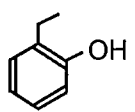
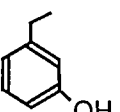
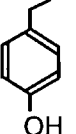
Enzyme	Products (molar %)				Molar ratio aromatic: sidechain hydroxylation	Relative total activity (%) ^b
	1-phenyl-ethanol	2-ethyl-phenol	3-ethyl-phenol	4-ethyl-phenol		
						
Wild-type	95.4 ± 1.4 ^b	0.0	4.6 ± 1.4 ^a		0.048	100
L110G	9.2 ± 3.1	8.8 ± 0.4	82.1 ± 2.7		9.9	32
L110C	23.6 ± 6.2	3.1 ± 2.1	73.3 ± 4.4		3.2	48
L110Y	40.2 ± 10.5	3.1 ± 0.6	56.8 ± 10.0		1.5	8.7
L110R	22.1 ± 1.6	1.3 ± 0.1	76.6 ± 1.5		3.5	63

Table 3.2: Products of ethyl benzene oxidation by Leu 110 mutants showing percentage product distribution, relative total activity and ring : side chain hydroxylation ratio.^a 3- and 4-ethyl phenol were not resolved in these experiments and so the mol fractions stated are the sum of both.^b Data are derived from three separate experiments from a single batch of drop frozen cells for each mutant and are shown in the form mean ± SD.^c Relative total activities with ethyl benzene as the substrate, which were corrected for differences in culture OD₆₀₀, are given as percentages of the rate of increase in total product concentrations obtained with wild-type *Ms. trichosporium* OB3b, which was 0.52 μM h⁻¹.

Fig 3.6) GCMS traces for wild type sMMO (A) and L110R mutant (B) showing total ion scan (bottom trace in red) and specific ion monitoring at 122 m/z (top trace in green). Identity of peaks was confirmed by comparing retention times against authentic standards (not shown).

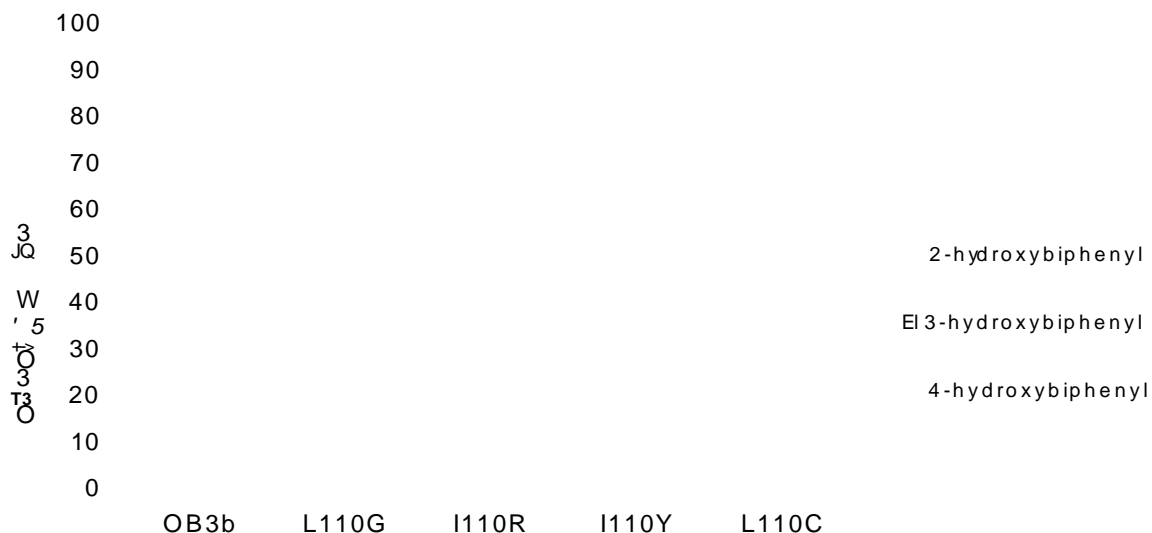


Fig 3.7) Distribution of biphenyl oxidation products by Leu 110 mutants. Data are derived from duplicate experiments from a single batch of drop frozen cells for each mutant and are shown in the form mean \pm SD

With biphenyl as the substrate, the wild-type produced predominantly 4-hydroxybiphenyl. Mutants with the larger tyrosine or arginine residue at position 110 showed a shift in regioselectivity with substantially more 2-hydroxybiphenyl produced than the wild-type. The mutants with the smaller glycine and cysteine residues at this position showed relaxed regiospecificity, producing the novel oxidation product 3-hydroxybiphenyl (Fig 3.7).

3.3.4) Neither mutants nor wild-type oxidized triaromatic hydrocarbons

Cells expressing wild-type sMMO and all four mutants at position 110 were initially screened for oxidation of the triaromatic compounds phenanthrene and anthracene in the same manner as used for the semiquantitative naphthalene assay, by addition of tetrazotised o-dianisidine, which would give coloured diazo dyes after reaction with the hydroxylated products. No visible colour changes were seen from mutants or wild-type, although a control of 9-phenanthrol gave a coloured product with a detection threshold of 5 pM which is comparable to the naphthalene test (Fig. 3.8). GC-MS was used to analyse assay reactions that had been incubated for 30 °C for 48 h, as described in the Material and Methods chapter, but no hydroxylated products could be found from either of the triaromatic substrates with wild-type *Ms. trichosporium* OB3b or any of the mutant strains. Presuming that phenanthrene and anthracene are able to diffuse into the cells, these results strongly suggest that neither wild-type sMMO nor the mutants are able to oxidize these bulky aromatic substrates.

1-naphthol standards

1 μmole/ml 100nmoles/ml 50nmoles/ml 10nmoles/ml 1nmole/ml

Fig 3.8) Colour formation of 1-naphthol and 9-phenanthrol standard solutions (1 ml) upon the addition of 100μl tetrazotized-o-dianisidine [0.5 mg ml⁻¹].

3.4 Analysis of results

3.4.1) Regioselectivity of WT sMMO

The results for the regioselectivity of *Ms. trichosporium* expressing the wild type sMMO are consistent with previously published results concerning the regioselectivity of sMMO towards aromatic substrates (Colby *et al.* 1977, Burrows *et al.* 1984). There seems to be a range of possible positions for the substrates in the active site with the wild type enzyme, as all aromatic substrates show more than one oxidation product. There also seems to be some correlation between the preferred sites of hydroxylation with the various aromatic substrates. If the substrates are considered to be roughly rectangular in shape, the wild-type enzyme shows a strong preference for hydroxylation nearest to the two short sides. This was observed with all the substrates assayed. When naphthalene was the substrate the primary oxidation product was 2-naphthol. Similarly the diaromatic substrate biphenyl was predominantly oxidized to 4-hydroxybiphenyl. With the monoaromatic substrates toluene and ethyl benzene both ring and side chain hydroxylation was seen with a mixture of benzyl alcohol and p-cresol being seen with toluene oxidation and a mixture of 1-phenylethanol and 4-ethylphenol being seen with ethyl benzene oxidation.

3.4.2) Mutants showed relaxed regioselectivity but showed no activity towards triaromatic substrates

The mutant-expressing strains showed lower rates of total product accumulation than the wild-type, ranging from 2.5 to 63 % of the wild-type activities. Examining the data from ethyl benzene and toluene as substrate, there does not seem to be a clear correlation between the property of the amino acid and the reduction in activity, and these results may also reflect differences in expression and stability between the mutants. However analysis of the proportions of oxidation products formed from the aromatic substrates, yielded information that is not biased by the level of expression.

The results indicate a correlation between the size amino acid at position 110 and altered regioselectivity for the mutant enzymes. The largest shift in regioselectivity with naphthalene as the substrate was observed with the larger arginine and tyrosine mutants. In both of these mutants there was significantly more 1-naphthol produced than 2-naphthol in comparison to the wild type enzyme. Conversely, the novel product from biphenyl oxidation, 3-hydroxybiphenyl, is seen only in the mutants with the smaller residues glycine and cysteine at this position. With the monoaromatic substrates a relaxation of regioselectivity was seen with both larger (Arg and Tyr) and smaller (Cys and Gly) mutants with novel oxidation products being produced with both toluene and ethyl benzene. However the shift from side-chain to ring hydroxylation of toluene was greatest in the mutants with the smaller residues at position 110 and the corresponding shift in regioselectivity in oxygenation of ethyl benzene was almost two orders of magnitude greater than that seen with any of the other mutants.

3.5 Summary

The data in this chapter clearly show that the Leu 110 residue has a role in regioselectivity of sMMO rather than that of a gating residue. The data in this chapter were collected from experiments carried out in whole cells over a 48 h period. It should be mentioned that the presence of other enzymes in the methanotroph metabolic pathway may have influenced the product distribution for the substrates in this and in previous studies using whole cells expressing sMMO. As will be discussed in more detail in later chapters, the presence of enzymes such as methanol dehydrogenase which has been shown to act on benzyl alcohol (Mountfort, 1990) and other aldehyde dehydrogenases (Patel *et al.* 1972; 1980) may act on the side chain oxidation products from substituted aromatics. Differences between product distribution from mutants and wild type sMMO reported in this chapter were recorded from assays conducted under identical conditions and hence indicate real differences in regioselectivity. However, side chain oxidized products may be under-

represented in the data due to their further metabolism by cellular enzymes other than sMMO.

Chapter 4: Mutagenesis based upon butane monooxygenase

4.1 Introduction

4.1.1) Comparative analysis of sMMO

Comparison of homologous enzymes with distinct catalytic properties can offer a powerful way to design site-directed mutants. A combination of sequence and three-dimensional structure information can be used to identify candidate residues that may be involved in key catalytic processes, which can then be investigated experimentally via mutagenesis. A substantial number of sMMO sequences are now available but these do not provide a large amount of information about the likely function of specific residues because the sMMOs that have been investigated have very similar catalytic properties (Cardy *et al.* 1991; McDonald *et al.* 1997; Dedysh *et al.* 1998, 2004; Dunfield *et al.* 2003; Hutchens *et al.*, 2004; Ward *et al.*, 2004; Lin *et al.* 2004; Ali *et al.* 2006; Dumont *et al.* 2006).

4.1.2) Comparison to butane monooxygenase

Butane monooxygenase (BMO), is an SDIMO with a relatively high similarity to sMMO that has distinct catalytic properties from sMMO. As mentioned previously, this bacterial multimeric enzyme catalyses the oxidation of butane to butanol using dioxygen as the oxidant. This enzyme has a much narrower substrate range than sMMO and has a very low specific activity of 3.6 nmol min⁻¹mg protein⁻¹ towards methane (Halsey *et al.* 2006). The cloning and sequence analysis of the BMO operon from *Thauera butanivorans* (formerly *Pseudomonas butanovora*) has shown that this enzyme shows high sequence identity at the amino acid level compared to

sMMO (Sluis *et al.* 2002, Kurth *et al.* 2008). The *bm oX* gene that encodes the hydroxylase α -subunit of BMO that contains the non haem diiron active site shows 63 % identity at the amino acid level to MmoX of *Methylosinus trichosporium* OB3b. These sequencing results enable us to create site directed mutants to compare the differences in catalytic activity between these two enzymes.

4.1.3) Comparison of a highly conserved hydrophobic pocket near the active site of BMO and sMMO

Crystallographic studies of sMMO from *Ms. trichosporium* OB3b by Elango *et al.* (1997) identified a hydrophobic pocket lined by 19 residues adjacent to the active site, hypothesised to be important in substrate binding. Of these 19 hydrophobic residues, 14 are conserved within BMO (Figs. 4.1, 4.2, 4.3). To begin to probe the differences in catalytic activity between BMO and MMO, mutants C151T, M184V and F282L were created. These mutants were highlighted as being of most interest and having the most significant in structure for each residue. The other two possible mutants, A120G and V239I had only minor changes in amino acid side chain with similar size and properties in each case.

MMO	ETMKVISNFLEVGGEYNAIAASAMLWDSATAAEQKNGYLAQVLDEIRHTHQ	150
BMO	EVMKLVSNFLETGEYGAIAGSALLWDTAQSPQQRNGYLAQVIDEIRHVNQ	147
	k	
MMO	CAFINHYYSKHYHDPAGHNDARRTRAIGPLWKGMKRVFADGFISGDAVEC	200
BMO	TAYVNYYYGKHYYDPAGHTNMRQLRAINPLYPGVKRAFEGEFLAGDAVES	197
	* *	
MMO	SVNLQLVGEACFTNPLIVAVTEWASANGDEITPTVFLSVETDELRRHMANG	250
BMO	SINLQLVGEACFTNPLIVSLTEWAAANGDEITPTVFLSIETDELRRHMANG	247
	*	
MMO	YQTVVSIANDPASAKFLNTDLNNAFWTQQKYFTPVLGYLFEYGSKFKVVEP	300
BMO	YQTIIVSIMNPNPETMKYLQTDLDNAFWTQHKFLTPFVGVVALEYGSKYKVEP	297
	*	

Fig 4.1) Amino acid alignment of methane monooxygenase and butane monooxygenase. The 19 residues within the hydrophobic pocket adjacent to the active site are highlighted in yellow. * indicates a difference in amino acid sequence between BMO and sMMO.

Fig 4.2) The active site of sMMO showing diiron centre (magenta spheres) and adjacent 19-residue hydrophobic binding region (Elango *et al.* 1997). The proposed substrate gate leu110 (conserved in BMO) and the five residues that are not conserved between sMMO and BMO are labeled. Diagram has been created from x-ray crystallography data (1MTY). The amino acids are coloured as follows: alanine (light green), cysteine (pale olive), glycine (white), glutamine (pink), isoleucine (dark green), leucine (green/grey), phenylalanine (dark grey), threonine (orange) and valine (violet).

Val181



Thr148

r

**•*

Q Q

Fig 4.3) The active site of BMO, showing amino acid positions corresponding to the 19-residue hydrophobic binding region of sMMO (Elango *et al.* 1997). The five residues in this region that are not conserved between sMMO and BMO are labelled along with the residue analogous to the proposed substrate gate of sMMO. Diagram has been created from x-ray crystallography data (1MTY). The amino acids are coloured as follows: alanine (light green), cysteine (pale olive), glycine (white), glutamine (pink), isoleucine (dark green), leucine (green/gray), phenylalanine (dark grey), threonine (orange) and valine (violet)

4.2 Construction and expression of mutants

4.2.1) Expression of mutants in *Ms. trichosporium* SMDM

The mutants C151T, M184V, and F282L were constructed within the pTJS175 expression vector and confirmed by DNA sequencing by Dr Elena Borodina (University of Warwick). The mutant plasmids were transformed into *E. coli* S17-1 and transferred to the sMMO negative host strain *Ms. trichosporium* SMDM by conjugation as described in the Materials and Methods chapter. The three mutants were grown in liquid cultures and on agar plates at a low copper to biomass ratio to induce expression of sMMO. A strong purple colour was detected for C151T and M184V, indicating the presence of naphthols which are the oxidation products of naphthalene, however, no activity was detected with the F282L mutant (Fig. 4.4). The F282L mutant was also assayed for butane and toluene oxidation activity using the GC and no oxidation products were detected with either substrate indicating an activity < 0.008 nmol min⁻¹.

C151T

Wild type OB3b

F282L

Fig 4.4) NMS agar plate showing positive naphthalene oxidation assay for *Ms. trichosporium* OB3b (wild type), *Ms. trichosporium* SMDM (pTJS175.C151T) and *Ms. trichosporium* SMDM (pTJS175.M184V).

4.2.2) Analysis of F282L soluble extract

A soluble extract of the F282L mutant expressing strain was prepared using the sonication method as described in the Materials and Methods section, along with soluble extract from the wild type strain *Ms. trichosporium* OB3b as a positive control and analysed using SDS PAGE. The protein bands corresponding to the α , β and γ hydroxylase subunits of sMMO in the F282L soluble extract are clearly visible (Fig. 4.5)



Fig 4.5) SDS PAGE gel showing Protein marker (M) and soluble extract from *Ms. trichosporium* OB3b (1) and mutant F282L (2). The hydroxylase subunits MmoX, MmoY and MmoZ are marked α , β and γ respectively.

4.2.3) The M184V mutant is an unstable enzyme

Soluble extract preparations of M184V and C151T were prepared as described in the Materials and Methods section along with the wild type strain *Ms. trichosporium* OB3b as a positive control and analysed by SDS PAGE. The α , β and γ hydroxylase subunits of sMMO were clearly visible in the wild type strain and C151T mutant expressing strain. However little or no visible protein bands for the M184V hydroxylase subunits were detected (Fig. 4.6). Assays with the substrates butane, pentane and hexane were carried out using soluble extracts of C151T, M184V and wild type OB3b however no activity was detected for M184V with any of these substrates.

M 1 2 3

Fig 4.6) SDS page gel showing Protein marker (M) and soluble extract from OB3b (1) and M184V (2) and C151T (3).

4.3 Oxidation of butane and naphthalene by the mutants showed no change in regioselectivity or activity compared to wild type sMMO

4.3.1) Oxidation of butane by BMO inspired site directed mutants

Butane oxidation assays were carried out using soluble extract to ensure that no particulate MMO was acting on the butane. Assays were carried out for 1 min, 5 min and 10 min for both wild-type OB3b and the C151T mutant. Analysis of M184V with the substrate butane was not possible due to the instability of the M184V mutant in soluble extract preparations. The primary products of butane oxidation are 1-butanol and 2-butanol, with butyraldehyde and 2-butanone as other possible products. The specific activities were quantified by using 1-propanol (2 μmol) as an internal standard. As products were detectable after 1 min this was the time chosen to ensure the specific activity was measured when the enzyme was at it most active. For both the wild type sMMO and the C151T mutant, hydroxylation of butane was observed only at the terminal carbon since 1-butanol was the only product detected. An extra peak was observed at ~ 10.6 min that was not seen in either the soluble extract with no substrate negative control or the control with only substrate and MOPS buffer (Fig. 4.7). This extra peak is possibly due to impurities in the butane that can be oxidized by sMMO. The specific activity of C151T against butane was 6 times less than wild type OB3b (Table 4.1).

8.0 9.0 10.0 11.0 12.0 13.0 14.0 15.0min

Fig 4.7) GC trace from OB3b Butane oxidation assay showing 1-butanol peak, retention time of 2-butanol and the unknown peak at 10.6 mins. Identity of the peaks was confirmed by comparing retention times against authentic standards (data not shown).

	Specific activity (nmol/min/mg)	activity (%)
Ob3b	78.0 ± 2.6	100
C151T	13.1 ± 1.0	16.8

Table 4.1: Specific activities for butane oxidation. Specific activities are a mean of triplicate results and expressed as nmoles product /min/mg soluble protein ± standard error.

4.3.2) Oxidation of naphthalene by BMO inspired site directed mutants

Both C151T and M184V showed no significant change in regioselectivity from the wild type when naphthalene was the substrate. As a result of the symmetry of the naphthalene molecule, there are only two possible products from a single hydroxylation event, 1-naphthol or 2-naphthol. The C151T and M184V mutants showed similar regioselectivity to the wild type enzyme with an almost equimolar amount of both isomers of naphthol and only a very slight excess of 2-naphthol in all cases (Table 4.2).

	1-naphthol (%)	2-naphthol (%)	specific activity (nmoles/min/mg)
Wild-type	46.49 ± 1.65	53.51 ± 1.65	33.89 ± 2.36
C151T	48.00 ± 0.84	52.00 ± 0.84	21.75 ± 0.48
M184V	46.22 ± 1.77	53.78 ± 1.77	21.26 ± 6.27

Table 4.2: Product distribution and specific activity with naphthalene as substrate. Specific activity is expressed as nmoles per minute per mg soluble protein. Data are derived from three separate experiments from a single batch of drop frozen cells for each mutant and are shown in the form mean ± SD

The assays were carried out at 30 °C for 30 min using whole cells with 5 mM formate to provide an excess of reducing equivalents for the reaction. The reaction was started by adding two naphthalene crystals (~5 mg total) to each assay and was stopped by plunging the tube into ice. The rate of oxidation of naphthalene was calculated using the colorimetric method described by the Wood group (Canada *et al.* 2002). Upon addition of the TOD reagent in the presence of naphthol oxidation products a diazo dye is formed (Wackett and Gibson 1982) which is measured by detecting an increase in absorbance at 540nm using a Jenway 6715 UV/Vis spectrophotometer and quantified by comparing against a standard curve of known standards for 1 and 2 naphthol. The specific activity of the C151T and M184V mutants expressed as nmole product per min per mg soluble protein (Table 4.2) are 64.1% and 62.7% that of the wild type OB3b respectively. It should be noted that these specific activities are with respect to the formation of 1-naphthol only, because the 1-naphthol-dye complex forms more quickly and the absorbance at 540 nm of the diazo dye formed from this isomer is much greater than that from 2-naphthol (Fig. 4.8)

Fig 4.8) Standard curve of concentrations of 1- and 2-naphthol against absorbance at 540 nm 15 s after addition of TOD reagent as described in the Materials and Methods chapter.

4.4 Oxidation of toluene, biphenyl and hexane by BMO inspired mutants shows relaxed regiospecificity compared to the wild type enzyme

4.4.1) Oxidation of toluene by BMO inspired mutants

Oxidation of toluene can produce four possible products. Oxidation of the methyl group produces benzyl alcohol whereas ring oxidation could produce *p*-cresol, *m*-cresol or *o*-cresol. Qualitative identification of toluene oxidation products was carried out using GCMS analysis and comparing and products identified by comparison of retention times against known standards and comparison of mass spectra against the NIST mass spectra library. For quantitative analysis, toluene oxidation products were run on a Shimadzu GC2010 with 1 μ l 2-phenyl ethanol as an internal standard. The specific activities for toluene for both C151T and M184V were calculated based upon total soluble protein and showed reduced activity compared to wild type OB3b (Table 4.4). For the M184V and C151T mutants, the oxidation products detected showed a similar distribution to those from the wild type enzyme with a majority of benzyl alcohol being produced (Table 4.3). No *m*-cresol or *o*-cresol was detected in either wild type sMMO or the C151T or M184V expressing mutants. When toluene was the substrate both C151T and M184V showed a statistically significant increase in ring hydroxylation compared to the wild type enzyme with 39% of the oxidation product as *p*-cresol compared with 29% in the wild type enzyme ($P=0.023$ and 0.028 respectively) (Table 4.3).

Mutant	benzyl alcohol (%)	p-cresol (%)
OB3b WT	71.38 ±2.89	28.62 ±2.89
C151T	60.86 ±0.35	39.14 ±0.35
M184V	60.77 ±1.20	39.23 ± 1.20

Table 4.3: Distribution of toluene oxidation products given as a percentage of total product. Assays were carried out in triplicate and are displayed as mean values ± standard error.

	Specific Activity	Relative Activity (%)
OB3b	132.4 ±51.7	100
C151T	91.6 ±26.1	68
M184V	42.7 ±5.4	35

Table 4.4: Specific activities of wild-type OB3b and C151T and M184V expressing mutants. Specific activities are given as nmole/min/mg soluble protein. Relative activity is shown against wild-type OB3b.

4.4.2) Oxidation of biphenyl by BMO inspired mutants

Analysis of the oxidation of biphenyl also shows a slight relaxation in regioselectivity compared to that of the wild type. The oxidation of biphenyl can produce three possible oxidation products depending on which position on the aromatic ring is oxidized. The oxidation assays were carried out using whole cells containing 5mM formate to provide plenty of reducing equivalents for the reaction. The C151T and M184V mutants showed > 97% of the biphenyl oxidation product as the 4-hydroxybiphenyl isomer (4hbp). There was a significant increase in the production of both 3-hydroxybiphenyl isomer (3hbp) and 2-hydroxybiphenyl (2hbp) from the C151T mutant compared to the wild type enzyme (P=0.021 and 0.04 respectively) (Table 4.5).

Cells	2-hydroxybiphenyl (%)	3-hydroxybiphenyl (%)	4-hydroxybiphenyl (%)
OB3b	0.16 ± 0.14	0.38 ± 0.27	99.46 ± 0.4
C151T	0.76 ± 0.11	1.84 ± 0.44	97.41 ± 0.25
M184V	<0.08	2.27 ± 0.97	97.73 ± 0.97

Table 4.5: Distribution of biphenyl oxidation products given as a percentage of total product. Assays were carried out in duplicate from a single batch of drop frozen cells for each mutant and are displayed as mean values ± standard error

4.4.3) Oxidation of hexane by BMO inspired mutants

The oxidation of hexane can yield 3 possible products depending on which carbon is oxidized: 1-hexanol, 2-hexanol or 3-hexanol. Hexane oxidation assays were carried out using soluble extract to ensure that only sMMO was oxidizing the substrate.

Soluble extract (2 ml) was incubated with 1 μ l hexane for 10 min at 30 °C and the reaction was started by adding NADH up to 5 mM. The internal standard used in these assays was 1-propanol (2 pmol), the assays were extracted with ether which was then allowed to evaporate at room temperature to a volume of ~50 μ l and run on the GC. The C151T mutant shows a slight relaxation of regioselectivity compared to the wild-type OB3b. Oxidation of hexane by wild-type OB3b shows 1-hexanol as the major oxidation product accounting for 65% of the total product detected. However, the C151T mutant shows a significantly altered product distribution compared to the wild type ($P < 0.001$) with only 48% of the hexane oxidation products as 1-hexanol (Table 4.6). In the wild type enzyme and the C151T mutant no 3-hexanol was detected. The specific activity of the C151T mutant was reduced 14-fold compared to that of the wild type sMMO (Table 4.7).

	1-hexanol (%)	2-hexanol (%)	3-hexanol (%)
OB3b	64.35 ± 0.05	35.65 ± 0.05	0
C151T	48.35 ± 1.22	51.65 ± 1.22	0

Table 4.6: Percentage product distribution of hexane oxidation of WT OB3b and C151T. Assays were carried out in triplicate and displayed as a mean result ± standard error

	Specific activity (nmoles/min/mg)	activity (%)
OB3b	0.27 ± 0.005	100
C151T	0.019 ± 0.0007	6.8

Table 4.7: Specific activities of WT OB3b and C151T mutants against hexane. Activities are expressed as nmoles product/mg/total soluble protein ± standard error.

4.5 Oxidation of mesitylene by the M184V mutant shows novel oxidation products.

4.5.1) A novel substrate for studying monooxygenase activity

The substrate mesitylene (1,3,5-trimethylbenzene) was chosen as a candidate for study due to its size and positions of the three methyl groups, meaning only two possible primary oxidation products would be produced. Ring hydroxylation of mesitylene would produce 2,4,6-trimethylphenol and side chain oxidation would produce 3,5-dimethylbenzyl alcohol, making it an ideal substrate for oxidation analysis.

4.5.2) Mesitylene oxidation assays over 24 h and 72 h showed no monohydroxylated products

Assays were carried out using whole cells over a period of 72 h and analysed via GCMS; however, no oxidation products were detected with wild type OB3b or the mutants M184V and C151T. It was noted that there was a large peak identified by its mass spectrum as 3,5-dimethyl benzoic acid. This corresponds to further oxidation of the side-chain hydroxylation product 3,5-dimethylbenzyl alcohol. An assay was set up for each mutant with an overnight incubation and again the large peak corresponding to 3,5-dimethylbenzoic acid was present, however, there were also

trace amounts of two products with a mass of 136 m/z , which correspond to the singly hydroxylated mesitylene products.

Since reducing the reaction time allowed detection of small amounts of the expected monohydroxylation products, it was possible that the initial products from the sMMO-catalysed reaction were the monohydroxylated moieties, which were then further oxidised by sMMO or another enzyme present in the methanotroph cells. The enzyme methanol dehydrogenase (MDH) was a possible candidate for such a reaction because it has been reported that MDH from *Ms. trichosporium* OB3b can oxidize benzyl alcohol to benzaldehyde (Mountfort 1990). However as MDH was shown by the author not to be active against benzaldehyde it is likely that another enzyme is responsible for the production of the benzoic acid derivative seen in these assays.

4.5.3) Mesitylene oxidation assays over 1 h showed monohydroxylated products

An assay was set up for 1 h and this time the oxidation products were clearly visible (Table 4.8). The C151T mutant showed similar characteristics to that of the wild type enzyme with hydroxylation predominating on the side chain with the product 3,5-dimethylbenzyl alcohol making up more than 99% of the total oxidation products. The specific activity of the cells expressing the C151T mutant sMMO towards mesitylene was also reduced, to 19 % of that observed in the wild type.

	2,4,6-trimethylphenol (%)	3,5-dimethylbenzyl alcohol (%)	3,5-dimethyl benzaldehyde (%)
OB3b	0.40 ± 0.34	99.60 ± 0.34	0.00
M184V	0.25 ± 0.42	33.30 ± 22.53	66.45 ± 22.33
C151T	0.82 ± 0.34	99.18 ± 0.34	0.00

Table 4.8: Percentage product distribution of Mesitylene oxidation products. Assays were carried out in triplicate from a single batch of drop frozen cells for each mutant and are displayed as mean values ± standard error.

The M184V mutant showed an extra oxidation product not expected. An extra peak was present identified by the mass spectra library as 3,5 dimethyl benzylaldehyde which was not detected in either OB3b or C151T. The significance of this unexpected result is covered in the discussions chapter.

4.6 Summary of results

The data in this chapter show that the M184V, C151T and F282L mutations have an effect on the stability and the activity of the sMMO enzyme. As the M184V mutant was unstable in soluble extracts, only whole cell assays could be carried out with this mutant. The F282L mutant had no detectable activity; however, the hydroxylase components could clearly be seen by SDS PAGE indicating that this is a stable mutant. The activity of the C151T mutant was reduced compared to the wild type enzyme with all substrates tested including butane and no shift towards terminal carbon oxidation as seen with butane monooxygenase, hence this site directed mutant does not confer a BMO-like phenotype upon the mutant enzyme. The regioselectivity of the C151T mutant was relaxed compared to the wild type enzyme with all substrates tested except butane. The greatest change in regioselectivity was seen with hexane as the substrate, where the major oxidation product shifted from 64.35 % 1-hexanol with the wild type enzyme, to 51.65 % 2-hexanol with the C151T mutant. The novel substrate mesitylene was the only substrate where a BMO-inspired mutant had increased activity compared to the wild type enzyme. The M184V mutant showed an 3.6-fold increase in activity over the wild type enzyme towards mesitylene and produced a novel oxidation product 3,5-dimethyl benzaldehyde not seen with the wild type OB3b or the C151T mutant.

Chapter 5: Random mutagenesis of *mmoX*

5.1 Introduction

5.1.1) A mutagenesis approach to studying sMMO substrate specificity

One of the key aims of this thesis is to look at the substrate range of sMMO and to try and identify the structural aspects that may limit the size of substrate that can be oxidized by the enzyme. A random mutagenesis approach was carried out with the intention of identifying new residues important in controlling substrate specificity. This is in addition to those which have been inferred from various crystal structure studies and were being tested via directed mutagenesis. Using a modification of the colorimetric naphthalene oxidation assay to screen for activity against the triaromatic compounds; a number of *m m oX* random mutant libraries were created and screened for activity against anthracene and phenanthrene.

5.1.2 Mutagenesis studies of related monooxygenases

Directed evolution is a term used to describe a variety of techniques where protein variants are created via random mutagenesis and mutants are selected that show a desired function. There are a number of ways of generating quasi-random mutants for selection or screening for activity including shuffling of homologous genes (Stemmer, 1994) and error prone PCR (Leung *et al.* 1989; Cadwell and Joyce 1992;

Zhou *et al.* 1994). No work has been published on the directed evolution of soluble methane monooxygenase although as described in chapter 1, directed evolution approaches have been used with a number of related bacterial diiron monooxygenases.

5.1.3) Directed evolution studies of aromatic monooxygenases

A random mutant library of *tomA012345* genes encoding toluene *ortho*-monooxygenase of *Burkholderia cepacia* G4 were created by Wood and co-workers (Canada *et al.* 2002) using DNA shuffling. A number of *tom* genes were digested with DNase I and randomly reassembled to create a mutant library. Screening of this library identified a mutant showing increased trichloroethylene degradation and also improved activity towards both diaromatic and triaromatic substrates. The sequence of the mutant led to the identification of Val 106 as an important residue in limiting the rate of these reactions. Directed evolution was also used by Wood and co-workers to identify residues important in the oxidation of nitrobenzene to 4-nitrocatechol by toluene 4-monooxygenase from *Pseudomonas mendocina* KR1 (Fishman *et al.* 2004). An error prone PCR technique was used to generate random mutations within the *tmoA*, *tmoB* and *tmoC* genes encoding encoding for the hydroxylase α -subunit, the hydroxylase γ -subunit and a Rieske type ferridoxin, respectively. Screening of this library identified a mutant with an 8-fold increase in the rate of 4-nitrocatechol production compared to the wild type enzyme when nitrobenzene was the substrate. This led to the identification of an Ile100 mutation as a possible candidate for the change in reactivity towards nitrobenzene, due to

comparison to the work carried out in the same laboratory on the analogous position of toluene *ortho* monooxygenase (Val 106 mentioned above). Further saturation mutagenesis work identified the mutant I100A as having > 16-fold increase in 4-nitrocatechol production compared to the wild type and the discovery that residue I100 is important in regioselectivity in this enzyme.

6.1.4) Directed evolution of alkene monooxygenase

A method has also been described using error prone PCR for directed evolution of another bacterial diiron monooxygenase related to soluble methane monooxygenase (Perry and Smith, 2006). The alkene monooxygenase from *Rhodococcus rhodochrous* B276 was expressed in the host *Streptomyces Hvidans* and a mutant library of the *amoC* gene created using the commercially available Genemorph random mutagenesis kit (Stratagene). This kit contains the Mutazyme error prone polymerase enzyme which has an easily controllable error rate and according to the manufacturer has reduced mutational bias compared to other error prone PCR enzymes such as *Taq* polymerase. Enantioselective GC analysis was carried out using a chiral column and mutants were screened for enhanced enantioselectivity towards the substrate propene.

Here, a method was devised using the pTJS175 expression system to create a random mutant library of the *mmoX* gene and a rapid colorimetric assay developed for high throughput screening of mutants with the ability to oxidize triaromatic compounds (Fig. 5.1).

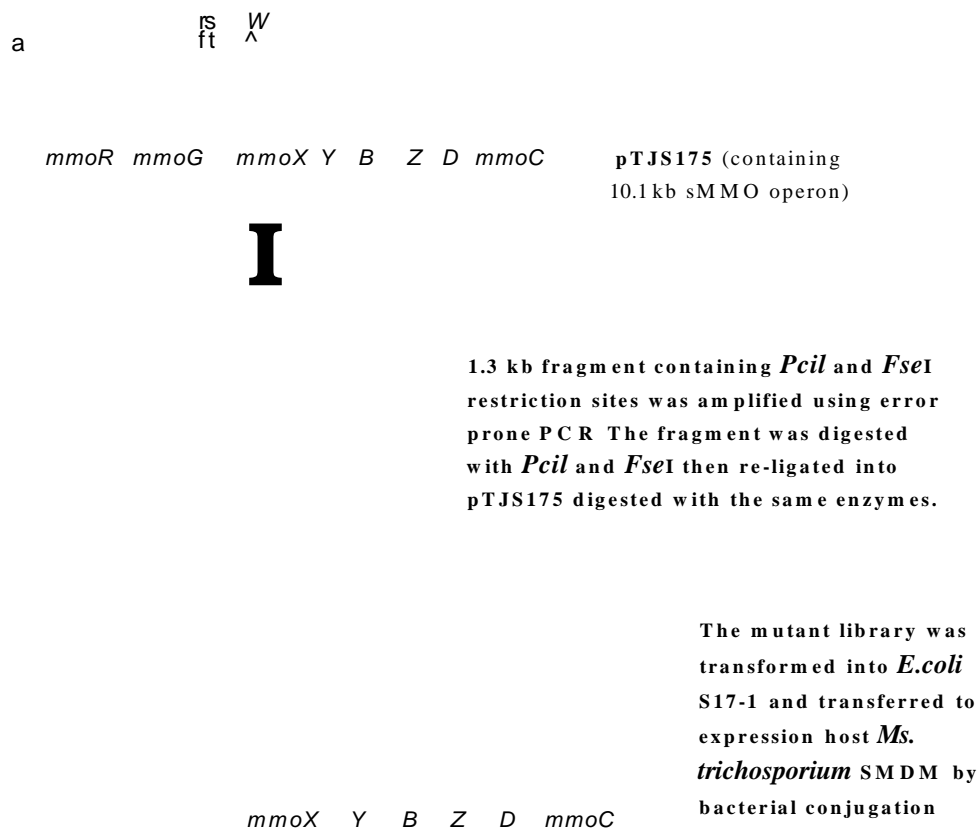


Fig. 5.1) Diagram showing the creation of an *mmoX* mutant library and expression within the sMMO negative host strain *Ms. trichosporium* SMDM

5.2 Development of a random mutagenesis method using *Taq* polymerase

5.2.1) Use of *Taq* polymerase for error prone PCR

For random mutagenesis *Taq* polymerase was chosen to amplify a portion of the *mmoX* gene using an error prone PCR reaction. The lack of a 3' to 5' proofreading activity and a high intrinsic error rate (depending on reaction conditions) of between 10^{-4} and 10^{-6} errors/nucleotide with this enzyme make it a perfect candidate for error prone PCR. A number of reaction conditions can be altered to reduce the fidelity of *Taq* polymerase and a method for error prone PCR based on Cadwell and Joyce (1992) was used to increase the mutation frequency whilst reducing the mutational bias as described in Materials and Methods section 2.3.6. One of the main drawbacks of using *Taq* polymerase for error prone PCR is the preference of this enzyme to produce A→G and T→C base pair changes. Using mismatched dNTPs with a much higher concentration of dCTP and dTTP compared to the concentrations of dATP and dGTP reduces this mutational bias (Cadwell *et al.* 1992). *Taq* polymerase requires a divalent metal cation for activation and this is normally MgCl₂ in a concentration that is equimolar to the dNTP concentration. By using a concentration of magnesium in excess of the dNTP concentration the fidelity of *Taq* polymerase can be greatly decreased, possibly due the stabilization of non complementary pairs (Eckert and Kunkel, 1991). The addition of MnCl₂ has been shown to further reduce the fidelity of *Taq* and is thought to act in the same way (Beckman *et al.* 1985). Finally the number of PCR cycles used greatly affects the fidelity of the polymerase, as more reaction cycles means more chance of an error in

amplification (Leung *et al.* 1989). By using these conditions an error rate of 10^{-4} mutations/kb was achieved (confirmed by sequencing of five cloned PCR products) [Fig. 5.2]

Fig 5.2) Partial sequence data of *mmoX* from wild type *Ms. trichosporium* OB3b showing base changes from a random mutant library clone. Base changes from the mutant library clone are shown in red below the wild type OB3b sequence. Corresponding translated protein data from wild type *Ms. trichosporium* OB3b (blue) and mutant library clone (green) with amino acid is boxed changes highlighted in red.

5.2.2) Creating the random mutant libraries

In order to insert the error prone PCR fragment into the sMMO operon two unique restriction sites needed to be found that could be used as an exchangeable cassette. The *Pci*/*Fse*I was chosen as it was the largest possible exchangeable cassette within the *mmoX* region that was available without engineering of the rest of the plasmid. The *Pci*/*Fse*I cassette is 790 bp in size and encodes for amino acids 1 - 167 of *mmoX*. *Taq* mutagenesis was carried out using primers TrmutP1 and TrmutP2 (Table 5.1) and amplifies a 1281 bp fragment flanking the *Pc*/I site and *Fse*I restriction sites. The error prone PCR product was digested with these enzymes and ligated into the larger fragment of pTJS175 also digested with *Pc*/I and *Fse*I (Fig. 5.1).

5.2.3) Transformation of *E. coli* S17-1

The *E. coli* conjugative strain S17-1 proved a difficult strain to transform. A number of methods were tried to transform the *E. coli* S17-1 strain including using CaCb prepared competent cells and a heat shock method (Sambrook *et al.* 1992). A high efficiency transformation method (Hanahan, 1983) and electroporation were also used as detailed in Materials and Methods section 2.5. For heat shock transformation mutant libraries were $1-7 \times 10^2$ colonies in size, whereas electroporation and Hanahan transformation methods were typically $1 - 3 \times 10^3$ in size. The mutant library was transformed into *E. coli* S17-1 cells using the Hanahan high efficiency method described above and transformed into *M. trichosporium* SMDM via bacterial conjugation (Materials and Methods section 2.6). Exconjugant colonies were visible after 5-7 days and patch plated onto NMS plates containing streptomycin, spectinomycin, nalidixic acid [20 µg/ml] and gentamicin [5 µg/ml]. Typically the mutant library size and subsequent conjugation rates were low with random mutant libraries being $1 - 3 \times 10^3$ clones in size.

Primer	Sequence 5'-3'	Description
TrmutP1	GCGGTCACTCATATTCC	210bp Upstream of Pc/I
TrmutP2	CGGATCATTGGCGATCG	281 bp Downstream of Fsel

Table 5.1)Sequences for primers used for error prone PCR of *m m oX* gene

5.3 Development of a colorimetric method for detecting oxidation of triaromatic compounds

In order for directed evolution studies to be effective, a suitable method of screening mutants for the desired function needed to be developed. A modification of the naphthalene oxidation assay has allowed efficient screening for the oxidation of triaromatic compounds phenanthrene and anthracene. As mentioned in chapter 3, this colorimetric assay showed similar detection limits for both 1-naphthol and 9-phenanthrol (Fig. 3.5). Each plate was incubated at 30 °C for 1 h in a sealed container with a few crystals of naphthalene or phenanthrene. Clones positive for oxidation were identified by the purple colour seen upon addition of tetrazotized-o-dianisidine [5 mg/ml]. Wood and co-workers reported a similar method to measure oxidation of both phenanthrene and anthracene using a spectrophotometer to quantify the coloured product (Canada *et al.* 2004).

5.4 Use of Genemorph random mutagenesis kit to create random mutant libraries

5.4.1) A new method for mutagenesis with reduced mutational bias and more controllable error rate

After screening 1200 mutants generated by random mutagenesis using *Taq* polymerase error prone PCR, no activity towards triaromatic compounds was detected. It has been shown that higher mutation rates using error prone PCR give rise to the most unique sequences yet few retain function and conversely that low mutation rates show many functional sequences yet few are unique (Suzuki *et al.*, 1996; Drummond *et al.* 2005). It was thought that possibly the mutation rate of *Taq* polymerase was too high or the mutational bias was excluding the desired mutant. The Genemorph II random mutagenesis kit (Stratagene) contains the Mutazyme polymerase which according to the manufacturers has no mutational bias and has a controllable error rate. By using the Mutazyme polymerase and altering the amount of DNA template in the reaction it is possible to influence the number of errors/kb. The lower the amount of target template the more amplifications are carried out and the higher the error rate. Up to 100 ng target DNA template is required for a higher mutation frequency of 9-14 mutations/kb. A medium mutation frequency of 4.5-9 mutations/kb is achieved with 100-500 ng target DNA and a low mutation frequency of 0-4.5 mutations/kb is achieved by using 500-1000 ng target DNA. For the random mutagenesis reactions 200 ng target DNA was used to achieve a medium mutation frequency around half that of the *Taq* error prone PCR. The 1281 bp target was first

amplified by high fidelity *Pfu* polymerase using primers Trm utp1/Trm utp2 (Table 5.2) and the PCR product used as template for the error prone PCR reactions. A Nanodrop spectrophotometer was used to measure the starting template DNA concentrations. A mutation frequency of 5-10 mutations/kb was achieved using this method (confirmed by sequencing of three cloned PCR products). The Genemorph PCR product was double digested with *FseI* and *PciI* and ligated into pTJS175 as with the taq random mutagenesis and transformed by electroporation into *E.coli* S17-1. As with the previous rounds of random mutagenesis with *Taq* polymerase, the mutant library generated in *E. coli* S17-1 was transferred to *Ms. trichosporium* SMDM by bacterial conjugation. Exconjugants were patch plated onto NMS agar plates containing streptomycin and spectinomycin [20 pg/ml], Exconjugants were screened for oxidation of phenanthrene and anthracene using the method described above however once again no activity was detected.

5.5 Summary

5.5.1) The colorimetric detection of triaromatic oxidation

The use of tetrazotized-*o*-dianisidine as a colorimetric test to detect oxidation of triaromatic makes the directed evolution towards oxidation of triaromatics a distinct possibility and by refining the methods described here it should be possible to identify the structural elements within wild type *m m oX* that prevent the oxidation of these larger compounds

5.5.2) *E. coli* strain S17-1 is difficult to transform

Although random mutagenesis was not successful in producing a mutant that could oxidise triaromatic compounds, a number of technical difficulties were overcome and future refinement of this method may lead to greater success in the directed evolution of sMMO. One major difficulty encountered with this system was the direct transformation into the conjugative *E. coli* S17-1 strain. In the creation of site directed mutants (see Methods section) the ligation reactions are first transformed into a strain of *E. coli* such as XL-1 or commercially available strains that have a much greater transformation efficiency. Such a strategy was judged unacceptable for cloning of libraries (i.e. large mixed populations) of mutants because it was considered that two rounds of amplification of the library in *E. coli* would greatly bias the mutant library before it could be screened in *Ms. trichosporium*. A number of different methods were investigated for transformation of *E. coli* S17-1 to obtain an acceptably high transformation frequency. The Hanahan method produced mutant libraries up to 3×10^3 clones in size. By using electroporation to transform the cells

the size of the library increased to 1×10^4 clones; however this is still a relatively small mutant library. Further changes in the preparation of electrocompetent *E. coli* S17-1 may lead to increased transformation efficiency and larger mutant libraries.

5.5.3) Difficulties encountered during the cloning stages

Another major obstacle to generation of libraries of random mutants of *mmoX* that has been overcome since the work in this chapter was performed relates to the expression vector. In the work described above the pTJS175 expression system was used and so *Pci*I and *Fse*I restriction sites had to be used as an exchangeable cassette. These enzymes are both very unstable and often did not digest the DNA well, making the creation of the random mutant library difficult. Multistep cloning strategies that would have allowed mutagenesis of a larger cassette using more stable restriction enzymes were avoided because (as detailed above) it was considered that the library should not be amplified more than once in *E. coli*. The 780bp *Pci*I-*Fse*I fragment only allows for 167 amino acids within the *mmoX* gene to be mutated. This is only 32% of the total protein and so may miss crucial amino acids which need to be mutated in order for triaromatic oxidation to take place. In later chapters the expression system pT2ML is described, where *Bam*HI/A/*cf*eI sites can be used to clone a 0.98kb cassette which would increase the amount of *mmoX* that could be mutated. However this expression system was not available when these experiments were carried out.

Chapter 6: Construction of a new expression vector pT2ML

8.1 Introduction

6.1.1 Cloning using the pTJS140/pTJS175 expression system

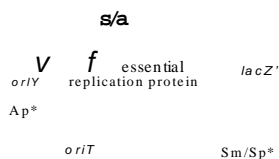
The current expression system used for site directed mutagenesis uses the broad host expression vector pTJS140 to allow cloning of mutants in *E. coli* and subsequent expression in *Ms. trichosporium* (Smith *et al.* 2002). This plasmid contains ampicillin, spectinomycin and streptomycin resistance markers and contains an origin of conjugative transfer (*ori/7*) and the broad host replicon from plasmid RK2 (*ori-RK2*) (Figurski *et al.* 1979, Blatny *et al.* 1997, Scott 2003). By using this system DNA modifications can be made in *E. coli* strains and the resulting plasmid transferred to an sMMO negative methanotroph host strain via bacterial conjugation as mentioned in the Materials and Methods chapter (section 2.6). This system although effective can be a slow process because subcloning within the plasmid pTJS176 is required for DNA manipulations within *mmoX* before the whole 10.1 kb operon is cloned into pTJS140. This requires two cloning steps and the insertion of a 10.1 kb insert into an 8 kb vector which can be a difficult cloning step. This chapter describes the modification of the pTJS140 system to remove the need for the subcloning step and allows for direct cloning into the sMMO operon via a 0.98 kb exchangeable cassette. This new expression system also allows for easier screening of *E. coli* colonies by PCR to identify plasmids containing the desired construct (Fig. 6.1).

NdeI and first *BamHI* site removed from pTJS140 by 4 primer overlap PCR to create plasmid pTN1



Delete 516 bp region of *mmoX* using *PstI* restriction sites

Second unwanted *BamHI* site removed by infilling using T4 polymerase to create plasmid pTN2



mmoR *mmoG* *AmmoX* *mmoY* *mmoB* *mmoZ* *orfY* *mmoC*

Clone sMMO operon into pTN2 via *KpnI* site

Clone *AmmoX* containing fragment into sMMO operon within pTJS176 to create pDIDI

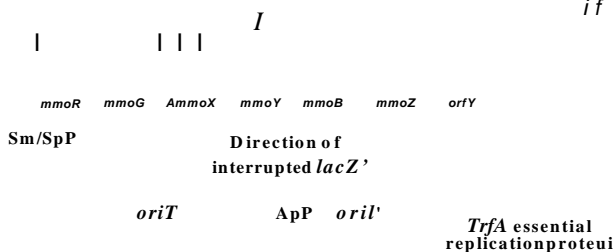


Fig 6.1) Diagram showing the stages in removing *BamHI* and *NdeI* sites from pTJS140 and subsequent creation of new expression vector pT2M L. Deletion of the 516bp region, cloning of the modified operon into pTN2 and creation of cloning vector pDIDI were carried out by Dr Malcolm Lock (Sheffield Hallam University).

6.2 Construction of new expression vector: pT2ML

6.2.1) Modification of pTJS140 to remove *Bam*HI and *Nde*I sites

As mentioned above the pTJS175 expression system required a subcloning step into the plasmid pTJS176. For every mutant created using the pTJS175 expression system two cloning steps were required. By removing the *Bam*HI and *Nde*I sites from pTJS140, a new expression vector was created that allowed direct cloning into the SMMO operon via a *Bam*HI/*Nde*I cassette.

Primer	Sequence 5'-3'	Description
TN140p1	CAC GCG AGG AAC TAT GAC GAC CAA GAA GC	Upstream external primer
TN140p2	GTA CTT CTC CCA GAT GAA TTT CGT GTA G	Reverse/complement of primer 3 below.
TN140p3	TAC ACG AAA TTC <u>ATC</u> TGG GAG AAG TAC	Mutagenic primer to remove <i>Nde</i> I, remnant of <i>Nde</i> I site underlined; mutation double underlined
TN140p4	G TCG ACT <u>CTA GAG GAC</u> CCC CGG GTA CCG AG	<i>Xba</i> I site underlined; mutation double underlined. Asp codon shown in bold

Table 6.1: Sequences of primers used for removal of an *Nde*I restriction site and one *Bam*HI restriction site by 4 primer overlap PCR from plasmid pTJS140

6.2.2) Removal of *Nde*I and first *Bam*HI site from pTJS175

The first stage in the creation of the new expression vector is to modify the broad host range expression vector pTJS140 by removing the *Nde*I site and the nearby *Bam*HI site to create plasmid pTN1. A four primer overlap extension PCR method as described in the Materials and Methods chapter (see section 2.3.5) was used to remove the *Nde*I and one of the *Bam*HI sites using the primers in Table 6.1. The

removal of the *NdeI* site was done by making a silent change with respect to the encoded amino acids and the alternative Ile codon is the most abundant in both *E. coli* and *Ms. trichosporium* genes. The removal of the *Bam*HI site is also a silent change and the Asp codon the most abundant in both *E. coli* and *Ms. trichosporium* (Table 6.1). These sites are contained within the *lacZ* and *trfA* essential replication protein and by making silent changes a stable working plasmid vector with a functional *lacZ* gene for blue/white selection was maintained (Fig. 6.1, Table 6.1). The two primary PCR products were 649 bp (TN140p1/TN140p2 upstream fragment) and 913 bp (TN140p3/TN140p4 downstream fragment) and these upstream and downstream fragments were used to create the 1534 bp combinatorial PCR product using primers TN140p1 and TN140p4 (Fig. 6.2). The 1534 bp fragment was digested with *SfiI* and *XbaI*, to give a 1447 bp fragment that was purified from a 1% agarose gel using the Qiagen gel extraction kit. In parallel, the pTJS140 vector was also digested with *SfiI* and *XbaI* and the larger fragment was purified from a 1% agarose gel before being treated with alkaline phosphatase. The 1447 bp insert and phosphatase treated vector were ligated using T4 DNA ligase and transformed into chemically competent *E. coli* XL1 and grown on LB agar plates containing 100 µg/ml ampicillin. Transformant colonies containing the putative progeny plasmid were grown overnight in LB containing ampicillin and the plasmid isolated using the Qiagen miniprep kit.

The new plasmid (pTN1) was identified on the basis that it only cut once when digested with *Bam*HI (confirming removal of 1 x *Bam*HI site) and by no cutting when digested with *NdeI*. The plasmid was also double digested with *SfiI* and *XbaI* to

confirm the presence of a 1447 bp fragment indicating that the insert used to create pTN1 was still intact.

M 1 2 M 3

Fig. 6.2A) 1% Agarose gel showing 1kb generuler DNA marker (M) 649 bp upstream (1) and 913 bp downstream (2) PCR products used for 4 primer mutagenesis.

Fig. 6.2B) 1% Agarose gel showing 1 kb generuler DNA marker (M) 1534 bp combinatorial PCR product (3) with removed *NdeI* and *BamHI* sites created by four primer overlap PCR

6.2.3) Removal of final *BamHI* site

In order to use the *BamHI* and *AclI* sites within the sMMO operon for direct cloning in the new expression vector, the final *BamHI* site within pTN1 was also removed by in-filling to create pTN2. The pTN1 plasmid was digested with *BamHI* and the linearized DNA was purified from a 1% agarose gel and treated with T4 polymerase in the presence of buffer and dNTPs to fill in the sticky ends to create blunt ends. The blunt ends were ligated using T4 DNA ligase and transformed into chemically competent *E. coli* XL1 and grown on LB agar plates containing ampicillin. Transformant colonies were grown overnight in LB containing ampicillin and plasmid DNA isolated by means of a miniprep kit. The correct plasmid was identified on the basis that it did not cut when digested with either *BamHI* or *NdeI*, showed a 1447bp fragment when double digested with *S7I* and *XbaI*, and showing linear DNA when digested with *KpnI* (Fig. 6.3).

M 1 M 2 3

Fig 6.3A) 1% Agarose gel showing 1kb generuler DNA marker (M), pTN1 partially digested using *SfiI* and *XbaI* confirming 1447bp insert fragment (1)

Fig 6.3B) 1% Agarose gel showing 1kb generuler DNA marker (M), uncut pTN1 digested using *BamHI* and *NdeI* (2) and linear pTN2 digested using *Kpnl* (3)

6.2.4) Deletion of 516 bp fragment from *mmoX*

In order to facilitate the screening process for successful transformation of site directed mutants of *mmoX*, a 516 bp section was removed from the *SamHI/A/cfeI* exchangeable cassette that includes most of *mmoX*. This work was carried out by Dr Malcolm Lock (Sheffield Hallam University). The use of a shortened *mmoX* gene within the new expression vector was designed to have two benefits. Firstly, only successful ligation of a complete *BamHVNdeI* cassette would encode an active sMMO enzyme so any activity observed was due to a recombinant clone and not due to a wild type phenotype resulting from re-circularization of the expression vector. Secondly, by using PCR primers flanking the *BamHVNdeI* sites, PCR could be used to identify colonies containing plasmids with the desired insert without the need to grow individual clones in liquid culture overnight and carry out miniprep plasmid

isolation. To accomplish this partial deletion of *mmoX* 1624 bp PCR fragment containing the *BamHI/NdeI* exchangeable cassette was amplified from the sMMO operon using primers P1/P4 (Table 6.2) and pTJS175 as the DNA template. The 0.98 kb BamHI cassette also contains two *PstI* sites which were used to remove the 516 bp fragment from the exchangeable cassette. The 1646 bp fragment was digested using *PstI* to give three fragments a 756 bp fragment (P1 to first *PstI* site), a 516 bp fragment (1st *PstI* site to 2nd *PstI* site) and a 372 bp fragment. The 758 bp and 372 bp fragments were purified from a 1% agarose gel using the Qiagen gel extraction kit and ligated using T4 DNA ligase overnight at 4 °C. The Ligase reaction mix was used as a DNA template for amplification of a 1.1 kb fragment by PCR using the P1 and P4 primers. This fragment was digested with BamHI and *NdeI* and ligated into the larger fragment of pTJS176 digested with the same enzymes and treated with alkaline phosphatase to create the plasmid pDIDI (Fig. 6.1).

6.2.5) Subcloning the modified sMMO operon into pTN1

The sMMO operon containing the *mmoX* deletion was excised from pDIDI using flanking *KpnI* sites and cloned into the unique *KpnI* cloning site within the *lacZ* gene of pTN2. The ligation mixture was transformed into *E. coli* XL1 supercompetent cells (stratagene) and plated onto LB agar plates containing ampicillin Xgal and IPTG. Blue and white selection was used to identify plasmids containing a disrupted *lacZ* gene indicating successful cloning within the *KpnI* site. The putative plasmid containing colonies were grown overnight in LB containing ampicillin and plasmidic DNA isolated by miniprep. The plasmids were digested with *KpnI* to confirm the 10.2 kb sMMO operon containing insert. To confirm the correct orientation of the 10 kb

insert within the pTN2 vector, restriction pattern analysis was carried out by digestion with *Xba*I. If the sMMO operon was inserted in the correct orientation then digestion with *Xba*I would show a band at ~2.2 kb and a band >10 kb in size (Fig. 6.4). To confirm the correct orientation of the insert, the plasmid was also digested with *Pvu*W (Fig. 6.5). This work was also carried out by Dr Malcolm Lock (Sheffield Hallam University).

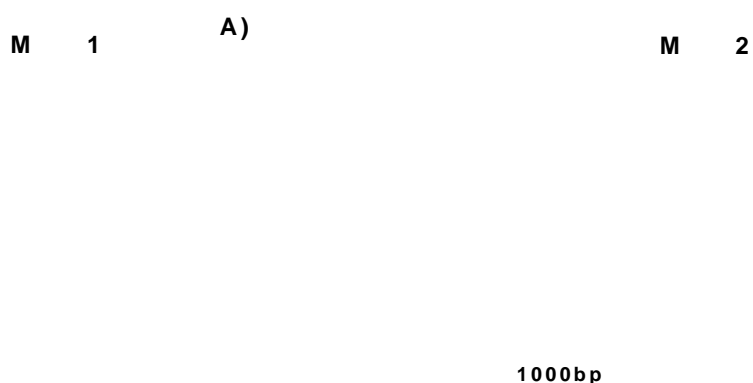


Fig 6.4A) Predicted banding pattern of pT2ML digested with *Xba*I.(Nebcutter, New England Biolabs

Fig 6.4B) 1% Agarose gel showing 1kb generuler DNA marker (M) and pT2ML digested with *Xba*I (1).

Fig 6.5A) Predicted banding pattern of pT2ML digested with *Pvu*W

Fig 6.5B)1% Agarose gel showing 1kb generuler DNA marker (M) and pT2ML digested with *Pvu*W.

6.3 Assessing the efficiency of pT2ML

6.3.1) Expression of recombinant wild-type sMMO in pT2ML

To assess the efficiency of the new expression system, a recombinant "wild type" was created that would restore wild type activity to the sMMO negative expression host using the new expression system. This plasmid designated pT2ML.WT1A was compared against wild type *Ms. trichosporium* OB3b to analyse the efficiency of the expression system. The WT1A plasmid was created by amplification of a 1.6 kb fragment from the sMMO operon by PCR using pTJS176 as the template and primers P1 and P4 which flank the *Bam*HI/*Nde*I exchangeable cassette (Table 6.2).

Primer	Sequence 5'-3'	Location
primer P1	ATTCGAGCTCAAACGTTCTGAAC	upstream of <i>Nde</i> I site
primer P4	GGGCTCTCGACGCCATATTTG	downstream of <i>Bam</i> HI site

Table 6.2) Sequence of primers used for screening of transformant colonies by colony template PCR

The PCR product was purified, digested with *Bam*HI and *Nde*I and ligated into the pT2ML expression vector using the same enzymes. The ligation reaction mixture was transformed into chemical competent *E. coli* XL1 and transformant colonies were screened using colony PCR with the P1 and P4 primers as described in the Materials and Methods chapter. Potential successful transformations were identified by a ~1.6 kb PCR product (Fig. 6.6). Any colonies containing pT2ML plasmid without insert were identified by a ~1.1 kb PCR product and were discarded as were any colonies failing to give a PCR product. Potential pT2ML.WT1 containing colonies were incubated overnight in liquid LB broth containing ampicillin and plasmids were

purified by miniprep. The correct expression plasmid was confirmed by DNA sequencing. The pT2ML.WT1A plasmid was transformed into *E. coli* S17-1 and transferred to the sMMO negative host strain *Ms. trichosporium* SMDM by conjugation as described in the Materials and Methods chapter. The WT1A mutant was grown in liquid culture and on agar plates at a low copper to biomass ratio to induce expression of sMMO. The activity of WT1a was confirmed by a positive naphthalene test.

M 1 2

Fig 6.6) 1% agarose gel showing 1 kb generuler DNA marker (M) and products from a colony PCR screen. Successful ligation of BamHI/NdeI digested insert into pT2ML shows a 1.6kb product (1). Recircularised vector shows 1.1 kb product (2, 3).

6.3.2) Comparison of wild type OB3b and pT2ML.WT1A activities towards naphthalene

A 50 ml culture of *Ms. trichosporium* SMDM (pT2ML.WT1A) cells in NMS medium was used to inoculate a 5 l fermentor with the same medium. Methane gas and air were pumped through at a 5:1 ratio and the temperature was maintained at 30°C (see section 2.1.2). The cells were tested for sMMO activity using the naphthalene test and after 3 weeks a strong positive reaction was detected. The cells were then harvested, resuspended in a minimal amount of 25 mM MOPS (1 mM benzamidine, 1 mM DTT, DNase [20 pg/ml]) and drop frozen in liquid nitrogen and stored in the -80°C freezer. A 50 ml culture of wild type *Ms. trichosporium* OB3b was also grown up in the 5 l fermentor, harvested and stored in the same way after a positive naphthalene test had been detected. For both batches of cells at harvest the OD_{600} was > 5 . An approximate value for the rate of naphthalene oxidation was measured using the spectrophotometer as described in the Materials and Methods section. The cells were incubated at 30 °C shaking at 180 rpm for 60 min then reaction stopped by incubating on ice for a further 5 min. The cells were pelleted at 17,000 * g and the supernatant used for the spectrophotometric assay. A 1% TOD solution was added to each cuvette and the colour formation reaction was allowed to take place for 15 s before being quenched by the addition of 120 μ l glacial acetic acid. The absorbance at 540 nm was recorded and plotted against a standard curve of 1-naphthol. The WT1A cells showed a slightly higher activity towards naphthalene than the OB3b cells in this case (Table 6.3).

Enzyme	1 -naphthol formation (nmoles/min)	relative activity (%)	± standard error
OB3b	0.40	100	0.07
WT1A	0.60	150	0.22

Table 6.3: Comparison of Activity of pT2ML.WT1A and wild type OB3b against naphthalene. Activity was determined by spectrophotometer (Materials and Methods section 2.8.4) and is displayed as a mean of three separate experiments from a single batch of drop frozen cells.

6.3.3) Comparison of wild type OB3b and pT2ML.WT1A activity towards butane

Cell free extract was prepared from drop frozen cells of both OB3b and WT1A as described in the Materials and Methods section 2.8.2 as follows. The cell suspension was passed three times through a French pressure cell and centrifuged at 55,000 x g for 90 min before the soluble extract was removed and frozen in liquid nitrogen. 2 ml of cell extract was incubated with 3 ml butane and NADH [5 pM] for 5 min at 30 °C. The reaction was stopped by incubating for 5 min on ice before an internal standard of 1-propanol (2 pmoles) was added and the reaction mixture extracted with ether. The ether was evaporated at room temperature until the volume was < 50 µl then run on Shimadzu GC2010 with an RTX-5 column as described in the Materials and Methods section 2.8.10 (Fig. 6.7a, Fig. 6.7b). The results show that the *Ms. trichosporium* WT1A mutant soluble extract has a 3-fold higher specific activity towards butane than the soluble extract of wild type *Ms. trichosporium* OB3b (Table 6.4).

Fig 6.7A) Partial chromatogram showing the 1-butanol product from the oxidation of butane by wild type OB3b

Fig 6.7B) Partial chromatogram showing the 1-butanol product from the oxidation of butane by pT2ML.WT1A

Enzyme	Specific activity (nmole min ⁻¹ mg ⁻¹)	% Relative activity	± Standard error
OB3b	0.42	100	0.02
WT1A	1.30	307	0.28

Table 6.4) Comparison of pT2ML.WT1A and wild type OB3b butane oxidation activity. Specific activities are shown as a mean of three separate experiments from a single batch of drop frozen cells.

6.4 Summary of the new expression vector pT2ML

The creation of the new expression vector pT2ML has decreased the number of cloning steps required in creating new site directed mutants within the hydroxylase a subunit of sMMO. The ability to clone fragments directly into the *mmoX* gene and to subsequently screen for the desired construct by PCR has facilitated the process of creating site directed mutants considerably. This new expression system has been compared to the wild type OB3b and the results from a single pair of fermentor runs show that WT1A showed substantially increased activity compared to the wild type enzyme.

The difference in specific activity observed between the wild-type *Ms. trichosporium* OB3b and recombinant wild type enzyme expressed in *Ms. trichosporium* WT1A may, judging from other results described here, be due at least in part to batch to batch variation between fermentor runs. It should be noted that these cells were harvested at a similar time to each other but were not grown to as high an OD_{600} as the wild-type OB3b and other site directed mutants described in chapters 3, 4 and 7. However it is clear from the results that the recombinant wild-type strain *Ms. trichosporium* WT1A produces sMMO expressing cells with at least the same specific activity as the original wild type strain.

Chapter 7: Mutation studies using the new expression vector

PT2ML

7.1) Introduction

As mentioned in the previous chapter, the new expression vector pT2ML was designed to simplify the site directed mutagenesis of *mmoX* from *Methylosinus trichosporium* OB3b. This new expression vector has restriction sites removed allowing a 1 kb *BamH**V**Nde*I fragment to be used as the exchangeable cassette. The deletion of a 0.5 kb sequence within this fragment has also allowed for quick screening for successful ligation of site directed mutants into this vector using colony PCR. In Chapter 6 it was shown that this expression system could produce functional recombinant sMMO with activity comparable to the wild type enzyme (6.3.2 - 6.3.3). In addition to the site directed mutants described in Chapters 3 and 4; two more site directed mutants have been created using this new system in order to complement the mutagenesis studies.

7.1.1) Role of Phe 188 as a substrate gating residue in sMMO

In Chapter 3 a number of site directed mutants were created at the position Leu110 to study the role of this amino acid as a gating residue. As mentioned in that chapter, this role for Leu 110 was proposed after the observation that the conformation of this residue changed during crystallisation of the sMMO hydroxylase in its oxidised state

and reduced states (Rosenzweig *et al.* 1997). The conformational change creates an opening between the hydrophobic cavity 1 and adjacent hydrophobic cavity 2 and it was suggested that this may indicate entry of substrate through these hydrophobic cavities to the active site. However, it was noted that additional movement of either this residue or Phe188 (Fig. 7.1) would be required to allow substrate access to the active site (Rosenzweig *et al.* 1997).

7.1.2) The Gly 113 mutant of butane monooxygenase

In Chapter 4, a number of mutants were created to probe the effects of changing key residues within the hydrophobic pocket of sMMO to the homologous residues within butane monooxygenase. In similar experiments with butane monooxygenase (Halsey *et al.* 2006) a number of residues within butane monooxygenase were mutated to their counterpart residues within sMMO. One of these butane monooxygenase mutants G113N showed changes in regioselectivity and altered kinetic data with a range of alkane substrates. The G113N mutant of butane monooxygenase showed a lower specific activity towards its natural substrate butane and a shift in regioselectivity was seen with both butane and propane from primarily terminal oxidation in the wild type to almost exclusively sub-terminal oxidation with the G113N mutant (Halsey *et al.* 2006). Methane oxidation assays carried out by measuring methanol accumulation showed that the initial rate of methanol formation was lower than that of the wild type butane monooxygenase. However, it was also observed that the G113N mutant of butane monooxygenase accumulated methanol to a level 3.5-fold higher than the wild type enzyme. Kinetic

analysis of this mutant showed that it has a greater affinity for both methane and methanol with K_m of 340 pM and 750 pM respectively, compared with 1100 pM and 1250 pM for the wild type enzyme (Cooley *et al.* 2009). These data indicate an importance of this residue in the function of butane monooxygenase with roles both in regioselectivity and activity towards these alkane substrates.

7.1.3) Designing new sMMO mutants F188A and N116G

The F188A site directed mutant has been created to investigate the effects of a smaller side chain at this position and what effect it has on the rate and regioselectivity of the enzyme. The mutation of a phenylalanine to an alanine at position 188 within *m m oX* provides a smaller side chain at this position yet maintains the hydrophobic nature of this residue. The residue Asn 116 within soluble methane monooxygenase (Fig. 7.1) corresponds to the Gly 113 residue of butane monooxygenase. To look at the role of this residue the mutant **N116G** was created, which changes the Asn residue to the corresponding Gly residue of butane monooxygenase. A number of assays have been carried out to probe the effect that these mutants have on the activity of sMMO.

Fig 7.1) Diagram showing the Asn116 (red) and Phe188 residues (blue). The diiron centre can be seen in orange and all other hydrophobic surfaces are coloured white.

7.2 Construction of mutants N116G and F188A using pT2ML expression vector

The mutants N116G and F188A were created by 4 primer overlap PCR using the appropriate primer sets (Table 7.1). The PCR product was purified, digested with BamHI and *NdeI* and ligated into the pT2ML expression vector using the same enzymes. The ligation reaction mixture was transformed into chemical competent *E. coli* XH and transformant colonies were screened using colony PCR with the P1 and P4 primers (Table 7.1).

Primer	Sequence (5'-3')	Description
P1	ATTTCGAGCTCAAACGTTCTGAAC	Forward primer 410 bp upstream of BamHI site
N116GP2	GA AGC GGC GAT GGC GCC ATA TTC GCC	Reverse complement of primer N116GP3
N116GP3	GGC GAA TAT GGC GCC ATC GCC GCT TC	Mutagenic primer containing the Asp → Gly mutation and silent change to incorporate the novel restriction site <i>SfiI</i>
F188AP2	A GCC GTC GGC CGC GAC GCG CTT	Reverse complement of primer F188AP3
F188AP3	AAG CGC GTC GCG GCC GAC GGC T	Mutagenic primer containing the Phe → Ala mutation and silent change to incorporate the novel restriction site <i>EagI</i>
P4	GGG CTC TCG ACG CCA TAT TTG	Reverse primer 251 bp downstream of <i>NdeI</i> site

Table 7.1) Mutant primer sets for the construction of site directed mutants N116G and F188A. Mutant codons are highlighted in bold, specific nucleotide changes are underlined, the novel *SfiI* restriction site (N116G) is highlighted in green and the *EagI* restriction site (F188A) is highlighted in yellow.

The desired clone was provisionally identified among the progeny on the basis of a ~1.6 kb PCR product. Any colonies containing the pT2ML plasmid without insert were identified a ~1.1 kb PCR product and were discarded as were any colonies failing to give a PCR product. Potential mutant containing colonies were incubated overnight in liquid LB broth containing ampicillin and plasmid was collected by miniprep. The 1.6 kb Colony PCR products from these colonies were then digested using either *SfiI* (N116G) or *EagI* (F188A) to identify the desired site directed

mutation (Fig. 7.2a, 7.2b). The correct mutant expression plasmids were further confirmed by DNA sequencing. The mutant plasmids were transformed into *E.coli* S17-1 and transferred to the sMMO negative host strain *Ms. trichosporium* SMDM by conjugation as described in the Materials and Methods chapter. The N116G and F188A mutants were grown in liquid cultures and on agar plates at a low copper to biomass ratio to induce expression of sMMO. The activity of the N116G and the F188A mutants was confirmed by a positive naphthalene test (Fig. 7.3).

Fig. 7.2A) Fig 7.2B) M 1 2 3 4

N 116 mutant Wild type

Fig 7.2a) Diagram showing the predicted DNA band size of P1-P4 PCR screening fragment digested with Sfil for the N116G mutant and wild type sMMO.

Fig 7.2B) Agarose gel showing 100 bp generuler DNA marker (M), 3 putative N116G PCR fragments diaested with Sfil (1-3) and a control diaest carried out on a wild tvoe *m m oX* PCR frament (4)

Fig 7.3) NMS agar plate showing positive naphthalene oxidation assay for *Ms. trichosporium* OB3b (wild type), *Ms. trichosporium* SMDM (pT2ML.N116G) and *Ms. trichosporium* SMDM (pT2ML.F188A). Naphthalene oxidation assay was carried out as described in Materials and Methods section 2.8.3

7.3 N116G and F188A show reduced rate with aromatic substrates but little or no change in regioselectivity

7.3.1 Oxidation of naphthalene by N116G and F188A

As mentioned previously oxidation of naphthalene can only occur at two positions on the aromatic ring to give either 1-naphthol or 2-naphthol as the oxidation products. The N116G and F188A mutants show a slight shift in regioselectivity with a slight excess of 1-naphthol produced compared to the wild type enzyme ($P=0.005$ and 0.004 respectively) where 2-naphthol is the major oxidation product (Fig. 7.4).

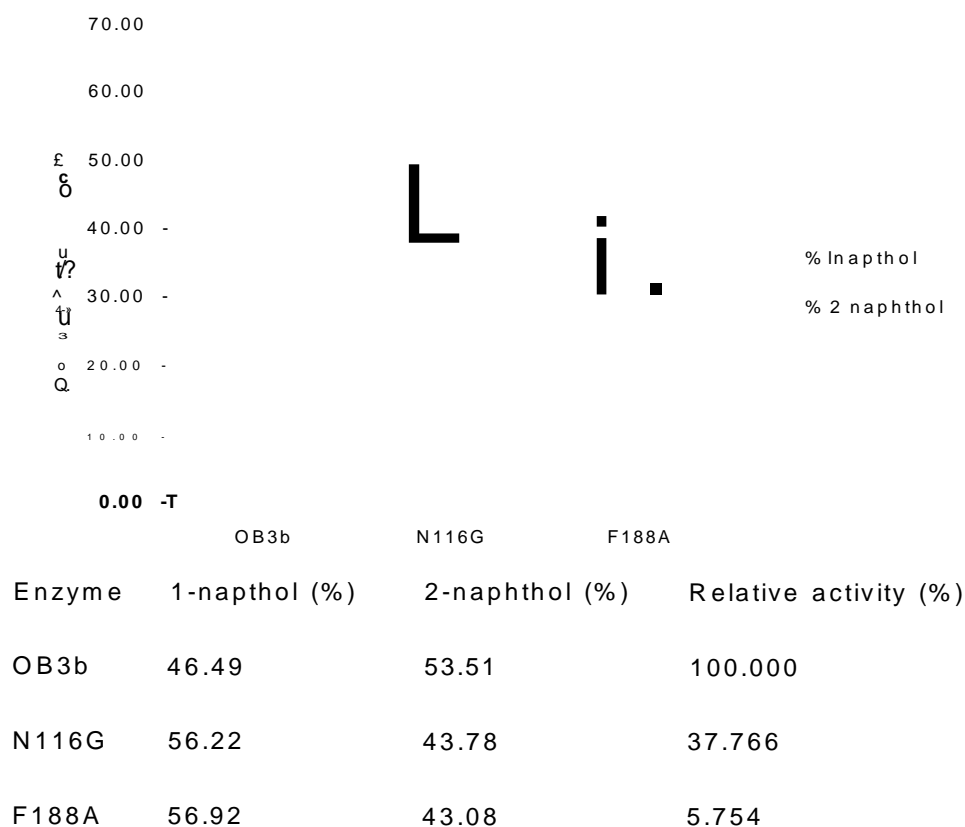


Fig 7.4) Percentage product distribution for naphthalene oxidation showing relative activity to OB3b which has been corrected for OD₆₀₀ and is given as 0.42 nmoles min⁻¹ at OD₆₀₀ = 1.

The approximate rate of naphthalene oxidation was calculated based on the colorimetric oxidation assay and absorbance at wavelength 540 nm measured upon addition of 1% TOD reagent as described in the Materials and Methods chapter. The amount of naphthalene was worked out from the product standard curve of 1-naphthol as seen in Chapter 4. The activity of both N116G and F188A towards naphthalene was significantly reduced. When compared to the wild type, the mutants showed 37.8% and 5.8% activity, respectively. As mentioned previously these specific activities are mostly with respect to the formation of 1-naphthol only because the absorbance of the diazo dye formed from this isomer at 540 nm is much greater than that from 2-naphthol (Chapter 4, Fig. 4.8)

7.3.2) Oxidation of ethylbenzene by N116G and F188A

The oxidation of the aromatic substrate ethylbenzene can yield five possible hydroxylated oxidation products: 1-phenylethanol, 2-phenylethanol, 2-ethylphenol, 3-ethylphenol and 4-ethylphenol. Assays were carried out with whole cells containing 5 mM sodium formate to provide reducing equivalents for the enzyme (as mentioned in the Materials and Methods section 2.8.1). Product analysis (Fig. 7.5) was carried out using a Shimadzu 2010 GC with a Restek RTX-5 column. As was seen in Chapter 3, oxidation of ethylbenzene by the wild type enzyme in 48 h assays produced only two oxidation products. A similar product distribution was also seen in 1 h assays where only 1-phenylethanol and 4-ethylphenol were detected. No novel oxidation products were detected with either N116G or F188A. 4-Ethylphenol was the predominant oxidation product with both mutants, which showed reduced activity compared to the wild type with this substrate (Table 7.2).

Fig 7.5). Part of a representative GC trace showing base line resolution of ethyl benzene oxidation products for an sMMO assay. Identity of peaks was confirmed by comparing retention times against authentic standards (not shown)

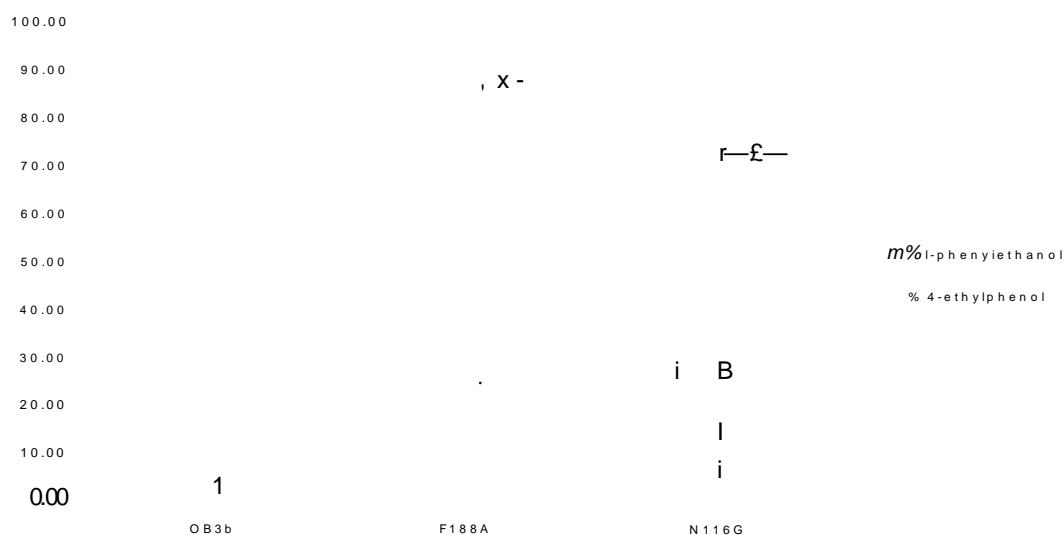


Fig 7.6) Graph showing product distribution from 1 h ethylbenzene oxidation assay. Data is given as a mean of three different experiments from a single batch of drop frozen cells for each mutant. Error bars show \pm standard error

A slight change of regioselectivity was observed with both mutants. The oxidation of ethylbenzene by the F188A mutant showed an increase in ring hydroxylation with 89% of the total product being 4-ethylphenol compared to 78% with the wild type ($P < 0.001$). The N116G mutant showed a slight increase in side chain hydroxylation compared to the wild type with 27.01% of the total product as 1-phenylethanol compared to 21.86% with the wild type enzyme ($P = 0.005$). Both mutants displayed a reduced specific activity towards ethylbenzene compared to the wild type enzyme.

(Fig. 7.6, Table 7.2)

Enzyme	1-phenylethanol t% > HO r	4-ethylphenol (%) f	Relative rate (%)
OB3b wild type	21.86 ± 0.67	78.14 ± 0.67	100.00
N116G	27.01 ± 1.45	72.99 ± 1.45	68.71
F188A	11.49 ± 1.67	88.51 ± 1.67	77.33

Table 7.2) Product distribution of ethylbenzene oxidation products. Relative rate has been corrected for differences in OD_{600} and is relative to the rate of wild type OB3b which was measured at 0.35 ± 0.02 nmole/min/mg protein

7.3.3) Oxidation of mesitylene by N116G and F188A

As mentioned previously the substrate mesitylene (1,3,5-trimethylbenzene) was chosen as a candidate for study due to its size and symmetry of the three methyl substituents, which mean that only two possible primary oxidation products were expected. All assays were set up for 1 h and the oxidation products (Fig. 7.7A, 7.7B) quantified by GCMS as mentioned in the Materials and Methods. The N116G mutant showed the same characteristics as the wild type enzyme, with a predominant side chain hydroxylation. When the F188A mutant was analysed, a 13 fold increase in ring hydroxylation was detected compared to the wild type enzyme (P=0.00197) (Table 7.3).

Enzyme	$\begin{array}{c} \text{OH} \\ \\ \text{H}_3\text{C} \cdot / \text{L} \cdot \text{C} \text{H}_3 \\ \text{V} \\ \text{CH}_3 \end{array}$ 2,4,6-trimethylphenol (%)	$\begin{array}{c} \text{CH}_2\text{OH} \end{array}$ 3,5-dimethyl benzyl alcohol (%)
Ob3b	0.40 ± 0.34	99.60 ± 0.34
N116G	0.41 ± 0.14	99.59 ± 0.14
F188A	5.42 ± 4.72	94.58 ± 4.72

Table 7.3) Percentage product distribution for mesitylene oxidation. Assays were carried out in triplicate from a single batch of drop frozen cells for each mutant and are displayed as mean values ± standard error.

Fig 7.7B

Abundance

TIC: M ESF2.D

Fig 7.7A) Partial GC trace showing the products from oxidation of mesitylene by N116G

Fig 7.7B) Partial GC trace showing the products from oxidation of mesitylene by F188A

7.3.4) Oxidation of biphenyl by N116G and F188A

Analysis of the oxidation of biphenyl by the N116G and F188A mutants also shows a slight relaxation in regioselectivity compared to the wild type. The oxidation of biphenyl can produce three possible oxidation products depending on which position on the aromatic ring is oxidized. The oxidation assays were carried out using whole cells plus 5 mM sodium formate to provide an excess of reducing equivalents for the reaction as mentioned in the Materials and Methods section. The F188A and N116G mutants showed similar regioselectivity compared to the wild type enzyme, with 4-hydroxybiphenyl representing 98-99 % of the oxidation products. A relaxation of regioselectivity was observed with both mutants, with more 2-hydroxybiphenyl and 3-hydroxybiphenyl being detected than with the wild type enzyme. The N116G mutant showed a 27.5 fold increase in the percentage of 2-hydroxybiphenyl produced and a 7.4-fold increase in 3-hydroxybiphenyl compared to the wild type enzyme however these are not seen as statistically significant ($P>0.05$). The F188A showed a statistically significant 46.5-fold increase in the percentage of 2-hydroxybiphenyl produced ($P=0.002$) and an 8-fold increase in the percentage of 3-hydroxybiphenyl which was not statistically significant ($P>0.05$) (Table 7.4).

Enzyme	2- hydroxybiphenyl (%)	3- hydroxybiphenyl (%)	4- hydroxybiphenyl (%)
Wild type	0.02 ± 0.03	0.05 ± 0.09	99.94 ± 0.13
N116G	0.55±0.16	0.37±0.16	99.08±0.17
F188A	0.93±0.03	0.40±0.19	98.66±0.2

Table 7.4) Percentage product distribution of biphenyl oxidation. Data is shown as a mean of 3 separate experiments from a single batch of drop frozen cells for each mutant and are shown ± standard error

7.3.5) Oxidation of toluene by N116G

Assays were carried out at 30°C using whole cells supplemented with 5 mM sodium formate. An internal standard was added and products were extracted into ether before evaporating at room temperature and running on a Shimadzu GC2010 with an RTX-5 column. As mentioned previously there are four possible hydroxylated products that could be formed from the oxidation of toluene by sMMO. The N116G mutant showed no novel oxidation products compared to the wild-type enzyme and (like the wild-type) showed benzyl alcohol as the major oxidation product under these reaction conditions. There was a slight increase in side chain hydroxylation compared to the wild type enzyme with N116G (P=0.032) (Fig. 7.8).



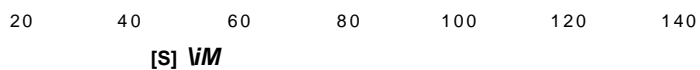
Enzyme	Benzyl Alcohol (%)	p-cresol (%)	relative rate (%)
OB3b	71.38 ± 2.89	28.62 ± 2.89	100
N116G	80.68 ± 0.06	19.32 ± 0.06	10.33

Fig 7.8) Product distribution of ethylbenzene oxidation products. Relative rate has been corrected for differences in $\sigma_{D 600}$ and is relative to the rate of wild type OB3b which was measured at 2.95 nmoles min⁻¹ at $\sigma_{D 600} = 1$.

7.4 Kinetic data for toluene oxidation by wild type OB3b and N116G

7.9a

Hanes w olf plot OB3b



7.9b

Hanes w olf plot N116G Toluene

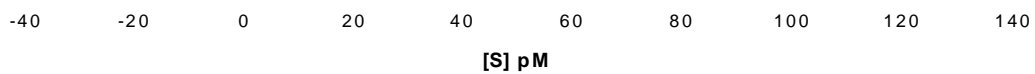


Fig 7.9a) Hanes Woolf plot for toluene oxidation by *Ms. trichosporium* OB3b. The trendline has been fitted to the data using Microsoft Excell software.

Fig 7.9b) Hanes Woolf plot for toluene oxidation by N116G. The trendline has been fitted to the data using Microsoft Excell software.

	K _m (pM)	V _{max} (nmoles/min)
OB3b	21.0 ± 7.0	22.1 ± 5.9
N116G	13.0 ± 9.0	5.7 ± 3.1

Table 7.6) K_m and V_{max} for OB3b and N116G calculated from Hanes Wolf plots (figs 9a + 9b). Data is corrected to a cultural OD₆₀₀ = 1.0

The kinetic data for toluene oxidation by both OB3b and N116G was collected by adding varying amounts of toluene saturated water to whole cells and measuring the amount of total product by Shimadzu 2010 GC with a Restek column as described in the methods. The amount of toluene added to each sample was also measured by GC and used to create a Hanes Wolf plot for OB3b and N116G. The K_m and V_{max} values were calculated by the following equation:

$$\frac{V}{[S]} = \frac{V_{max}}{K_m + [S]} + \frac{V_{max}}{[S]}$$

Where [S] is the substrate concentration and V is the reaction velocity. The K_m of the N116G enzyme is 13.0 pM, only slightly lower than 21.0 pM for the wild type. This indicates that in comparing wild type sMMO and the N116G mutant, there is no detectable difference in affinity for the substrate toluene. However the V_{max} of the N116G mutant showed >3.8 fold decrease at 5.7 nmoles min⁻¹ compared to 22.1 nmoles min⁻¹ for the wild type (Table 7.6). Although it is accepted that these data are limited, it is clear that the maximum rate of the N116G mutant is greatly reduced compared to the wild type enzyme.

7.5 The mutants showed no measurable activity towards alkanes or tri-aromatic substrates

Soluble extracts of the F188A and N116G mutants were prepared and assayed with the alkanes: butane, pentane and hexane as described in the Materials and Methods chapter. Oxidation assays were carried out over a range of reaction times ranging from 1-30 min however no activity could be detected with either N116G or F188A. Activity was detected with the wild-type enzyme in parallel experiments.

Oxidation assays for up to 48 h were also attempted with anthracene and phenanthrene as substrates using both using biomass on agar plates and liquid cultures. No hydroxylated products were detected for the N116G, F188A or the wild type enzyme with these triaromatic substrates.

7.6 Summary

The N116G and F188A mutants were created to complement work carried out in previous chapters. The N116G mutant showed similar results to the previous mutants analysed in Chapter 4. No increase in butane oxidation was observed and although small changes in regioselectivity of the N116G mutant compared to the wild type were seen, no shift towards terminal carbon oxidation was seen. This shows that this site directed mutation is not enough to confer a "BMO-like" phenotype upon this mutant. The specific activity of the N116G mutant was reduced compared to the wild type with all substrates measured. The kinetic data for the oxidation of toluene shows that the N116G mutant has a similar affinity for the substrate compared to the wild-type enzyme but has a significantly reduced maximum oxidation rate. The F188A mutant showed a regioselectivity to the wild type enzyme. A shift in

regioselectivity of naphthalene and biphenyl was seen and an increase in ring hydroxylation was seen with ethylbenzene and mesitylene compared to the wild-type. This residue has been implicated along with the residue Leu 110 in having a gating role controlling substrate access (Rosenzweig *et al.* 1997). No evidence has been found to suggest that the F188 residue has a gating role in sMMO. The F188A mutant also has only a little effect on the regioselectivity of the enzyme compared to the L110 mutants seen in Chapter 3.

Chapter 8: Discussions

8.1 Leu 110 is not the limiting factor preventing oxidation of triaromatic compounds by wildtype sMMO

The possibility of leu 110 as a gating residue that controls access of substrate to the active site led to the hypothesis that this residue may be the limiting factor in preventing oxidation of larger triaromatic compounds by sMMO. In the hydroxylase α -subunit of the related toluene *ortho*-monooxygenase from *Burkholderia cepacia* G4, the Val 106 residue occupies the equivalent position to Leu 110 in sMMO (Shields *et al.* 1995). A similar site directed mutagenesis experiment in the same enzyme by the Wood group showed that the V106A mutant exhibited increased activity towards the three ring aromatic compounds phenanthrene, anthracene and fluorene (Canada *et al.* 2002). It was thought that opening the gate by putting a smaller residue at this position allowed easier access for larger substrates to the active site of toluene *ortho*-monooxygenase.

Site directed mutagenesis of *mmoX* was carried out to create mutants with varying sized side chains at position 110. Mutants with less bulky side chains at position 110 were assayed to see whether these residues provided more space to allow access of larger triaromatic substrates into the active site. When the Leu 110 residue was mutated to either the smaller Gly and Cys residues or the larger Tyr and Arg

residues oxidation of triaromatic compounds could not be detected by a colorimetric assay based on the naphthalene test or by GCMS with total ion or selected ion monitoring. Selected ion monitoring was used to screen for ions of m/z 194, corresponding to singly charged ions of monohydroxylated triaromatic compounds, with very high degrees of sensitivity (<1 pM). Hence neither the wild type nor any of the site directed mutants (including the smaller Gly and Cys mutants) can detectably oxidize triaromatic compounds. This suggests that the Leu 110 residue is not the limiting factor and further mutations are required for the oxidation of triaromatic compounds by sMMO.

It has been shown that the corresponding V106A mutant of the homologous toluene *ortho*-monooxygenase showed increased triaromatic oxidation (Canada *et al.* 2002). However it should be noted that toluene, the natural substrate for this enzyme is a much larger compound than the natural substrate methane, of sMMO.

Crystallographic studies of the toluene-4-monooxygenase and toluene *o*-xylene monooxygenase (Sazinsky *et al.* 2004; Bailey *et al.* 2008) have shown that the aromatic monooxygenases have a much more accessible active site than the sMMOs, probably due to the larger size of their natural substrates. The access of substrates to the active site within sMMO is likely to be via a series of hydrophobic cavities that can form a channel allowing access to the active site and so constrictions in this substrate entry/ exit channel may prevent entry of triaromatic compounds even when the Leu 110 residue has adopted an "open" conformation. If there are several constrictions on the pathway that substrates take to and from the active site of sMMO, a number of mutations may be needed to allow access of triaromatic compounds and other very large substrates.

8.2 Leu 110 is an important residue in determining the regioselectivity of sMMO

The data shown in Chapter 3 (Tables 3.1 - 3.4) show that this Leu 110 is extremely important in determining the regioselectivity of sMMO. With the wild type enzyme, oxidation of aromatic substrates predominantly occurs at the short ends of the roughly rectangular substrate molecule. With toluene as substrate, the oxidation products are benzyl alcohol and p-cresol (Table 3.2). With naphthalene the primary oxidation product is 2-naphthol (Table 3.1); with biphenyl the primary oxidation product is 4-hydroxybiphenyl (Table 3.4) and with ethylbenzene both 1-phenylethanol and 4-ethylbenzene were seen as oxidation products (Table 3.3). However, all mutations at position 110 showed a shift away from this oxidation at the "short end" of the roughly rectangular substrates with increasing amounts of 1-naphthol from naphthalene, and 2- and 3- hydroxy products from substituted monaromatics and biphenyl. This result was unexpected since a "gating role" for Leu 110 suggested that mutations to smaller residues would be more likely to allow substrates into the active site and conversely mutations to larger residues would be more likely to restrict access to the active site. These results showed that rather than increasing or restricting access to the active site, both bulkier side chain mutations and smaller side chain mutations had similar effects in relaxing regioselectivity.

As mentioned previously a number of mutagenesis studies have been carried out on various monoaromatic monooxygenases at the corresponding position to Leu 110. Mutation at Val 106 of toluene-ortho-monooxygenase and Ile 100 of toluene-4-

monooxygenase have indicated that this residue is important for gating access of substrate to the active site (Canada *et al.* 2002; Tao *et al.* 2004; McClay *et al.* 2005). However some mutations at this position such as the lie 100 mutants of toluene *o*-*xylene* monooxygenase, have also shown the importance of this residue in regioselectivity of these enzymes (Vardar and Wood, 2004; Notomista *et al.* 2009).

The results here indicate that Leu 110 is an important residue in determining the precision of regioselectivity with aromatic substrates. This may be mediated via the conformational changes shown to affect this residue in its various crystal forms. It should be noted that in the crystal structures of sMMO published to date, if Leu 110 lies on the substrate entry pathway, it needs to adopt a conformational change which opens the aperture connecting cavities 1 and 2 wider than is seen with any of the crystal structures (Elango *et al.* 1997; Rosenzweig *et al.* 1997; Sazinsky and Lippard, 2005). This is thought to come about from conformational changes during the assembly of the whole enzyme complex. However to date no crystal structure of the entire sMMO complex has been observed. The “open” and “closed” forms of Leu 110 may act as a “clamp” holding the aromatic substrates in an orientation that promotes terminal oxidation of the aromatic substrates. The Swiss-model program was used to model the active sites of mutants L110C and L110R (Fig. 8.1) based on the crystal structure published for the sMMO hydroxylase of *Ms. trichosporium* OB3b (Elango *et al.* 1997). These mutants adopt a conformation where the distance between the sidechain and the diiron site is greater than that of the wild type Leu 110 residue. Increasing the distance between the residue and the diiron site allows for greater movement of the substrate within the active site. This results in an increase in subterminal oxidation of aromatic compounds and relaxed regiospecificity.

Fig 8.1) Diagram showing distances from diiron site for A) Leu 110, B) Cys 110 and C) Arg 110. The models were created based using Swiss-model automated modelling and is based on the *Ms. trichosporium* sM M O hydroxylase crystal structure (pdb accession code 1M HY)

8.3 The presence of other enzymes in the methanotroph cells affects product distribution

It should be noted that the product distribution of oxidation products can alter with time. One way that this can happen is via the action of other enzymes in the methanotroph metabolic pathway further oxidizing the initial oxidation products.

When toluene oxidation was carried out in whole cells of wild type *Ms. trichosporium* OB3b over a 48 h period as described in Chapter 3 (Table 3.2), the product distribution showed the major oxidation product as 63% p-cresol. However when a 5 min oxidation assay was carried out with toluene, the wild type *Ms. trichosporium* OB3b cells showed benzyl alcohol as the major oxidation product at 71% (Table 4.4). This difference in product distribution is most likely due to the action of methanol dehydrogenase working on the benzyl alcohol. This enzyme has been shown to have an activity towards benzyl alcohol that is 52% that of the activity towards the natural substrate methanol (Mountfort, 1990).

Similarly oxidation of ethyl benzene by wild-type OB3b cells for 1 h gave 78% 4-ethylphenol as the primary oxidation product (Fig. 7.4, 7.5). However when wild-type OB3b cells were left for 48 h incubations with ethyl benzene the major oxidation product was 95% 1-phenyl ethanol (Table 3.3). When mesitylene was the substrate, assays had to be run for 1 h because 24 h and 72 h assays showed none of the expected oxidation products. However trace amounts of 3,5-dimethyl benzoic acid were detected at all three timescales, indicating further oxidation of the 3,5-dimethyl benzyl alcohol product (Table 4.9, Fig. 7.6).

Methanol dehydrogenase is not the only enzyme in the metabolic pathway that could alter the product distribution in reactions initiated by the action of sMMO. A general aldehyde dehydrogenase has been described in *Ms. trichosporium* OB3b capable of further oxidizing the primary oxidation products (Patel *et al.* 1980). A secondary alcohol specific dehydrogenase has also been described within *Ms. trichosporium* which may also act upon the oxidation products of various substrates tested in this work (Hou *et al.* 1979, 1981). In particular this secondary alcohol dehydrogenase has been shown to have a high activity towards 2-butanol which may be one of the factors why this oxidation product was not detected by either the wild type or any of the mutants. These enzymes are soluble and therefore are also expected to be present within the soluble extract used for the assays; hence, the only way completely to exclude their action would be to use purified sMMO protein.

In light of the presence other enzymes, every effort was taken to make assay times as short as possible to get the most accurate data and to minimize the effects of other enzymes upon the assays. Since a large concentration of NADH or formate is added at the start of the reaction, during the initial phase of the reaction there is an excess of reducing equivalents which presumably favour the action of the monooxygenase (which require reducing equivalents). However as the reducing equivalents get used up there will be an increase in oxidized cofactors required by the other enzymes such as methanol dehydrogenase. The data from the longer assay times are still valid as long as comparison of mutants and wild type enzymes are carried out over the same time period and the possibility of further oxidation of

(some of the) products is taken into account when interpreting the results. However, comparisons have not been made between results from assays carried out over different time periods such as the toluene oxidation assays in Chapter 3 and Chapter 4, because it is generally not possible to separate effects of changes in substrate distribution from the sMMO enzyme from the effects of the subsequent enzymes.

8.4 Different expression levels between batches affects rate

analysis

Another problem encountered in this project was variation in expression levels between different batches of the same strains, when the culture conditions had been changed (e.g. varying lengths of time for growth). In Chapter 6, the activity of the wild-type strain *Ms. trichosporium* OB3b was compared against the activity from *Ms. trichosporium* SMDM containing recombinant wild-type sMMO genes on the plasmid pT2ML-WT, the new expression plasmid encoding for the wild type enzyme. In this case both batches were grown in the fermentor until the cultures tested positive for sMMO activity ($OD_{600} = 5-6$) using the naphthalene oxidation test and then they were harvested. These batches were assayed using butane and naphthalene as the substrates. Since both cultures were grown to similar optical densities using the same conditions, the results were used to compare the new expression system against the wild type enzyme. The cells expressing the wild type enzyme using the new expression system were shown to have activity similar to that of wild type *Ms. trichosporium* OB3b (Table 6.3 - 6.4). However in Chapter 4, the same butane and naphthalene assays were carried out with a batch of wild type *Ms. trichosporium* OB3b that were harvested at a much higher optical density ($OD_{600} = \sim 10$). When naphthalene was assayed with this batch of cells the activity had 83-fold increase compared to the batch of wild type OB3b cells grown to a lower optical density (Table 4.2). Similarly when butane was the substrate wild type OB3b cells grown at a higher optical density showed a 185-fold increase compared to those grown at a lower optical density (Table 4.3, 6.4). The vast difference in expression levels between these batches highlights the need to work with purified proteins for more detailed characterization of the recombinant enzymes.

8.5 Site directed mutations based upon BMO do not confer “BMO-like” regioselectivity.

The site directed mutagenesis of residues near the active site of sMMO to the homologous residues within butane monooxygenase has allowed the comparison of these two enzymes. As mentioned previously, of the 19 reported putative substrate-interacting residues around the active site of sMMO there are 14 that are conserved within BMO (Sluis *et al.* 2002). However, although there is a high degree of similarity between these two enzymes there are some large differences in their activity. The butane monooxygenase enzyme has a much smaller substrate range compared to sMMO and has very low activity towards methane. The butane monooxygenase enzyme oxidizes alkanes with a strong bias towards primary oxidation at the terminal carbon (Arp 1999). In contrast to this sMMO shows a mixture of both terminal and subterminal oxidation with varying stoichiometric ratios depending on the substrate used (Colby and Dalton, 1977; Burrows *et al.* 1984; Fox *et al.* 1990). The active site residues which differed between sMMO and butane monooxygenase were studied to investigate their roles in determining the differences in activity shown by these two enzymes. The butane monooxygenase-based sMMO site-directed mutants showed very similar results to wild type sMMO with respect to the regioselectivity of the enzyme with almost all substrates studied. Various aromatic and aliphatic substrates were oxidized by these mutant enzymes and, with the exception of the oxidation of mesitylene by the M184V mutant (discussed later in this chapter) there was no change in the regioselectivity of any of these mutants compared to the wild type enzyme (Tables 4.1 - 4.9, Figs. 4.4 - 4.5).

As mentioned previously butane monooxygenase oxidizes butane and propane predominantly to 1-butanol and 1-propanol, respectively. The G113N mutation of butane monooxygenase led to 92 % of the oxidation product accumulating as 2-butanol when butane was the substrate compared with up to 90% 1-butanol produced by wild type butane monooxygenase (Arp, 1999; Halsey *et al.* 2006). Propane oxidation by the G113N butane monooxygenase mutant was exclusively sub terminal at a rate which was 2.7 fold greater than that of the wild type enzyme (Halsey *et al.* 2006). This mutant also showed evidence of an altered regioselectivity towards dichloro and trichloroethylene. Hence the G113N mutant, where a BMO residue was replaced by its sMMO equivalent, made BMO more similar to sMMO.

The corresponding mutation within sMMO is the N116G mutant, which had very little activity towards any of the alkanes tested including butane and propane. Activity of this mutant towards aromatic compounds was detectable; however, there was no evidence of altered regioselectivity in the oxidation of ethylbenzene, mesitylene, biphenyl or toluene compared to the wild type enzyme. A slight change in regioselectivity was seen with the oxidation naphthalene by this mutant. The wild type enzyme showed the major naphthalene oxidation product as 2-naphthol (57%). This product distribution was changed when N116G oxidized naphthalene with 56% 1-naphthol as the major oxidation product (Fig. 6.3, Table 6.2).

The C151T mutant showed a decreased proportion of in terminal oxidation with all substrates assayed with the exception of butane; where no secondary alcohol product was detected with either the wild type or the C151T mutant. The oxidation of

naphthalene, mesitylene and biphenyl by C151T showed very little change in regioselectivity compared to the wild type enzyme. The C151T mutant showed a 1.5% reduction in 2-naphthol production compared to the wild type when naphthalene was the substrate (Table 4.2). The oxidation of mesitylene by this mutant showed only a 0.8% reduction in the predominant oxidation product 3,5 dimethyl-benzyl alcohol compared to the wild type. However this was a 5 fold increase in the production of the 2,3,5-trimethylphenol ring hydroxylation product (Table 4.9). The oxidation of biphenyl showed a 2% reduction in the predominant 4-hydroxybiphenyl and a 9.7 fold increase in the oxidation product 3-hydroxybiphenyl compared to wild type sMMO (Table 4.6). When toluene was the substrate the amount of benzyl alcohol produced was reduced from 71% with the wild type to 60% with the C151T mutant. In all these cases the major oxidation product remained the same as the wild type sMMO. The greatest change in regioselectivity between wild type sMMO and the C151T mutant was seen with the substrate hexane. The product distribution of hexane oxidation by wild type sMMO shows 1-hexanol as the predominant oxidation product at 64.3% of the total hexane oxidation products (Table 4.8). This is altered in the C151T mutant to 51% 2-hexanol as the major hexane oxidation product, a change showing the largest increase sub terminal oxidation detected with all substrates tested with this mutant.

8.6 Single mutations of sMMO active site residues to BMO counterparts are not sufficient to confer a BMO-like activity

The various site directed mutagenesis studies carried out by the Arp group on butane monooxygenase have provided some insight into the role of particular residues within the BMO enzyme (Halsey *et al.* 2006, 2007; Doughty *et al.* 2007; Cooley *et al.* 2009). By creating the corresponding mutants within sMMO it was hoped that the roles of key differences within the highly conserved active site and proposed substrate binding cavity of these two homologous enzymes, could be probed to gain insight into what makes these highly similar enzymes have such different activities and substrate ranges. The G113N mutant of butane monooxygenase showed a decrease in specific activity towards butane and an increase in specific activity towards methane and so was reported as being particularly significant in determining the differences in the activity between butane monooxygenase and sMMO. The corresponding N116G mutant within sMMO was created to probe the significance of this residue. The activity of this enzyme towards butane was assayed by GC as described earlier and activity was too low to be detected using this method ($<0.01 \text{ nmol min}^{-1} \text{ mg protein}^{-1}$).

The activity of another butane monooxygenase mutant L279F also showed reduced activity towards all substrates assayed however it did show altered regioselectivity towards alkane substrates and chloroethylenes. The corresponding mutant F282L within sMMO produced an enzyme with hydroxylase subunits that were detectable by SDS PAGE indicating that the enzyme was synthesised and accumulated in the cells. However no activity was detected with this mutant and any of the substrate oxidation assays described including short chain alkanes (propane, butane, hexane), alkenes (propylene), substituted monoaromatics (toluene, ethyl benzene) and diaromatics (naphthalene). In contrast to this the M184V sMMO mutant which has good whole cell activity with all the aromatic substrates tested and gives a strong purple product with the colorimetric naphthalene oxidation assay.

The unsuccessful attempts to recover the analogous V181M mutant via site directed mutagenesis of butane monooxygenase led to the conclusion that perhaps this mutation yielded a butane α -hydroxylase that could not support butane oxidation (Halsey *et al.* 2006). These results show that the role of these key amino acid differences between the two enzymes are more complex than first thought. The site directed mutagenesis of these residues within sMMO to their counterparts within BMO does not confer a "BMO-like" activity upon these mutant enzymes in terms of oxidation rate or regioselectivity. The creation of a mutant within BMO that has reduced butane activity and increased methane activity does not mean that the reverse mutation within sMMO will have the opposite effect. The stability of these mutants is also a factor to consider as mutants have been made in both enzymes that have interesting properties whereas the corresponding mutant in the homologous mutant is unstable and/or inactive.

The results here do show that mutating residues that differ between sMMO and BMO created novel mutants with properties that shed light into how the SDIMOs work. The creation of a C151T mutant with reduced terminal oxidation activity implicates this residue as being important in determining regioselectivity. This work has also produced another mutant M184V described below, which shows altered regioselectivity towards the novel substrate mesitylene that has implications for substrate trafficking within sMMO.

8.7 The M184V mutant is an unstable enzyme

In the studies of the M184V sMMO mutation it was discovered that this mutant that only had activity in whole cells. Preparations of soluble extract had no activity and no hydroxylase subunits could be seen when soluble extract samples were run on an SDS PAGE. These results indicate that this mutation yielded a hydroxylase α -subunit that was less stable than the wild type enzyme. It is possible that the packing of proteins within the bacterial cell allowed the mutant hydroxylase to maintain its structural integrity but that in the soluble extract the reduction in packing density meant that integrity was lost and led to breakdown of the enzyme.

Fig 8.2) Active site of sM M O showing diiron centre (orange spheres) and residues chosen for site directed mutagenesis in this study. Leu110 (red), Asn116 (magenta), Cys151 (pink), Met184 (green), Phe188 (yellow) and Phe282 (white). The distance between M 184 and the diiron centre is displayed as a dotted line. Figure was constructed using X-ray crystallographic data (PDB accession code 1M HY).

8.8 Evidence of substrate trafficking via hydrophobic cavities 1, 2 and 3

Although the majority of the “BMO-like” mutants showed no great difference in product distribution compared to the wild type enzyme there was one notable exception. When the substrate mesitylene was oxidised by the wild type enzyme the oxidation product was almost exclusively 3,5-dimethylbenzyl alcohol. However with the M184V mutant there was also a second oxidation product identified by GCMS as 3,5-dimethylbenzaldehyde. This product most likely arose from further oxidation of the primary oxidation product 3,5-dimethylbenzyl alcohol. One possibility for this result is that the mutation prevents the oxidation product from exiting the active site as easily and so is further oxidized to the aldehyde form. This may suggest that these hydrophobic cavities are part of the exit channel involved in product egress from the active site and this mutation prevents product egress directly or that this mutation indirectly causes a conformational change elsewhere within the hydroxylase which prevented the mesitylene oxidation product exiting the active site. Another possibility is that the mutation gave rise to an enzyme with a lower K_m for 3,5-dimethylbenzyl alcohol and so the mutant had greater affinity for the oxidation product. However, the location of this residue is 10.99 Å away from the closest iron atom within the diiron centre (Fig. 8.2) and so is unlikely to be involved directly in the binding of the product to the active site during the oxidation reaction and so this would most likely be due to a secondary effect brought about by conformational changes due to the M184V mutation.

A number of different product bound sMMO hydroxylase crystal structures all have a continuous channel from solvent to the active site via hydrophobic cavities 1, 2 and 3 (Chapter 1, Fig. 1.5; Sazinsky *et al*/2004). The interface between hydrophobic cavities 1 adjacent to the active site and cavity 2 contain the Leu 110 and Phe 188 residues. As explained previously, the different conformations of the Leu 110 residue in oxidized and reduced forms of sMMO identified by Rosenzweig *et al.* (1997) led to the "leucine gate" hypothesis. The crystal structures of various alcohols bound to the active site showed an open configuration connecting cavities 1 and 2 similar to the "open" conformation observed by Rosenzweig and co-worker possibly indicating that a conformational change takes place that allows exit of hydroxylated product from the active site. Within cavity 2 there were a number of different residues that were seen to adopt alternative configurations upon binding of product to the active site including Met-184 and Phe-282. It was also noted that with these crystal structures, movement of the Phe-282 residue was essential for the accommodation of oxidation product within this cavity. The results presented here show that the F282L mutant was stable but unreactive. One possible explanation for this would be if this mutant were no longer able to adopt a conformation that would allow passage of substrate through this cavity. There are a number of possibilities for substrate entry and exit from the active site, either via a gap between the four helix bundle co-ordinating the active site, via interconnecting hydrophobic cavities or by a mixture of the two. These results show that the cavities 1 and 2 are important in substrate trafficking with this enzyme. Since when mesitylene was used as a substrate, a mutation of residue M184 within cavity 2 resulted in further oxidation of the primary oxidation product 3,5-dimethylbenzyl alcohol to the corresponding aldehyde. This is presumably due to

increased retention of the primary oxidation product within the active site arising from a conformational change within cavity 2 which restricts substrate exit.

8.9 Summary

The results discussed in this thesis have given important insights into the role of specific residues in the activity of sMMO. Although the results did not establish whether Leu 110 has the proposed gating function restricting access to the active site, it was shown that among all sMMO residues studied to date, Leu 110 has the greatest influence on regioselectivity of sMMO towards aromatic substrates.

Although the random mutagenesis experiments did not yield a mutant capable of oxidizing triaromatic substrates this method seems to be the best approach to produce a mutant sMMO enzyme capable of oxidizing these compounds by allowing the screening of large mutant libraries using the simple colorimetric assay described. By modifying the methods described here and utilizing the new expression vector it may be possible to create a random mutant library that spans the whole of the *mmoX* gene and so greatly increase the chances of discovering a triaromatic oxidizing sMMO mutant. Although amino acid sequence information suggests that the active sites of butane monooxygenase are highly similar with very few differing residues, none of the mutants that were made to produce an sMMO that was "more similar to butane monooxygenase" conferred any of the distinguishing characteristics of the latter enzymes. The single amino acid changes made here did not make the properties of sMMO more similar to those of BMO. It is possible that other point mutations would have this effect on sMMO or that a combination of mutations (perhaps including those already made singly) would be needed. This did however indicate a number of residues which were implicated in affecting regiospecificity, in particular the C151T mutant which showed relaxed regiospecificity with all substrates

tested. The use of a new substrate mesitylene (1,3,5-trimethylbenzene) has proved useful for product distribution and activity due to the limited number of possible positions for oxidation. The use of this new substrate has identified the M184V mutation within hydrophobic cavity 2 (Fig. 8.3) as having a significant effect on the enzyme activity and supports the suggested role of interconnected hydrophobic cavities in substrate trafficking.

References

1. ABBRUZZESE, A., PARK, M. H. and FOLK, J. E. (1986). Deoxyhypusine hydroxylase from rat testis, partial purification and characterization. *The Journal of Biological Chemistry*, 261 (7), 3085-3089.
2. ALI, H., SCANLAN, J., DUMONT, M. G. and MURRELL, J. C. (2006). Duplication of the mmoX gene in methylosinus sporium: Cloning, sequencing and mutational analysis. *Microbiology (Reading, England)*, 152 (Pt 10), 2931-2942.
3. ANDERSSON, M. E., HOGBOM, M., RINALDO-MATTHIS, A, ANDERSSON, K. K., SJOBERG, B. M. and NORDLUND, P. (1999). The crystal structure of an azide complex of the diferrous R2 subunit of ribonucleotide reductase displays a novel carboxylate shift with important mechanistic implications for diiron-catalyzed oxygen activation *Journal of the American Chemical Society*, 121 (11), 2346-2352.
4. ANTHONY, C. (1982). *The biochemistry of methylotrophs*. London, UK, Academic press.
5. ARP, D. J. (1999). Butane metabolism by butane-grown 'pseudomonas butanovora'. *Microbiology (Reading, England)*, 145 (5), 1173-1180.
6. BAILEY, L. J. and FOX, B. G. (2009). Crystallographic and catalytic studies of the peroxide-shunt reaction in a diiron hydroxylase. *Biochemistry*, 48 (38), 8932-8939.
7. BAILEY, L. J., MCCOY, J. G., PHILLIPS, G. N., Jr and FOX, B. G. (2008). Structural consequences of effector protein complex formation in a diiron hydroxylase. *Proceedings of the National Academy of Sciences of the United States of America*, 105 (49), 19194-19198.
8. BALASUBRAMANIAN, R., SMITH, S. M., RAWAT, S., YATSUNYK, L. A., STEMMLER, T. L. and ROSENZWEIG, A. C. (2010). Oxidation of methane by a biological dicopper centre. *Nature*, 465 (7294), 115-119.
9. BASU, P., KATTERLE, B., ANDERSSON, K. K. and DALTON, H. (2003). The membrane-associated form of methane mono-oxygenase from *Methylococcus capsulatus* (Bath) is a copper/iron protein. *The Biochemical Journal*, 369 (Pt 2), 417-427.

10. BECKMAN, R. A., MILDEVAN, A. S. and LOEB, L. A. (1985). On the fidelity of DNA replication: Manganese mutagenesis in vitro *Biochemistry*, 24 (21), 5810-5817.
11. BERTONI, G., MARTINO, M., GALLI, E. and BARBIERI, P. (1998). Analysis of the gene cluster encoding toluene/o-xylene monooxygenase from *Pseudomonas stutzeri* 0X1. *Applied and Environmental Microbiology*, 64 (10), 3626-3632.
12. BLATNY, J. M., BRAUTASET, T., WINTHER-LARSEN, H. C., HAUGAN, K. and VALLA, S. (1997). Construction and use of a versatile set of broad-host-range cloning and expression vectors based on the RK2 replicon. *Applied and Environmental Microbiology*, 63 (2), 370-379.
13. BODROSSY, L., MURRELL, J. C., DALTON, H., KALMAN, M., PUSKAS, L. G. and KOVACS, K. L. (1995). Heat-tolerant methanotrophic bacteria from the hot water effluent of a natural gas field *Applied and Environmental Microbiology*, 61 (10), 3549-3555.
14. BOLLINGER, J. M., TONG, W. H., RAVI, N., HUYNH, B. H., EDMONSON, D. E. and STUBBE, J. (1994). Mechanism of assembly of the tyrosyl radical- $\text{Fe}(\text{III})$ cofactor of *E. coli* ribonucleotide reductase. 2. kinetics of the excess Fe^{2+} reaction by optical, EPR, and moessbauer spectroscopies *Journal of the American Chemical Society*, 116 (18), 8015 - 8023.
15. BORODINA, E., NICHOL, T., DUMONT, M. G., SMITH, T. J. and MURRELL, J. C. (2007). Mutagenesis of the "leucine gate" to explore the basis of catalytic versatility in soluble methane monooxygenase. *Applied and Environmental Microbiology*, 73 (20), 6460-6467.
16. BURROWS, K. J., CORNISH, A., SCOTT, D. and HIGGINS, I. J. (1984). Substrate specificities of the soluble and particulate methane monooxygenases of *Methylosinus trichosporium* OB3b *Microbiology*, 130 (12), 3327 - 3333.
17. BUZY, A., MILLAR, A. L., LEGROS, V., WILKINS, P. C., DALTON, H. and JENNINGS, K. R. (1998). The hydroxylase component of soluble methane monooxygenase from *Methylococcus capsulatus* (Bath) exists in several forms as shown by electrospray-ionisation mass spectrometry. *European Journal of Biochemistry / FEBS*, 254 (3), 602-609.

18. BYRNE, A. M., KUKOR, J. J. and OLSEN, R. H. (1995). Sequence analysis of the gene cluster encoding toluene-3-monooxygenase from *Pseudomonas pickettii* PK01. *Gene*, 154 (1), 65-70.
19. CADWELL, R. C. and JOYCE, G. F. (1992). Randomization of genes by PCR mutagenesis. *Genome Research*, 2 (1), 28 - 33.
20. CAHOON, E. B., LINDQVIST, Y., SCHNEIDER, G. and SHANKLIN, J. (1997). Redesign of soluble fatty acid desaturases from plants for altered substrate specificity and double bond position *Proceedings of the National Academy of Sciences of the United States of America*, 94 (10), 4872-4877.
21. CANADA, K. A., IWASHITA, S., SHIM, H. and WOOD, T. K. (2002). Directed evolution of toluene ortho-monooxygenase for enhanced 1-naphthol synthesis and chlorinated ethene degradation. *Journal of Bacteriology*, 184 (2), 344-349.
22. CARAGLIA, M., MARRA, M., GIUBERTI, G., D'ALESSANDRO, A. M., BUDILLON, A., DEL PRETE, S., LENTINI, A., BENINATI, S. and ABBRUZZESE, A. (2001). The role of eukaryotic initiation factor 5A in the control of cell proliferation and apoptosis. *Amino Acids*, 20 (2), 91-104.
23. CARDY, D. L. N., LAIDLER, V., SALMOND, G. P. C. and MURRELL, J. C. (1991). Molecular analysis of the methane monooxygenase (MMO) gene cluster of *Methylosinus trichosporium* OB3b *Molecular Microbiology*, 5 (2), 335 - 342.
24. CARLSON, J., FUCHS, J. A. and MESSING, J. (1984). Primary structure of the escherichia coli ribonucleoside diphosphate reductase operon *Proceedings of the National Academy of Sciences of the United States of America*, 81 (14), 4294-4297.
25. CAVANAUGH, C. M., LEVERING, P. R., MAKI, J. S., MITCHELL, R. and LIDSTROM, M. E. (1987). Symbiosis of methylotrophic bacteria and deep-sea mussels *Nature*, 325 (6102), 346 - 348.
26. CHAN, S. I., CHEN, K. H., YU, S. S., CHEN, C. L. and KUO, S. S. (2004). Toward delineating the structure and function of the particulate methane monooxygenase from methanotrophic bacteria *Biochemistry*, 43 (15), 4421 - 4430.
27. CHAN, S. I., WANG, V. C., LAI, J. C., YU, S. S., CHEN, P. P., CHEN, K. H., CHEN, C. L. and CHAN, M. K. (2007). Redox potentiometry studies of

- particulate methane monooxygenase: Support for a trinuclear copper cluster active site *Angewandte chemie*, 119 (12), 2038 - 2040.
28. CHEN, K. Y. and LIU, A. Y. (1997). Biochemistry and function of hypusine formation on eukaryotic initiation factor 5A. *Biological Signals*, 6 (3), 105-109.
 29. CHOI, D. -W, KUNZ, R. C., BOYD, E. S., SEMRAU, J. D., ANTHOLINE, W. E., HAN, J. -I, ZAHN, J. A., BOYD, J. M., DE LA MORA, A. M. and DISPIRITO, A. A. (2003; 2003). The membrane-associated methane monooxygenase (pMMO) and pMMO-NADH:Quinone oxidoreductase complex from *Methylococcus capsulatus* bath *Journal of Bacteriology*, 185 (19), 5755 - 5764.
 30. CLIMENT, I., SJOEBERG, B. M. and HUANG, C. Y. (1992). Site-directed mutagenesis and deletion of the carboxyl terminus of escherichia coli ribonucleotide reductase protein R2. effects on catalytic activity and subunit interaction *Biochemistry*, 31 (20), 4801 - 4807.
 31. COLBY, J. and DALTON, H. (1976). Some properties of a soluble methane mono-oxygenase from *Methylococcus capsulatus* strain Bath. *The Biochemical Journal*, 157 (2), 495-497.
 32. COLBY, J. and DALTON, H. (1978). Resolution of the methane mono-oxygenase of *Methylococcus capsulatus* (Bath) into three components, purification and properties of component C, a flavoprotein *The Biochemical Journal*, 171 (2), 461-468.
 33. COLBY, J., STIRLING, D. I. and DALTON, H. (1977). The soluble methane mono-oxygenase of *Methylococcus capsulatus* (Bath), its ability to oxygenate n-alkanes, n-alkenes, ethers, and alicyclic, aromatic and heterocyclic compounds. *The Biochemical Journal*, 165 (2), 395-402.
 34. COOLEY, R. B., DUBBELS, B. L., SAYAVEDRA-SOTO, L. A., BOTTOMLEY, P. J. and ARP, D. J. (2009). Kinetic characterization of the soluble butane monooxygenase from *Thauera butanivorans*, formerly '*Pseudomonas butanovora*'. *Microbiology (Reading, England)*, 155 (6), 2086-2096.
 35. CSAKI, R., BODROSSY, L., KLEM, J., MURRELL, J. C. and KOVACS, K. L. (2003). Genes involved in the copper-dependent regulation of soluble methane monooxygenase of *Methylococcus capsulatus* (Bath): Cloning, sequencing and mutational analysis. *Microbiology (Reading, England)*, 149 (7), 1785-1795.

36. DALTON, H. (2005). The leeuwenhoek lecture 2000 the natural and unnatural history of methane-oxidizing bacteria. *Philosophical Transactions of the Royal Society of London. series B, biological sciences*, 360 (1458), 1207-1222.
37. DAVIES, S. L. and WHITTENBURY, R. (1970). Fine structure of methane and other hydrocarbon-utilizing bacteria *Microbiology*, 61 (2), 227 - 232.
38. DECHAINED, E. G. and CAVANAUGH, C. M. (2006). Symbioses of methanotrophs and deep-sea mussels (mytilidae: Bathymodiolinae). *Progress in Molecular and Subcellular Biology*, 41 , 227-249.
39. DEDYSH, S. N. (1998). Isolation of acidophilic methane-oxidizing bacteria from northern peat wetlands *Science*, 282 (5387), 281 - 284.
40. DEDYSH, S. N., BERESTOVSKAYA, Y. Y., VASYLIEVA, L. V., BELOVA, S. E., KHMELENINA, V. N., SUZINA, N. E., TROTSENKO, Y. A., LIESACK, W. and ZAVARZIN, G. A. (2004). *Methylocella tundrae* sp. nov., a novel methanotrophic bacterium from acidic tundra peatlands *International Journal of Systematic and Evolutionary Microbiology*, 54 (Pt 1), 151-156.
41. DEDYSH, S. N., DUNFIELD, P. F., DERAQSHANI, M., STUBNER, S., HEYER, J. and LIESACK, W. (2003). Differential detection of type II methanotrophic bacteria in acidic peatlands using newly developed 16S rRNA-targeted fluorescent oligonucleotide probes. *FEMS Microbiology Ecology*, 43 (3), 299-308.
42. DEWITT, J. G., BENTSEN, J. G., ROSENZWEIG, A. C., HEDMAN, B., GREEN, J., PILKINGTON, S., PAPAETHYMIU, G. C., DALTON, H., HODGSON, K. O. and LIPPARD, S. J. (1991). X-ray absorption, moessbauer, and EPR studies of the dinuclear iron center in the hydroxylase component of methane monooxygenase *Journal of the American Chemical Society*, 113 (24), 9219-9235.
43. DOUGHTY, D. M., HALSEY, K. H., VIEVILLE, C. J., SAYAVEDRA-SOTO, L. A., ARP, D. J. and BOTTOMLEY, P. J. (2007). Propionate inactivation of butane monooxygenase activity in *Pseudomonas butanovorans* Biochemical and physiological implications. *Microbiology (Reading, England)*, 153 (11), 3722-3729.
44. DOUGHTY, D. M., KURTH, E. G., SAYAVEDRA-SOTO, L. A., ARP, D. J. and BOTTOMLEY, P. J. (2008). Evidence for involvement of copper ions and

- redox state in regulation of butane monooxygenase in *Pseudomonas butanovora*. *Journal of Bacteriology*, 190 (8), 2933-2938.
45. DOUGHTY, D. M., SAYAVEDRA-SOTO, L. A., ARP, D. J. and BOTTOMLEY, P. J. (2006). Product repression of alkane monooxygenase expression in *Pseudomonas butanovora*. *Journal of Bacteriology*, 188 (7), 2586-2592.
 46. DRUMMOND, D. A., IVERSON, B. L., GEORGIU, G. and ARNOLD, F. H. (2005). Why high-error-rate random mutagenesis libraries are enriched in functional and improved proteins *Journal of Molecular Biology*, 350 (4), 806-816.
 47. DUBBELS, B. L., SAYAVEDRA-SOTO, L. A. and ARP, D. J. (2007). Butane monooxygenase of *Pseudomonas butanovora* Purification and biochemical characterization of a terminal-alkane hydroxylating diiron monooxygenase. *Microbiology (Reading, England)*, 153 (6), 1808-1816.
 48. DUMONT, M. G., RADAJEWSKI, S. M., MIGUEZ, C. B., MCDONALD, I. R. and MURRELL, J. C. (2006). Identification of a complete methane monooxygenase operon from soil by combining stable isotope probing and metagenomic analysis. *Environmental Microbiology*, 8 (7), 1240-1250.
 49. DUNFIELD, P. F., BELOVA, S. E., VOROB'EV, A. V., CORNISH, S. L. and DEDYSH, S. N. (2010). *Methylocapsa aurea* sp. nov., a facultative methanotroph possessing a particulate methane monooxygenase, and emended description of the genus methylocapsa. *International Journal of Systematic and Evolutionary Microbiology*, 60 (11), 2659-2664.
 50. DUNFIELD, P. F., KHMELENINA, V. N., SUZINA, N. E., TROTSENKO, Y. A. and DEDYSH, S. N. (2003). *Methylocella silvestris* sp. nov., a novel methanotroph isolated from an acidic forest cambisol *International Journal of Systematic and Evolutionary Microbiology*, 53 (Pt 5), 1231-1239.
 51. DUNFIELD, P. F., YURYEV, A., SENIN, P., SMIRNOVA, A. V., STOTT, M. B., HOU, S., LY, B., SAW, J. H., ZHOU, Z., REN, Y., WANG, J., MOUNTAIN, B. W., CROWE, M. A., WEATHERBY, T. M., BODELIER, P. L., LIESACK, W., FENG, L., WANG, L. and ALAM, M. (2007). Methane oxidation by an extremely acidophilic bacterium of the phylum verrucomicrobia. *Nature*, 450 (7171), 879-882.
 52. ECKERT, K. A. and KUNKEL, T. A. (1991). DNA polymerase fidelity and the polymerase chain reaction *PCR Methods and Applications*, 1 (1), 17-24.

53. ECKERT, K. A. and KUNKEL, T. A. (1990). High fidelity DNA synthesis by the *Thermus aquaticus* DNA polymerase *Nucleic Acids Research*, 18 (13), 3739 - 3744.
54. EKBERG, M., POTSCHE, S., SANDIN, E., THUNNISSEN, M., NORDLUND, P., SAHLIN, M. and SJOBERG, B. M. (1998). Preserved catalytic activity in an engineered ribonucleotide reductase R2 protein with a nonphysiological radical transfer pathway, the importance of hydrogen bond connections between the participating residues *The Journal of Biological Chemistry*, 273 (33), 21003-21008.
55. ELANGO, N., RADHAKRISHNAN, R., FROLAND, W. A., WALLAR, B. J., EARHART, C. A., LIPSCOMB, J. D. and OHLENDORF, D. H. (1997). Crystal structure of the hydroxylase component of methane monooxygenase from *Methylosinus trichosporium* OB3b. *Protein Science : A publication of the protein society*, 6 (3), 556-568.
56. ERICSON, A., HEDMAN, B., HODGSON, K. O., GREEN, J., DALTON, H. BENTSEN, J. G., BEER, R. H. and LIPPARD, S. J. (1988). Structural characterization by EXAFS spectroscopy of the binuclear iron center in protein A of methane monooxygenase from *Methylococcus capsulatus* (bath) *Journal of the American Chemical Society*, 110 (7), 2330 - 2332.
57. FEINGERSCH, R., SHAINSKY, J., WOOD, T. K. and FISHMAN, A. (2008). Protein engineering of toluene monooxygenases for synthesis of chiral sulfoxides. *Applied and Environmental Microbiology*, 74 (5), 1555-1566.
58. FIGURSKI, D. H. and HELINSKI, D. R. (1979). Replication of an origin-containing derivative of plasmid RK2 dependent on a plasmid function provided in trans *Proceedings of the National Academy of Sciences of the United States of America*, 76 (4), 1648-1652.
59. FISHMAN, A., TAO, Y., BENTLEY, W. E. and WOOD, T. K. (2004). Protein engineering of toluene 4-monooxygenase of *Pseudomonas mendocina* KR1 for synthesizing 4-nitrocatechol from nitrobenzene. *Biotechnology and Bioengineering*, 87 (6), 779-790.
60. FISHMAN, A., TAO, Y. and WOOD, T. K. (2004). Toluene 3-monooxygenase of *Ralstonia pickettii* PK01 is a para-hydroxylating enzyme. *Journal of Bacteriology*, 186 (10), 3117-3123.

61. FOX, B. G., SHANKLIN, J., AI, J., LOEHR, T. M. and SANDERS-LOEHR, J. (1994). Resonance raman evidence for an Fe-O-Fe center in stearyl-ACP desaturase. primary sequence identity with other diiron-oxo proteins. *Biochemistry*, 33 (43), 12776-12786.
62. FOX, Brian G., BORNEMAN, James G., WACKETT, Lawrence P. and LIPSCOMB, John D. (1990). Flaloalkene oxidation by the soluble methane monooxygenase from *Methylosinus trichosporium* OB3b: Mechanistic and environmental implications *Biochemistry*, 29 (27), 6419 - 6427.
63. GESSER, Hyman D., HUNTER, Norman R. and PRAKASH, Chandra B. (1985). The direct conversion of methane to methanol by controlled oxidation *Chemical reviews*, 85 (4), 235 - 244.
64. GILBERT, B., MCDONALD, I. R., FINCH, R., STAFFORD, G. P., NIELSEN, A. K. and MURRELL, J. C. (2000). Molecular analysis of the pmo (particulate methane monooxygenase) operons from two type II methanotrophs *Applied and Environmental Microbiology*, 66 (3), 966 - 975.
65. GREEN, J. and DALTON, H. (1985). Protein B of soluble methane monooxygenase from *Methylococcus capsulatus* (Bath). A novel regulatory protein of enzyme activity. *The Journal of Biological Chemistry*, 260 (29), 15795-15801.
66. GREEN, J. and DALTON, H. (1989). Substrate specificity of soluble methane monooxygenase. mechanistic implications. *The Journal of Biological Chemistry*, 264 (30), 17698-17703.
67. GREEN, J., PRIOR, S. D. and DALTON, H. (1985). Copper ions as inhibitors of protein C of soluble methane monooxygenase of *Methylococcus capsulatus* (Bath). *European Journal of Biochemistry, FEBS*, 153 (1), 137-144.
68. GUY, J. E., ABREU, I. A., MOCHE, M., LINDQVIST, Y., WHITTLE, E. and SHANKLIN, J. (2006). A single mutation in the castor Delta 9-18:0-desaturase changes reaction partitioning from desaturation to oxidase chemistry. *Proceedings of the National Academy of Sciences of the United States of America*, 103 (46), 17220-17224.
69. HAKEMIAN, A. S. and ROSENZWEIG, A. C. (2007). The biochemistry of methane oxidation. *Annual Review of Biochemistry*, 76 , 223-241.
70. HAKEMIAN, A. S., KONDAPALLI, K. C., TELSER, J., HOFFMAN, B. M., STEMMLER, T. L. and ROSENZWEIG, A. C. (2008). The metal centers of

particulate methane monooxygenase from *Methylosinus trichosporium* OB3b
Biochemistry, 47 (26), 6793 - 6801.

71. HALSEY, K. H., DOUGHTY, D. M., SAYAVEDRA-SOTO, L. A., BOTTOMLEY, P. J. and ARP, D. J. (2007). Evidence for modified mechanisms of chloroethene oxidation in *Pseudomonas butanovora* mutants containing single amino acid substitutions in the hydroxylase alpha-subunit of butane monooxygenase. *Journal of Bacteriology*, 189 (14), 5068-5074.
72. HALSEY, K. H., SAYAVEDRA-SOTO, L. A., BOTTOMLEY, P. J. and ARP, D. J. (2006). Site-directed amino acid substitutions in the hydroxylase alpha subunit of butane monooxygenase from *Pseudomonas butanovora*: Implications for substrates knocking at the gate. *Journal of Bacteriology*, 188 (13), 4962-4969.
73. HANAHAN, D. (1983). Studies on transformation of *Escherichia coli* with plasmids *Journal of Molecular Biology*, 166 (4), 557 - 580.
74. HAZEN, T. C., CHAKRABORTY, R., FLEMING, J. M., GREGORY, I. R., BOWMAN, J. P., JIMENEZ, L., ZHANG, D., PFIFFNER, S. M., BROCKMAN, F. J. and SAYLER, G. S. (2009). Use of gene probes to assess the impact and effectiveness of aerobic in situ bioremediation of TCE. *Archives of Microbiology*, 191 (3), 221-232.
75. HOU, C. T., PATEL, R., LASKIN, A. I., BARNABE, N. and MARCZAK, I. (1979). Microbial oxidation of gaseous hydrocarbons: Production of methyl ketones from their corresponding secondary alcohols by methane- and methanol-grown microbes *Applied and Environmental Microbiology*, 38 (1), 135-142.
76. HOU, C. T., PATEL, R., BARNABE, N. and MARCZAK, I. (1981). Stereospecificity and other properties of a novel secondary-alcohol-specific alcohol dehydrogenase *European Journal of Biochemistry*, 119 (2), 359 - 364.
77. HOU, S., MAKAROVA, K. S., SAW, J. H., SENIN, P., LY, B. V., ZHOU, Z., REN, Y., WANG, J., GALPERIN, M. Y., OMELCHENKO, M. V., WOLF, Y. I., YUTIN, N., KOONIN, E. V., STOTT, M. B., MOUNTAIN, B. W., CROWE, M. A., SMIRNOVA, A. V., DUNFIELD, P. F., FENG, L., WANG, L. and ALAM, M. (2008). Complete genome sequence of the extremely acidophilic methanotroph isolate V4, *Methylophilum inferorum*, a representative of the bacterial phylum verrucomicrobia. *Biology Direct*, 3 , 26.

78. HUTCHENS, E., RADAJEWSKI, S., DUMONT, M. G., MCDONALD, I. R. and MURRELL, J. C. (2003). Analysis of methanotrophic bacteria in mobile cave by stable isotope probing *Environmental Microbiology*, 6 (2), 111 -120.
79. Intergovernmental Panel on Climate Change and SOLOMON, S. S. (2007). *Climate change 2007: The Physical Science Basis: Contribution of working group I to the fourth assessment report of the intergovernmental panel on climate change* Cambridge, Cambridge University Press for the intergovernmental Panel on Climate Change.
80. ISLAM, T., JENSEN, S., REIGSTAD, L. J., LARSEN, O. and BIRKELAND, N. K. (2008). Methane oxidation at 55 degrees C and pH 2 by a thermoacidophilic bacterium belonging to the verrucomicrobia phylum. *Proceedings of the National Academy of Sciences of the United States of America*, 105 (1), 300-304.
81. JAHNG, D., KIM, C. S., HANSON, R. S. and WOOD, T. K. (1996). Optimization of trichloroethylene degradation using soluble methane monooxygenase of *Methylosinus trichosporium* OB3b expressed in recombinant bacteria *Biotechnology and Bioengineering*, 51 (3), 349-359.
82. JENKINS, M. B., CHEN, J. H., KADNER, D. J. and LION, L. W. (1994). Methanotrophic bacteria and facilitated transport of pollutants in aquifer material. *Applied and Environmental Microbiology*, 60 (10), 3491-3498.
83. KANG, K. R., KIM, Y. S., WOLFF, E. C. and PARK, M. H. (2007). Specificity of the deoxyhypusine hydroxylase-eukaryotic translation initiation factor (eIF5A) interaction: Identification of amino acid residues of the enzyme required for binding of its substrate, deoxyhypusine-containing eIF5A. *The Journal of Biological Chemistry*, 282 (11), 8300-8308.
84. KHADEM, A. F., POL, A., JETTEN, M. S. and OP DEN CAMP, H. J. (2010). Nitrogen fixation by the verrucomicrobial methanotroph '*Methyloacidiphilum fumarolicum*' SolV. *Microbiology (reading, england)*, 156 (4), 1052-1059.
85. KHMELENINA, V. N. (1997). Isolation and characterization of halotolerant alkaliphilic methanotrophic bacteria from tuva soda lakes *Current Microbiology*, 35 (5), 257-261.
86. KIM, Y. S., KANG, K. R., WOLFF, E. C., BELL, J. K., MCPHIE, P. and PARK, M. H. (2006). Deoxyhypusine hydroxylase is a fe(II)-dependent, HEAT-repeat enzyme, identification of amino acid residues critical for fe(II) binding and

- catalysis [corrected]. *The Journal of Biological Chemistry*, 281 (19), 13217-13225.
87. KITMITTO, A., MYRONOVA, N., BASU, P. and DALTON, H. (2005). Characterization and structural analysis of an active particulate methane monooxygenase trimer from *Methylococcus capsulatus* (Bath) *Biochemistry*, 44 (33), 10954- 10965.
 88. KOPP, D. A. and LIPPARD, S. J. (2002). Soluble methane monooxygenase: Activation of dioxygen and methane. *Current Opinion in Chemical Biology*, 6 (5), 568-576.
 89. KREBS, C., CHEN, S., BALDWIN, J., LEY, B. A., PATEL, U., EDMONDSON, D. E., HUYNH, B. H. and BOLLINGER, J. M. (2000). Mechanism of rapid electron transfer during oxygen activation in the R2 subunit of *Escherichia coli* ribonucleotide reductase. 2. evidence for and consequences of blocked electron transfer in the W48F variant *Journal of the American Chemical Society*, 122 (49), 12207 - 12219.
 90. KREBS, C., DAVYDOV, R., BALDWIN, J., HOFFMAN, B. M., BOLLINGER, J. M. and HUYNH, B. H. (2000). Mossbauer and EPR characterization of the S=9/2 Mixed-valence Fe(II)Fe(III) cluster in the cryoreduced R2 subunit of *Escherichia coli* ribonucleotide reductase *Journal of the American Chemical Society*, 122 (22), 5327 - 5336.
 91. KURTH, E. G., DOUGHTY, D. M., BOTTOMLEY, P. J., ARP, D. J. and SAYAVEDRA-SOTO, L. A. (2008). Involvement of BmoR and BmoG in n-alkane metabolism in '*Pseudomonas butanovora*'. *Microbiology (Reading, England)*, 154(1), 139-147.
 92. LEAHY, J. G., BATCHELOR, P. J. and MORCOMB, S. M. (2003). Evolution of the soluble diiron monooxygenases. *FEMS Microbiology Reviews*, 27 (4), 449-479.
 93. LEE, S. K., NESHEIM, J. C. and LIPSCOMB, J. D. (1993). Transient intermediates of the methane monooxygenase catalytic cycle *The Journal of Biological Chemistry*, 268 (29), 21569-21577.
 94. LEE, S. W., KEENEY, D. R., LIM, D. H., DISPIRITO, A. A. and SEMRAU, J. D. (2006). Mixed pollutant degradation by *Methylosinus trichosporium* OB3b expressing either soluble or particulate methane monooxygenase: Can the

- tortoise beat the hare? *Applied and Environmental Microbiology*, 72 (12), 7503-7509.
95. LEUNG, D. W., CHEN, E. and GOEDEL, D. V. (1989). A method for random mutagenesis of a defined DNA segment using a modified polymerase chain reaction. *Technique*, 1, 11-15.
 96. LIEBERMAN, R. L. and ROSENZWEIG, A. C. (2005). Crystal structure of a membrane-bound metalloenzyme that catalyses the biological oxidation of methane. *Nature*, 434 (7030), 177-182.
 97. LIN, J. L., JOYE, S. B., SCHOLTEN, J. C., SCHAFER, H., MCDONALD, I. R. and MURRELL, J. C. (2005). Analysis of methane monooxygenase genes in mono lake suggests that increased methane oxidation activity may correlate with a change in methanotroph community structure *Applied and Environmental Microbiology*, 71 (10), 6458-6462.
 98. LINDNER, A. S., ADRIAENS, P. and SEMRAU, J. D. (2000). Transformation of ortho -substituted biphenyls by *Methylosinus trichosporium* OB3b: Substituent effects on oxidation kinetics and product formation *Archives of microbiology*, 174(1-2), 35-41.
 99. LINDQVIST, Y., HUANG, W., SCHNEIDER, G. and SHANKLIN, J. (1996). Crystal structure of delta9 stearoyl-acyl carrier protein desaturase from castor seed and its relationship to other di-iron proteins *The EMBO journal*, 15 (16), 4081-4092.
 100. LITTLE, C. D., PALUMBO, A. V., HERBES, S. E., LIDSTROM, M. E., TYNDALL, R. L. and GILMER, P. J. (1988). Trichloroethylene biodegradation by a methane-oxidizing bacterium *Applied and Environmental Microbiology*, 54 (4), 951-956.
 101. LIU, K. E., VALENTINE, A. M., WANG, D., HUYNH, B. H., EDMONDSON, D. E., SALIFOGLU, A. and LIPPARD, S. J. (1995). Kinetic and spectroscopic characterization of intermediates and component interactions in reactions of methane monooxygenase from *Methylococcus capsulatus* (Bath) *Journal of the American Chemical Society*, 117 (41), 10174 - 10185.
 102. LLOYD, J. S., BHAMBRA, A., MURRELL, J. C. and DALTON, H. (1997). Inactivation of the regulatory protein B of soluble methane monooxygenase from *Methylococcus capsulatus* (Bath) by proteolysis can be overcome by a

- gly to gin modification. *European Journal of Biochemistry / FEBS*, 248 (1), 72-79.
103. LLOYD, J. S., DE MARCO, P., DALTON, H. and MURRELL, J. C. (1999). Heterologous expression of soluble methane monooxygenase genes in methanotrophs containing only particulate methane monooxygenase. *Archives of Microbiology*, 171 (6), 364-370.
104. LLOYD, J. S., FINCH, R., DALTON, H. and MURRELL, J. C. (1999). Homologous expression of soluble methane monooxygenase genes in *Methylosinus trichosporium* OB3b. *Microbiology (Reading, England)*, 145 (2), 461-470.
105. LONTOH, S. and SEMRAU, J. D. (1998). Methane and trichloroethylene degradation by *Methylosinus trichosporium* OB3b expressing particulate methane monooxygenase. *Applied and Environmental Microbiology*, 64 (3), 1106-1114.
106. LUND, J., WOODLAND, M. P. and DALTON, H. (1985). Electron transfer reactions in the soluble methane monooxygenase of *Methylococcus capsulatus* (Bath). *European Journal of Biochemistry / FEBS*, 147 (2), 297-305.
107. MARTINHO, Marlene, CHOI, Dong W., DISPIRITO, Alan A., ANTHOLINE, William E., SEMRAU, Jeremy D. and MUNCK, Eckard (2007). Mossbauer studies of the membrane-associated methane monooxygenase from *Methylococcus capsulatus* (Bath): Evidence for a diiron center *Journal of the American Chemical Society*, 129 (51), 15783 - 15785.
108. MCCLAY, K., BOSS, C., KERESZTES, I. and STEFFAN, R. J. (2005). Mutations of toluene-4-monooxygenase that alter regiospecificity of indole oxidation and lead to production of novel indigoid pigments. *Applied and Environmental Microbiology*, 71 (9), 5476-5483.
109. MCCORMICK, M. S., SAZINSKY, M. H., CONDON, K. L. and LIPPARD, S. J. (2006). X-ray crystal structures of manganese(II)-reconstituted and native toluene/o-xylene monooxygenase hydroxylase reveal rotamer shifts in conserved residues and an enhanced view of the protein interior. *Journal of the American Chemical Society*, 128 (47), 15108-15110.
110. MCDONALD, I. R., UCHIYAMA, H., KAMBE, S., YAGI, O. and MURRELL, J. C. (1997). The soluble methane monooxygenase gene cluster of the

- trichloroethylene-degrading methanotroph methylocystis sp. strain M *Applied and Environmental Microbiology*, 63 (5), 1898-1904.
111. MILLER, A. R., KEENER, W. K., WATWOOD, M. E. and ROBERTO, F. F. (2002). A rapid fluorescence-based assay for detecting soluble methane monooxygenase. *Applied Microbiology and Biotechnology*, 58 (2), 183-188.
112. MITCHELL, K. H., ROGGE, C. E., GIERAHN, T. and FOX, B. G. (2003). Insight into the mechanism of aromatic hydroxylation by toluene 4-monooxygenase by use of specifically deuterated toluene and p-xylene. *Proceedings of the National Academy of Sciences of the United States of America*, 100 (7), 3784-3789.
113. MITCHELL, K. H., STUDTS, J. M. and FOX, B. G. (2002). Combined participation of hydroxylase active site residues and effector protein binding in a *para* to *ortho* modulation of toluene 4-monooxygenase regioselectivity. *Biochemistry*, 41 (9), 3176-3188.
114. MITIC, N., SCHWARTZ, J. K., BRAZEAU, B. J., LIPSCOMB, J. D. and SOLOMON, E. I. (2008). CD and MCD studies of the effects of component B variant binding on the biferrrous active site of methane monooxygenase. *Biochemistry*, 47 (32), 8386-8397.
115. MOUNTFORT, D. O. (1990). Oxidation of aromatic alcohols by purified methanol dehydrogenase from *Methylosinus trichosporium* OB3b *Journal of Bacteriology*, 172 (7), 3690-3694.
116. MURRAY, L. J., GARCIA-SERRES, R., MCCORMICK, M. S., DAVYDOV, R., NAIK, S. G., KIM, S. H., HOFFMAN, B. M., HUYNH, B. H. and LIPPARD, S. J. (2007). Dioxygen activation at non-heme diiron centers: Oxidation of a proximal residue in the I100W variant of toluene/o-xylene monooxygenase hydroxylase. *Biochemistry*, 46 (51), 14795-14809.
117. MURRAY, L. J., GARCIA-SERRES, R., NAIK, S., HUYNH, B. H. and LIPPARD, S. J. (2006). Dioxygen activation at non-heme diiron centers: Characterization of intermediates in a mutant form of toluene/o-xylene monooxygenase hydroxylase. *Journal of the American Chemical Society*, 128 (23), 7458-7459.
118. MURRAY, L. J. and LIPPARD, S. J. (2007). Substrate trafficking and dioxygen activation in bacterial multicomponent monooxygenases. *Accounts of Chemical Research*, 40 (7), 466-474.

119. MURRAY, L. J., NAIK, S. G., ORTILLO, D. O., GARCIA-SERRES, R., LEE, J. K., HUYNH, B. H. and LIPPARD, S. J. (2007). Characterization of the arene-oxidizing intermediate in ToMOH as a diiron(III) species. *Journal of the American Chemical Society*, 129 (46), 14500-14510.
120. MYRONOVA, N., KITMITTO, A., COLLINS, R. F., MIYAJI, A. and DALTON, H. (2006). Three-dimensional structure determination of a protein supercomplex that oxidizes methane to formaldehyde in *Methylococcus capsulatus* (Bath) *Biochemistry*, 45 (39), 11905 - 11914.
121. NAKAMURA, T., HOAKI, T., HANADA, S., MARUYAMA, A., KAMAGATA, Y. and FUSE, H. (2007). Soluble and particulate methane monooxygenase gene clusters in the marine methanotroph methylomicrobium sp. strain NI. *FEMS Microbiology Letters*, 277 (2), 157-164.
122. NEWMAN, L. M. and WACKETT, L. P. (1995). Purification and characterization of toluene 2-monooxygenase from *Burkholderia cepacia* G4. *Biochemistry*, 34 (43), 14066-14076.
123. NGUYEN, H. H., ELLIOTT, S. J., YIP, J. H. and CHAN, S. I. (1998). The particulate methane monooxygenase from *Methylococcus capsulatus* (Bath) is a novel copper-containing three-subunit enzyme, isolation and characterization *The Journal of Biological Chemistry*, 273 (14), 7957-7966.
124. NGUYEN, H. H., SHIEMKE, A. K., JACOBS, S. J., HALES, B. J., LIDSTROM, M. E. and CHAN, S. I. (1994). The nature of the copper ions in the membranes containing the particulate methane monooxygenase from *Methylococcus capsulatus* (Bath) *The Journal of Biological Chemistry*, 269 (21), 14995-15005.
125. NIELSEN, A. K., GERDES, K., DEGN, H. and COLIN, M. J. (1996). Regulation of bacterial methane oxidation: Transcription of the soluble methane mono-oxygenase operon of *Methylococcus capsulatus* (Bath) is repressed by copper ions *Microbiology*, 142 (5), 1289 - 1296.
126. NIELSEN, A. K., GERDES, K. and MURRELL, J. C. (1997). Copper-dependent reciprocal transcriptional regulation of methane monooxygenase genes in *Methylococcus capsulatus* and *Methylosinus trichosporium* *Molecular Microbiology*, 25 (2), 399-409.
127. NOTOMISTA, E., CAFARO, V., BOZZA, G. and DI DONATO, A. (2009). Molecular determinants of the regioselectivity of toluene/o-xylene

- monooxygenase from *Pseudomonas* sp. strain 0X1. *Applied and Environmental Microbiology*, 75 (3), 823-836.
128. OLSEN, R. H., KUKOR, J. J. and KAPHAMMER, B. (1994). A novel toluene-3-monooxygenase pathway cloned from *Pseudomonas pickettii* PK01. *Journal of Bacteriology*, 176 (12), 3749-3756.
129. PARK, J. H., ARAVIND, L., WOLFF, E. C., KAEVEL, J., KIM, Y. S. and PARK, M. H. (2006). Molecular cloning, expression, and structural prediction of deoxyhypusine hydroxylase: A FIEAT-repeat-containing metalloenzyme. *Proceedings of the National Academy of Sciences of the United States of America*, 103 (1), 51-56.
130. PARK, M. H. (2006). The post-translational synthesis of a polyamine-derived amino acid, hypusine, in the eukaryotic translation initiation factor 5A (eIF5A). *Journal of Biochemistry*, 139 (2), 161-169.
131. PATEL, R., HOU, C., DERELANKO, P. and FELIX, A. (1980). Purification and properties of a heme-containing aldehyde dehydrogenase from *Archives of Biochemistry and Biophysics*, 203 (2), 654 - 662.
132. PATEL, R. N., BOSE, H. R., MANDY, W. J. and HOARE, D. S. (1972). Physiological studies of methane- and methanol-oxidizing bacteria: Comparison of a primary alcohol dehydrogenase from *Methylococcus capsulatus* (Texas strain) and pseudomonas species M27 *Journal of Bacteriology*, 110 (2), 570-577.
133. PERRY, A. and SMITFI, T. J. (2006). Protocol for mutagenesis of alkene monooxygenase and screening for modified enantiocomposition of the epoxypropane product *Journal of Biomolecular Screening*, 11 (5), 553-556.
134. PIKUS, J. D., MITCHELL, K. H., STUDTS, J. M., MCCLAY, K., STEFFAN, R. J. and FOX, B. G. (2000). Threonine 201 in the diiron enzyme toluene 4-monooxygenase is not required for catalysis. *Biochemistry*, 39 (4), 791-799.
135. PIKUS, J. D., STUDTS, J. M., MCCLAY, K., STEFFAN, R. J. and FOX, B. G. (1997). Changes in the regiospecificity of aromatic hydroxylation produced by active site engineering in the diiron enzyme toluene 4-monooxygenase. *Biochemistry*, 36 (31), 9283-9289.
136. POL, A., HEIJMANS, K., HARHANGI, H. R., TEDESCO, D., JETTEN, M. S. and OP DEN CAMP, H. J. (2007). Methanotrophy below pH 1 by a new verrucomicrobia species. *Nature*, 450 (7171), 874-878.

137. REEBURGH, W. S., WHALEN, S. C. and ALPERIN, M. J. (1993). The role of methylotrophy in the global methane budget. In: MURRELL, J. C. and KELLY, D. P. (eds.). *Microbial growth on C1 compounds*. Andover, UK, Intercept, 1-14.
138. REISNER, E., ABIKOFF, T. C. and LIPPARD, S. J. (2007). Influence of steric hindrance on the core geometry and sulfoxidation chemistry of carboxylate-rich diiron(II) complexes. *Inorganic Chemistry*, 46 (24), 10229-10240.
139. RINALDO, D., PHILIPP, D. M., LIPPARD, S. J. and FRIESNER, R. A. (2007). Intermediates in dioxygen activation by methane monooxygenase: A QM/MM study. *Journal of the American Chemical Society*, 129 (11), 3135-3147.
140. ROSENZWEIG, A. C., BRANDSTETTER, H., WHITTINGTON, D. A., NORDLUND, P., LIPPARD, S. J. and FREDERICK, C. A. (1997). Crystal structures of the methane monooxygenase hydroxylase from *Methylococcus capsulatus* (Bath): Implications for substrate gating and component interactions. *Proteins*, 29 (2), 141-152.
141. RUI, L., KWON, Y. M., FISHMAN, A., REARDON, K. F. and WOOD, T. K. (2004). Saturation mutagenesis of toluene *ortho*-monooxygenase of *Burkholderia cepacia* G4 for enhanced 1-naphthol synthesis and chloroform degradation. *Applied and Environmental Microbiology*, 70 (6), 3246-3252.
142. RUI, L., REARDON, K. F. and WOOD, T. K. (2005). Protein engineering of toluene *ortho*-monooxygenase of *Burkholderia cepacia* G4 for regiospecific hydroxylation of indole to form various indigoid compounds. *Applied Microbiology and Biotechnology*, 66 (4), 422-429.
143. SAHLIN, M., LASSMANN, G., POTSCH, S., SLABY, A., SJOBERG, B. M. and GRASLUND, A. (1994). Tryptophan radicals formed by iron/oxygen reaction with *Escherichia coli* ribonucleotide reductase protein R2 mutant Y122F. *The Journal of Biological Chemistry*, 269 (16), 11699-11702.
144. SAMBROOK, Joseph, FRITSCH, E. F. and MANIATIS, T. (1989). *Molecular cloning: A laboratory manual* Cold Spring Harbor, N.Y., Cold Spring Harbor Laboratory.
145. SAZINSKY, M. H., BARD, J., DI DONATO, A. and LIPPARD, S. J. (2004). Crystal structure of the toluene/*o*-xylene monooxygenase hydroxylase from *Pseudomonas stutzeri* OX1. insight into the substrate specificity, substrate channeling, and active site tuning of multicomponent monooxygenases. *The Journal of Biological Chemistry*, 279 (29), 30600-30610.

146. SAZINSKY, M. H. and LIPPARD, S. J. (2005). Product bound structures of the soluble methane monooxygenase hydroxylase from *Methylococcus capsulatus* (Bath): Protein motion in the alpha-subunit. *Journal of the American Chemical Society*, 127 (16), 5814-5825.
147. SCANLAN, J., DUMONT, M. G. and MURRELL, J. C. (2009). Involvement of MmoR and MmoG in the transcriptional activation of soluble methane monooxygenase genes in *Methylosinus trichosporium* OB3b. *FEMS Microbiology letters*, 301 (2), 181-187.
148. SCHMALJOHANN, R. (1991). Oxidation of various potential energy sources by the methanotrophic endosymbionts of *siboglinum poseidoni* (pogonophora). *Mar. Ecol. Prog. Ser.* 76:143-148.
149. SCHWARTZ, J. K., WEI, P. P., MITCHELL, K. H., FOX, B. G. and SOLOMON, E. I. (2008). Geometric and electronic structure studies of the binuclear nonheme ferrous active site of toluene-4-monooxygenase: Parallels with methane monooxygenase and insight into the role of the effector proteins in O₂ activation. *Journal of the American Chemical Society*, 130 (22), 7098-7109.
150. SCOTT, H. (2003). Sequences of versatile broad-host-range vectors of the RK2 family *Plasmid*, 50 (1), 74 - 79.
151. SHANKLIN, J. and SOMERVILLE, C. (1991). Stearoyl-acyl-carrier-protein desaturase from higher plants is structurally unrelated to the animal and fungal homologs *Proceedings of the National Academy of Sciences of the United States of America*, 88 (6), 2510-2514.
152. SHIELDS, M. S., REAGIN, M. J., GERGER, R. R., CAMPBELL, R. and SOMERVILLE, C. (1995). TOM, a new aromatic degradative plasmid from *Burkholderia (Pseudomonas) cepacia* G4. *Applied and Environmental Microbiology*, 61 (4), 1352-1356.
153. SIMON, R., PRIEFER, U. and PUHLER, A. (1983). A broad host range mobilization system for in vivo genetic engineering: Transposon mutagenesis in gram negative bacteria *Bio/Technology*, 1 (9), 784 - 791.
154. SJOBERG, B. M (1997). Ribonucleotide reductases - a group of enzymes with different metallosites and a similar reaction mechanism. *Structure and Bonding*, 88 , 139-173.

155. SLUIS, M. K., SAYAVEDRA-SOTO, L. A. and ARP, D. J. (2002). Molecular analysis of the soluble butane monooxygenase from '*Pseudomonas butanovora*'. *Microbiology (Reading, England)*, 148 (11), 3617-3629.
156. SMITH, T. J. and MURRELL, J. C. (2009). Methanotrophy/methane oxidation. In: SCHAECHTER, M. (ed.). *Encyclopedia of Microbiology*; Elsevier, 3, 293 - 298.
157. SMITH, T. J., SLADE, S. E., BURTON, N. P., MURRELL, J. C. and DALTON, H. (2002). Improved system for protein engineering of the hydroxylase component of soluble methane monooxygenase. *Applied and Environmental Microbiology*, 68 (11), 5265-5273.
158. STAFFORD, G. P., SCANLAN, J., MCDONALD, I. R. and MURRELL, J. C. (2003). rpoN, mmoR and mmoG, genes involved in regulating the expression of soluble methane monooxygenase in *Methylosinus trichosporium* OB3b. *Microbiology (Reading, England)*, 149 (7), 1771-1784.
159. STAINTHORPE, A. C., LEES, V., SALMOND, G. P., DALTON, H. and MURRELL, J. C. (1990). The methane monooxygenase gene cluster of *Methylococcus capsulatus* (Bath). *Gene*, 91 (1), 27-34.
160. STANLEY, S. H., PRIOR, S. D., LEAK, D. J. and DALTON, H. (1983). Copper stress underlies the fundamental change in intracellular location of methane mono-oxygenase in methane-oxidizing organisms: Studies in batch and continuous cultures *Biotechnology letters*, 5 (7), 487 - 492.
161. STEIN, L. Y., YOON, S., SEMRAU, J. D., DISPIRITO, A. A., CROMBIE, A., MURRELL, J. C., VUILLEUMIER, S., KALYUZHNYA, M. G., OP DEN CAMP, H. J., BRINGEL, F., BRUCE, D., CHENG, J. F., COPELAND, A., GOODWIN, L., HAN, S., HAUSER, L., JETTEN, M. S., LAJUS, A., LAND, M. L., LAPIDUS, A., LUCAS, S., MEDIGUE, C., PITLUCK, S., WOYKE, T., ZEYTUN, A. and KLOTZ, M. G. (2010). Genome sequence of the obligate methanotroph *Methylosinus trichosporium* OB3b. *Journal of Bacteriology*, 192 (24), 6497-6498.
162. STEMMER, W. P. (1994). Rapid evolution of a protein in vitro by DNA shuffling *Nature*, 370 (6488), 389-391.
163. STOECKER, K., BENDINGER, B., SCHONING, B., NIELSEN, P. H., NIELSEN, J. L., BARANYI, C., TOENSHOFF, E. R., DAIMS, H. and WAGNER, M. (2006). Cohn's crenothrix is a filamentous methane oxidizer

- with an unusual methane monooxygenase. *Proceedings of the National Academy of Sciences of the United States of America*, 103 (7), 2363-2367.
164. STOLYAR, S., FRANKE, M. and LIDSTROM, M. E. (2001). Expression of individual copies of methylococcus capsulatus bath particulate methane monooxygenase genes *Journal of Bacteriology*, 183 (5), 1810-1812.
165. STUBBE, JoAnne, NOCERA, Daniel G., YEE, Cyril S. and CHANG, Michelle C. Y. (2003). Radical initiation in the class I ribonucleotide reductase: Long-range proton-coupled electron transfer? *Chemical Reviews*, 103 (6), 2167 - 2202.
166. SUZUKI, Motoshi, CHRISTIANS, Fred C., KIM, Baek, SKANDALIS, Adonis, BLACK, Margaret E. and LOEB, Lawrence A. (1996). Tolerance of different proteins for amino acid diversity *Molecular Diversity*, 2 (1-2), 111-118.
167. TAO, Y., BENTLEY, W. E. and WOOD, T. K. (2005). Regiospecific oxidation of naphthalene and fluorene by toluene monooxygenases and engineered toluene 4-monooxygenases of *Pseudomonas mendocina* KR1. *Biotechnology and Bioengineering*, 90 (1), 85-94.
168. TAO, Y., FISHMAN, A., BENTLEY, W. E. and WOOD, T. K. (2004). Altering toluene 4-monooxygenase by active-site engineering for the synthesis of 3-methoxycatechol, methoxyhydroquinone, and methylhydroquinone. *Journal of Bacteriology*, 186 (14), 4705-4713.
169. TAO, Y., FISHMAN, A., BENTLEY, W. E. and WOOD, T. K. (2004). Oxidation of benzene to phenol, catechol, and 1,2,3-trihydroxybenzene by toluene 4-monooxygenase of *Pseudomonas mendocina* KR1 and toluene 3-monooxygenase of *Ralstonia pickettii* PK01. *Applied and Environmental Microbiology*, 70 (7), 3814-3820.
170. TINBERG, C. E. and LIPPARD, S. J. (2009). Revisiting the mechanism of dioxygen activation in soluble methane monooxygenase from *M. capsulatus* (Bath): Evidence for a multi-step, proton-dependent reaction pathway. *Biochemistry*, 48 (51), 12145-12158.
171. TINDALL, Kenneth R. and KUNKEL, Thomas A. (1988). Fidelity of DNA synthesis by the *Thermus aquaticus* DNA polymerase *Biochemistry*, 27 (16), 6008-6013.
172. TSIEN, H. C. and HANSON, R. S. (1992). Soluble methane monooxygenase component B gene probe for identification of methanotrophs that rapidly

- degrade trichloroethylene *Applied and Environmental Microbiology*, 58 (3), 953-960.
173. UHLIN, U. and EKLUND, H. (1994). Structure of ribonucleotide reductase protein R1 *Nature*, 370 (6490), 533-539.
174. UKAEGBU, U. E., HENERY, S. and ROSENZWEIG, A. C. (2006). Biochemical characterization of MmoS, a sensor protein involved in copper-dependent regulation of soluble methane monooxygenase. *Biochemistry*, 45 (34), 10191-10198.
175. VARDAR, G., TAO, Y., LEE, J. and WOOD, T. K. (2005). Alanine 101 and alanine 110 of the alpha subunit of *Pseudomonas stutzeri* OX1 toluene-o-xylene monooxygenase influence the regiospecific oxidation of aromatics. *Biotechnology and Bioengineering*, 92 (5), 652-658.
176. VARDAR, G. and WOOD, T. K. (2004). Protein engineering of toluene-o-xylene monooxygenase from *Pseudomonas stutzeri* OX1 for synthesizing 4-methylresorcinol, methylhydroquinone, and pyrogallol. *Applied and Environmental Microbiology*, 70 (6), 3253-3262. (a)
177. VARDAR, G. and WOOD, T. K. (2005). Alpha-subunit positions methionine 180 and glutamate 214 of *Pseudomonas stutzeri* OX1 toluene-o-xylene monooxygenase influence catalysis. *Journal of Bacteriology*, 187 (4), 1511-1514.
178. VARDAR, G. and WOOD, T. K. (2005). Protein engineering of toluene-o-xylene monooxygenase from *Pseudomonas stutzeri* OX1 for enhanced chlorinated ethene degradation and o-xylene oxidation. *Applied Microbiology and Biotechnology*, 68 (4), 510-517. (b)
179. VIGLIOTTA, G., NUTRICATI, E., CARATA, E., TREDICI, S. M., DE STEFANO, M., PONTIERI, P., MASSARDO, D. R., PRATI, M. V., DE BELLIS, L. and ALIFANO, P. (2007). *Clonothrix fusca* roze 1896, a filamentous, sheathed, methanotrophic gamma-proteobacterium. *Applied and Environmental Microbiology*, 73 (11), 3556-3565.
180. VOROBEV, A. V., BAANI, M., DORONINA, N. V., BRADY, A. L., LIESACK, W., DUNFIELD, P. F. and DEDYSH, S. N. (2010). *Methyloferula stellata* gen. nov., sp. nov., an acidophilic, obligately methanotrophic bacterium possessing only a soluble methane monooxygenase *International Journal of Systematic and Evolutionary Microbiology*.

181. VU, V. V., EMERSON, J. P., MARTINHO, M., KIM, Y. S., MUNCK, E., PARK, M. H. and QUE, L., Jr (2009). Human deoxyhypusine hydroxylase, an enzyme involved in regulating cell growth, activates O₂ with a nonheme diiron center. *Proceedings of the National Academy of Sciences of the United States of America*, 106 (35), 14814-14819.
182. WARD, N., LARSEN, O., SAKWA, J., BRUSETH, L., KHOURI, H., DURKIN, A. S., DIMITROV, G., JIANG, L., SCANLAN, D., KANG, K. H., LEWIS, M., NELSON, K. E., METHE, B., WU, M., HEIDELBERG, J. F., PAULSEN, I. T., FOUTS, D., RAVEL, J., TETTELIN, H., REN, Q., READ, T., DEBOY, R. T., SESHADRI, R., SALZBERG, S. L., JENSEN, H. B., BIRKELAND, N. K., NELSON, W. C., DODSON, R. J., GRINDHAUG, S. H., HOLT, I., EIDHAMMER, I., JONASEN, I., VANAKEN, S., UTTERBACK, T., FELDBLYUM, T. V., FRASER, C. M., LILLEHAUG, J. R. and EISEN, J. A. (2004). Genomic insights into methanotrophy: The complete genome sequence of *Methylococcus capsulatus* (Bath). *PLoS biology*, 2 (10), e303.
183. WHITTENBURY, R., PHILLIPS, K. C. and WILKINSON, J. F. (1970). Enrichment, isolation and some properties of methane-utilizing bacteria *Microbiology*, 61 (2), 205 - 218. (a)
184. WHITTINGTON, D. A. and LIPPARD, S. J. (2001). Crystal structures of the soluble methane monooxygenase hydroxylase from *Methylococcus capsulatus* (Bath) demonstrating geometrical variability at the dinuclear iron active site *Journal of the American Chemical Society*, 123 (5), 827 - 838. (b)
185. WHITTLE, E. J., TREMBLAY, A. E., BUIST, P. H. and SHANKLIN, J. (2008). Revealing the catalytic potential of an acyl-ACP desaturase: Tandem selective oxidation of saturated fatty acids. *Proceedings of the National Academy of Sciences of the United States of America*, 105 (38), 14738-14743.
186. WOODLAND, M., PATIL, D., CAMMACK, R. and DALTON, H. (1986). ESR studies of protein A of the soluble methane monooxygenase from *Methylococcus capsulatus* (Bath) *Biochimica et Biophysica Acta (BBA) - Protein Structure and Molecular Enzymology*, 873 (2), 237 - 242. (a)
187. WOODLAND, M. P. and DALTON, H. (1984). Purification and characterization of component A of the methane monooxygenase from *Methylococcus capsulatus* (Bath) *The Journal of Biological Chemistry*, 259 (1), 53-59. (b)

188. YEN, K. M. and KARL, M. R. (1992). Identification of a new gene, *tmoF*, in the *Pseudomonas mendocina* KR1 gene cluster encoding toluene-4-monooxygenase. *Journal of Bacteriology*, 174 (22), 7253-7261.
189. YEN, K. M., KARL, M. R., BLATT, L. M., SIMON, M. J., WINTER, R. B., FAUSSET, P. R., LU, H. S., HARCOURT, A. A. and CHEN, K. K. (1991). Cloning and characterization of a *Pseudomonas mendocina* KR1 gene cluster encoding toluene-4-monooxygenase. *Journal of Bacteriology*, 173 (17), 5315-5327.
190. ZAHN, J. A. and DISPIRITO, A. A. (1996). Membrane-associated methane monooxygenase from *Methylococcus capsulatus* (Bath) *Journal of Bacteriology*, 178 (4), 1018-1029.

Appendix 1 media preparation

1.1) Preparation of Nitrate Mineral Salts Medium (0.1mg/Ltr CuS04.5H20)

Preparation of 1 x NMS Medium

- © 100 ml 10 x NMS salts solution.
- © 1 ml Sodium Molybdate solution
- © 1 ml Trace Elements Solution.
- © 0.1 ml Fe EDTA solution.
- © Dilute up to 1 L sdH20
- © Autoclave at 15 psi for 15 minutes.

For solid agar plates 1.5 % bacteriological agar (wt/v) is added to NMS medium prior to autoclaving. When the NMS is cool enough to hold in the hand, aseptically add 10 ml phosphate buffer. If this is done too early the phosphate will precipitate out.

10 x NMS salts solution

- © 10 g KN03
- © 10 g MgS04.7H20 (4.8g MgS04)
- © 2g CaCl2.2H20
- © up to 1 L sdH20

FE EDTA solution

- © 3.8 g Fe EDTA
- © up to 100 ml sdH20
- Q

Sodium Molybdate solution

- © 0.5 g NaMo04.2H20
- © up to 1 L sdH20

Trace elements solution

- 9 0.1 g $C_{11}SO_{4.5}H_{20}$
- 0.5 g $FeSO_{4.7}H_{20}$
- o 0.4 g $ZnSO_{4.7}H_{20}$
- 0.015 g $H_{3}B_{03}$
- o 0.05 g $CoCl_{2.6}H_{20}$
- © 0.25 g EDTA (di sodium salt)
- © 0.02 g $MnCl_{2.4}H_{20}$
- o 0.01 g $NiCl_{2.6}H_{20}$
- © up to 1 L with sdH_{20}

Dissolve the above in the specified order in distilled water and dilute to 250 ml. Store in the dark (wrap around with Aluminium foil).

Phosphate Buffer

- © 49.7 g $Na_2HPO_4 \cdot 2H_2O$
- 39 g KH_2PO_4
- o Up to 1 L sdH_{20}

pH should be 6.8 without altering. Sterilise by autoclaving in 100 ml aliquots and store at room temp.

1.2) Liquid LB media:

- © 10 g Tryptone
- © 5 g yeast extract
- © 10 g NaCl
- © 100 μ l 5M NaOH
- ® up to 1 L sdH_{20}
- © Autoclave at 15 psi for 15 minutes

For solid agar plates 1.5 % bacteriological agar (wt/v) is added to LB medium prior to autoclaving

1.3) SOB and SOC media

SOB Broth

- © 20.0 g of tryptone
- © 5.0 g of yeast extract
- © 0.5 g of NaCl
- © Add deionized H₂O to a final volume of 1 L
- © Autoclave at 15 psi for 15 min

Add 10 ml of filter-sterilized 1 M MgCl² and 10 ml of filter-sterilized 1 M MgSO₄ prior to use

SOC Broth

(prepared immediately before use)

- © 2 ml of filter-sterilized 20 % (w/v) glucose or 1 ml of filter-sterilized
- © 2 M glucose
- © SOB medium (autoclaved) to a final volume of 100 ml

Appendix 2 Buffer preparation

1.1) Preparation of buffers for genomic tip protocol

B1 buffer

- 18.61 g Na₂EDTA-2H₂O
- o 6.06 g Tris base
- © 800 ml distilled water.
- © 50 ml 10% Tween-20 solution (v/v)
- © 50 ml 10% Triton X-100 solution, (v/v)
- © Adjust the pH to 8.0 with HCl.
- © Up to 1 L sdH₂O

B2 buffer

- © 286.59 g guanidine HCl
- 700 ml sdH₂O
- ® 200 ml 100% Tween-20 (v/v)
- © Up to 1 L sdH₂O

QBT buffer

- © 43.83 g NaCl,
- ® 10.46 g MOPS
- © 800 ml distilled water.
- Adjust the pH to 7.0 with NaOH.
- Add 150 ml pure isopropanol
- © 15 ml 10% Triton X-100 solution (v/v)
- ® Up to 1 L sdH₂O

QC buffer

- o 58.44 g NaCl,
- © 10.46 g MOPS (free acid)
- © 800 ml distilled water.
- ® Adjust the pH to 7.0 with NaOH.
- © Add 150 ml isopropanol,
- o Up to 1 L sdH₂O

QF buffer

- 73.05 g NaCl
- © 6.06 g Tris base
- 800 ml distilled water.
- © Adjust the pH to 8.5 with HCl.
- o Add 150 ml pure isopropanol.
- © Up to 1 L sdH₂O

1.2) Buffers for Hanahan Plasmid transformation method

DnD Solution

- © 1.53 g D U
- 100 pi of 1 M Potassium acetate solution (pH 7.5)
- 9 ml Dimethylsulfoxide (DMSO)
- 900 pi sdH₂O

TFB transformation buffer

- © 0.74 g KCl
- 0.89 g MnCl₂·4H₂O
- © 0.15g CaCl₂·2 H₂O
- ® 0.08 g Hexamine cobalt chloride
- 2 ml of 0.5 M 2-(N-Morpholino)ethanesulfonic acid potassium salt solution (pH6.3)
- © Up to 100 ml sdH₂O

Appendix 3 SDS PAGE reagents and protocol

RUNNING BUFFER

- © 7.2 g Glycine
- © 1.5 g Tris
- © 0.5 g SDS
- © dH₂O up to 500 ml

RESOLVING BUFFER (3 M Tris-HCl pH 8.8)

STACKING BUFFER (0.5 M TrisHCl pH 6.8)

RESOLVING GEL (12.5 %)

- Ⓜ 4.84 ml 40 % acrylamide/bis solution
 - 2.5 ml resolving buffer
 - 2.65 ml H₂O
- © 0.1 ml 10 % glycerol (v/v)
- © 0.1 ml 10% SDS
- © 0.5 ml 10 % APS (fresh made)
- © 5 pi TEMED (add last)

STACKING GEL

- © 0.83 ml 40 % acrylamide/bis solution
- Ⓜ 1.36 ml stacking buffer
- © 2.8 ml H₂O
- © 50 pi 10 % SDS(v/v)
- © 50 pi 10 % glycerol (v/v)
- Ⓜ 0.5 ml 10 % APS (wt/v)
- © 5 pi TEMED (add last)

SAMPLE BUFFER (2x) (gel loading)

- Ⓜ 250 pi stacking buffer
- « 200 pi 100 % glycerol
- q 80 pi 0.5 % bromophenol blue
- © 100 pi (3-mercaptoethanol (100 %)
- o 1.2 ml 10% SDS (wt/v)

STAIN SOLUTION

- Ⓢ 450 ml methanol
- 450 ml sdH₂O
- Ⓢ 100 ml glacial acetic acid
- Ⓢ 2.5 g coomassie brilliant blue R

DESTAIN SOLUTION

- 300 ml methanol
- « 100 ml glacial acetic acid
- 600 ml sdH₂O

SDS PAGE Protocol

- Ⓢ clip together glass plates including rubber lining
- Ⓢ pour resolving gel until few mm below level of wells
- Ⓢ overlay gel with 700 μ l ethanol or isopropanol
 - after gel has set (-30 min) wash off ethanol with water and blot off excess
- Ⓢ assemble stacking gel and pour over resolving gel
- Ⓢ allow to set
 - remove clips and rubber seal, assemble gel tank and add running buffer
- Ⓢ boil 10 μ l sample for 10 min
- Ⓢ add 10 μ l sample buffer to each sample
 - run at 130 v 150 ma for 30 min turn to 150 v for 1hr or until dye reaches bottom of gel.

Appendix 4 Ethanol free NADH preparation

Preparation of 100mM NADH

- o 0.7635 g NADH
- © 10mlsdH₂O
- o Divide into 1 ml aliquots

Ether extraction of NADH

- q Add 250 µl diethyl ether to 1ml NADH
- ® Remove top layer
- © Add 250 µl diethyl ether
- © Remove top layer
- ® dry overnight in Eppendorf 5301 concentrator
- ® Add 1ml sdH₂O and vortex till dissolved.

Store at in foil at -15 °C, use within 1 week.

Mutagenesis of the “Leucine Gate” To Explore the Basis of Catalytic Versatility in Soluble Methane Monooxygenase[∇]

Elena Borodina,^{1†} Tim Nichol,^{2†} Marc G. Dumont,¹ Thomas J. Smith,^{2*} and J. Colin Murrell¹

Department of Biological Sciences, University of Warwick, Coventry CV4 7AL, United Kingdom,¹ and Biomedical Research Centre, Sheffield Hallam University, Howard Street, Sheffield S1 1WB, United Kingdom²

Received 11 April 2007/Accepted 7 August 2007

Soluble methane monooxygenase (sMMO) from methane-oxidizing bacteria is a multicomponent nonheme oxygenase that naturally oxidizes methane to methanol and can also cooxidize a wide range of adventitious substrates, including mono- and diaromatic hydrocarbons. Leucine 110, at the mouth of the active site in the α subunit of the hydroxylase component of sMMO, has been suggested to act as a gate to control the access of substrates to the active site. Previous crystallography of the wild-type sMMO has indicated at least two conformations of the enzyme that have the “leucine gate” open to different extents, and mutagenesis of homologous enzymes has indicated a role for this residue in the control of substrate range and regioselectivity with aromatic substrates. By further refinement of the system for homologous expression of sMMO that we developed previously, we have been able to prepare a range of site-directed mutations at position 110 in the α subunit of sMMO. All the mutants (with Gly, Cys, Arg, and Tyr, respectively, at this position) showed relaxations of regioselectivity compared to the wild type with monoaromatic substrates and biphenyl, including the appearance of new products arising from hydroxylation at the 2- and 3- positions on the benzene ring. Mutants with the larger Arg and Trp residues at position 110 also showed shifts in regioselectivity during naphthalene hydroxylation from the 2- to the 1- position. No evidence that mutagenesis of Leu 110 could allow very large substrates to enter the active site was found, however, since the mutants (like the wild type) were inactive toward the triaromatic hydrocarbons anthracene and phenanthrene. Thus, our results indicate that the “leucine gate” in sMMO is more important in controlling the precision of regioselectivity than the sizes of substrates that can enter the active site.

Soluble methane monooxygenase (sMMO) is one of two enzyme systems via which methane-oxidizing bacteria catalyze the oxygenation of methane to methanol, which is the particularly challenging first step in the metabolism of the kinetically unreactive methane molecule (28). sMMO is a multicomponent enzyme encoded by the six-gene operon *mmoXYBZDC*, in which the active binuclear iron center (8, 45) that is the site of methane oxidation resides within the α subunit of the hydroxylase component, encoded by *mmoX* (5). It may be because methane is a small and unfunctionalized substrate that the hydrophobic pocket on the hydroxylase component of sMMO that has evolved to bind methane is also able to accommodate a very wide range of hydrocarbons and other molecules. Indeed, sMMO, whose known substrates number over 100, range in size from methane to naphthalene (2) and biphenyl (23), and also include carbon monoxide and ammonia (37), must surely be among the most catalytically versatile of all known enzymes.

The unusual catalytic versatility of sMMO has led to interest in its potential as a biocatalyst for bioremediation and synthetic chemistry as well as an interest in how the structure of the enzyme facilitates so wide a substrate range. The hydrophobic substrate binding site of sMMO, which is believed to be re-

sponsible for binding its wide range of substrates, is adjacent to the active binuclear iron center and is deeply buried in the 250-kDa ($\alpha\beta\gamma$)₂ hydroxylase component (9, 12, 31), presumably to prevent the solvent from quenching the highly oxidizing diferryl intermediate Q (22, 33, 35) that is needed to oxygenate methane and other recalcitrant substrates. Access to the active site is likely to be via another hydrophobic pocket, cavity two, which is part of a chain of buried cavities that communicate between the active site and the solvent. Between cavity two and the active site lies the “leucine gate,” residue Leu 110. Different crystal forms of the hydroxylase differ in the conformation of Leu 110, such that in the crystal state it can either block the pathway between cavity two and the active site or (in the alternative conformation) open a 2.6-Å-diameter channel between the two cavities. A larger conformational change, such as may be caused by interaction with the other components of the sMMO complex, could open this “leucine gate” further to allow passage of substrates and products (30), reasonably acting to control the access of substrates to the active site.

Other monooxygenases homologous to sMMO, which naturally oxidize molecules considerably larger than methane, have narrower substrate ranges than sMMO (21). There is an X-ray crystal structure for one of these enzymes, toluene *o*-xylene monooxygenase, in which the opening to the active site is wider than that observed in sMMO (33). While a more open active site is consistent with the larger natural substrate of this enzyme, it is clear that the active site of sMMO can open sufficiently to allow entry of aromatic substrates.

Mutagenesis studies of homologous monooxygenases whose natural substrates are monoaromatic hydrocarbons have indi-

* Corresponding author. Mailing address: Biomedical Research Centre, Sheffield Hallam University, Howard Street, Sheffield S1 1WB, United Kingdom. Phone: 44 114 225 3042. Fax: 44 114 225 3066. E-mail: t.j.smith@shu.ac.uk.

† E. Borodina and T. Nichol made equal contributions to this work.

[∇] Published ahead of print on 17 August 2007.

TABLE 1. Plasmids and *M. trichosporium* strains

Plasmid or strain	Description	Source or reference
Plasmids		
p34S-Gm	Broad-host-range TnMod-derived plasmid, 3.6 kb; Ap ^r Gm ^r	7
pBBR1MCS5	Broad-host-range cloning vector, 4.8 kb; Gm ^r Mob ⁺ lacZ'	20
pBBR1MCS5b	Broad-host-range cloning vector, 4.3 kb; Gm ^r Mob ⁺ lacZ'	This study
pK18mobsacB	Mobilizable plasmid with narrow-host-range (pUC18-derived) replicon, 3.8 kb; oriT Km ^r lacZ' sacB	34
pUC19	Cloning vector, 2.7 kb; Ap ^r lacZ'	43
pMD2	10-kb KpnI insert of pTJS176, containing <i>mnoRGXYBZDC</i> , cloned into pBBR1MCS5b; Gm ^r	This study
pMD-Mdel1	pUC19 containing a 2.2-kb fragment spanning <i>mnoG</i> of <i>M. trichosporium</i> and a 1.2-kb fragment containing ' <i>mnoC</i> '; Ap ^r	This study
pMD-Mdel2	pMD-Mdel1 with the 0.87-kb Gm ^r cassette of p34S-Gm cloned into the BamHI site between <i>mnoG</i> and ' <i>mnoC</i> '; Gm ^r Ap ^r	This study
pMD-Mdel3	pK18mobsacB containing the 4.3-kb <i>mnoG</i> -Gm ^r -' <i>mnoC</i> ' fragment from pMD-Mdel2; Gm ^r Kn ^r	This study
pNPB101	PUC18 carrying the 1.0-kb XbaI-NdeI fragment of pSJH1a, including <i>mnoX</i> '	This study
pTJS140	Broad host-range cloning vector, 7.5 kb; Mob ⁺ Ap ^r Sp ^r Sm ^r lacZ'	38
pTJS175	10-kb KpnI insert of pTJS173 cloned into pTJS140 in the same direction as lacZ'; Ap ^r Sp ^r Sm ^r	38
pTJS176	10-kb KpnI insert of pTJS173 cloned into pMTL24; Ap ^r	38
<i>M. trichosporium</i> strains		
OB3b	Wild-type, sMMO-positive strain	Laboratory stock
Mutant F	Kn ^r ; sMMO-minus double crossover mutant of OB3b partially deleted in <i>mnoX</i>	26
SMDM	Gm ^r ; sMMO-minus double crossover mutant of OB3b deleted in <i>mnoXYBZD</i> and the first 3 codons of <i>mnoC</i>	This study
SMDM-sMMO	SMDM into which pTJS175 had been introduced by means of conjugation	This study

cated that the position equivalent to Leu 110 is indeed important in the interaction between these enzymes and their substrates. In a directed evolution study of toluene 2-monoxygenase of *Burkholderia cepacia* G4 (4), a Val-to-Ala mutation at position 106, equivalent to Leu 110 in sMMO, gave increased naphthalene and phenanthrene oxidation but no change in regioselectivity with naphthalene. Both the mutant and the wild type gave 1-naphthol as the predominant product. This was consistent with the proposed gating role of this residue, i.e., the mutation affected the rates of oxidation of large substrates but did not greatly affect regioselectivity. Similar results were found in a saturation mutagenesis study of toluene 4-monoxygenase, where the V100L mutant showed a twofold increase in the rate of oxidation of 2-methoxyphenol; here, a modest loss of regiospecificity was observed, but the mutant (like the wild type) gave 3-methoxyresorcinol as the major product (41). A reduction in the rate of oxindole formation from indole by the Ala, Cys, and Val mutations of the equivalent Ile 100 residue in toluene 4-monoxygenase (40) was also consistent with such a function, although a change in the predominant product of phenol hydroxylation from catechol to hydroquinone (i.e., a shift in regioselectivity from the 2- to the 4- position) in the I100Q mutant of toluene *o*-xylene monoxygenase (42) indicates that the site equivalent to Leu 110 may have a role in determining regioselectivity as well as substrate access. Results from mutagenesis of the nearby site Gly 113 in soluble butane monoxygenase have also suggested that a conformational change involving the "leucine gate" (Leu 109 in this enzyme) may be necessary for product release from the active site, since the G113N mutant showed a reduced inhibition by nascent methanol produced by oxidation of methane (13).

In order to probe the role of Leu 110 in sMMO, we here report further refinements in the homologous expression system for sMMO that we previously developed (25, 38) in order to overcome problems associated with expression of the enzyme in *Escherichia coli*. Several mutations at position 110 in the α subunit of the hydroxylase have been analyzed using bulky aromatic substrates in order to evaluate the role of this residue in the sMMO system and to compare its function to that of the equivalent residues in the aromatic monoxygenases.

MATERIALS AND METHODS

Bacterial strains, plasmids, and culture conditions. Details of plasmids and methanotroph strains used during this study are given in Table 1. Plasmid construction and site-directed mutagenesis were accomplished using *E. coli* strains INV α F', TOP10 (Invitrogen), and XL-10 GOLD (Stratagene). The donor strain for conjugation of plasmids into *Methylosinus trichosporium* was *E. coli* S17-1 (36). *E. coli* strains were cultivated at 37°C in LB medium or on LB agar plates. Strains of *M. trichosporium* were cultivated at 30°C on nitrate mineral salts (NMS) agar plates and in NMS medium in flask and fermentor culture, using methane as the carbon and energy source, as described previously (38). As previously described, cells were cultivated in a fermentor in NMS medium containing 0.1 mg liter⁻¹ (0.4 μ M) of CuSO₄ · 5H₂O and induction of sMMO occurred when the culture optical density at 600 nm (OD₆₀₀) exceeded about 5.0, when the copper-to-biomass ratio became low enough to induce sMMO genes. Where necessary, antibiotics were added to culture media at the following working concentrations: ampicillin, 50 to 100 μ g ml⁻¹; gentamicin, 5 μ g ml⁻¹; kanamycin, 50 μ g ml⁻¹.

General DNA methods. General methods for DNA purification and analysis and cloning with *E. coli* were performed according to Sambrook et al. (32). Where necessary, to facilitate difficult plasmid manipulations, commercially prepared competent *E. coli* cells (TOP10 [Invitrogen] or Solo Pack GOLD [Stratagene]) were used. DNA probes were labeled by random priming (10, 11) using hexanucleotide primers and deoxynucleoside triphosphates from Roche according to the manufacturer's instructions. An agarose gel-purified DNA fragment (25 to 50 ng) was labeled with [α -³²P]dGTP (50 μ Ci) for 1 h at 37°C with Klenow

polymerase (Invitrogen). The unincorporated label was removed using Micro-Spin columns (Amersham Pharmacia Biotech). The probes were denatured by the addition of NaOH to a final concentration of 0.4 M and incubated for 2 min at room temperature before being added to the hybridization solution.

Construction of plasmids. In order to allow subsequent manipulations of the sMMO operon by using BamHI, the BamHI site was deleted from the vector pBBR1MCS-5 (20) by removing the fragment of the multiple cloning site that contained it with ClaI and BstBI and religating the plasmid backbone via the compatible cohesive ends thus produced, giving the vector pBBR1MCS-5b. The 10-kb fragment containing the *mnoXYBZDC* operon from *M. trichosporium* OB3b and flanking sequences was excised from pTJS176 (38) with KpnI and cloned into the unique KpnI site of pBBR1MCS-5b, giving plasmid pMD2. To direct deletion of the chromosomal copy of the sMMO-encoding operon, the plasmid pMD-MdeI3 was then constructed as detailed in Fig. 1.

Site-directed mutagenesis and preparation of cells expressing the mutant enzymes. Site-directed mutagenesis of the *mnoX* gene, encoding the α subunit of the sMMO hydroxylase, was performed via the four-primer overlap extension method (15) as described previously (38). Primers used for mutagenesis are given in Table 2. Dye termination sequencing was used to confirm the absence of unwanted mutations from PCR-derived portions of the cloned mutant sMMO genes. The mutant *mnoX* genes, assembled into an intact *mnoXYBZDC* operon in the sMMO expression plasmid pTJS175 (38), were introduced into *M. trichosporium* SMDM by conjugation (25, 38). The recombinant sMMO strains were initially grown on NMS plates containing antibiotics (gentamicin and kanamycin) and screened for sMMO activity by using the naphthalene oxidation test (1, 2). Cells for more-detailed analysis were prepared by growing the recombinant *M. trichosporium* cells in a fermentor to an OD_{600} greater than 5 in order to induce mutant enzyme expression from the native sMMO promoter in pTJS175, which is induced by low copper-to-biomass ratio in the culture.

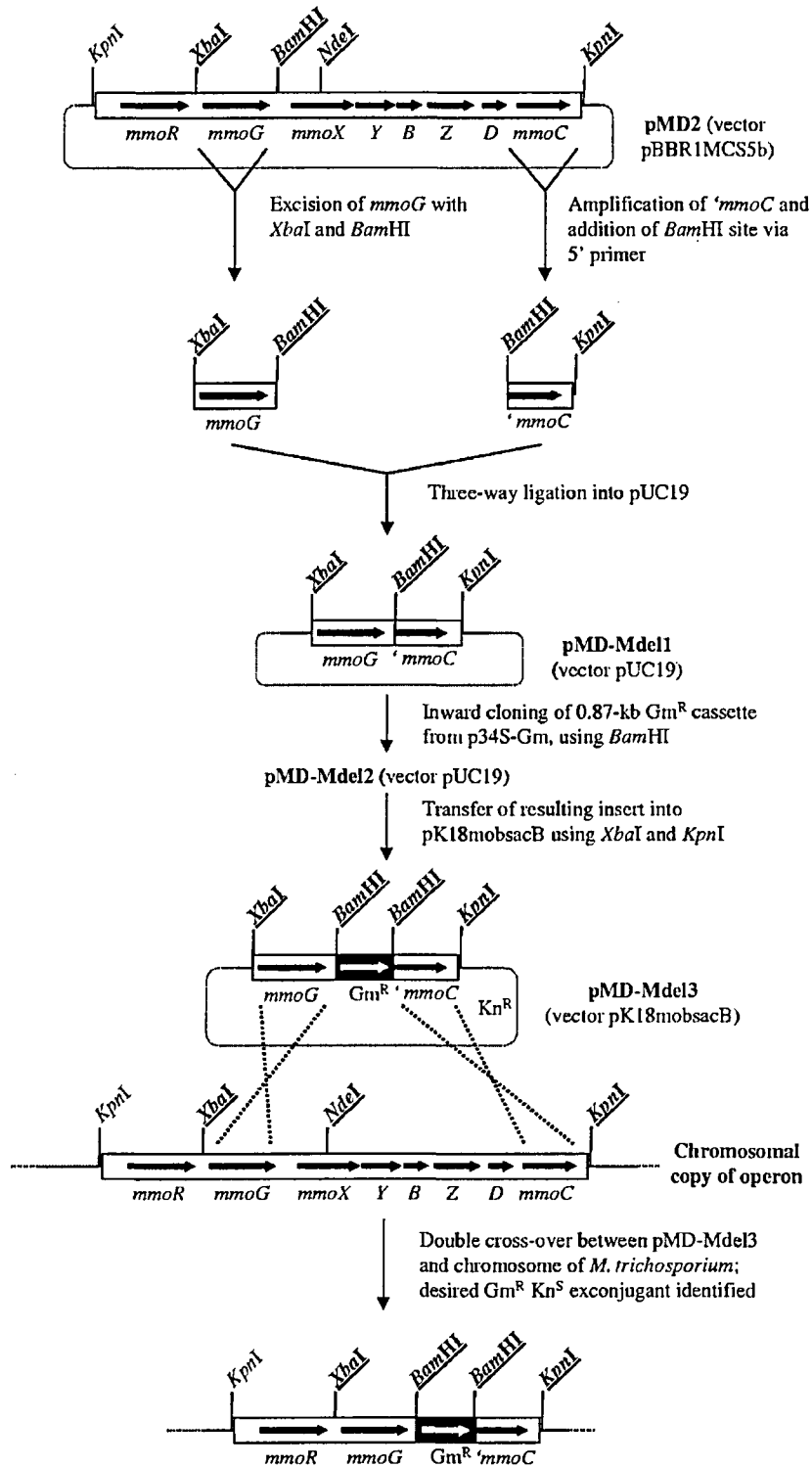
sMMO assays. sMMO is the only enzyme system expressed in *M. trichosporium* that is able to oxygenate aromatic hydrocarbon substrates. As a result, assays with these substrates can be performed using whole-sMMO-expressing cells. The semiquantitative naphthalene oxidation test, which is based on the derivatization of the naphthol products of naphthalene oxidation to pink/purple diazo dyes, was performed on cultures in liquid medium and on agar plates as described previously (1, 2). After oxidation of aromatic hydrocarbons by cells expressing mutant or wild-type sMMO, product analysis was performed as follows. Methanotroph cells were resuspended in 25 mM MOPS (morpholinepropanesulfonic acid) buffer (pH 7.0) to an OD_{600} of greater than 5. Each assay was conducted with 5 ml of cell suspension or 10 ml where biphenyl was the substrate. Oxidation substrate was added, together with sodium formate (10 mM), to ensure a plentiful supply of the reducing equivalents required by sMMO. The amounts of oxidation substrate used were 50 μ l for liquid substrates (toluene or ethylbenzene) and 1 mg for solid substrates (naphthalene, biphenyl, phenanthrene, or anthracene). The reaction mixture was incubated aerobically at 30°C for 48 h with shaking (250 rpm) in a closed 30-ml glass vial held in a horizontal position. The hydroxylated products were extracted into 1.0 ml of diethyl ether, which was then evaporated to a volume of 50 μ l before analysis. The products of toluene and biphenyl oxidation were characterized by means of gas chromatography (GC), using a 6890 GC apparatus (Hewlett-Packard) fitted with a Stabilwax capillary column with a Carbowax polyethylene glycol coating (50 m by 0.32 mm; coating thickness, 1 μ m) and coupled to a flame ionization detector. The column temperature at the beginning of the separation was held at 100°C for 5 min, after which it was ramped to 180°C at 2°C min⁻¹ and held for 15 min at 180°C. The flow rate of carrier gas (nitrogen) was 1.5 ml min⁻¹, and the split ratio was 10:1. When the substrate was naphthalene or ethylbenzene, products were analyzed via GC-mass spectrometry (MS) using a 5890 GC (Hewlett-Packard) coupled to a Trio-1 MS. Here, the GC was fitted with a Hewlett-Packard HP-5 column with a (5% phenyl) methyl polysiloxane coating (50 m by 0.32 mm; coating thickness, 0.25 μ m) and operated with a carrier gas (nitrogen) flow rate of 1.5 ml min⁻¹. With ethyl benzene as the substrate, the split ratio was 30:1 and the column temperature was ramped from 80°C to 250°C at 4°C min⁻¹ and held for 1 min at 250°C. When naphthalene was the substrate, the separations were carried out without a split and the column temperature was ramped from 80°C to 126°C at 10°C min⁻¹, from 126°C to 129°C at 0.1°C min⁻¹, and then from 129°C to 250°C at 10°C min⁻¹. When biphenyl was the substrate, the products were separated via a PerkinElmer autosystem GC using the Hewlett-Packard HP-5 column (details described above) coupled to a flame ionization detector. The separations were carried out without a split. The carrier gas (nitrogen) flow rate was 1 ml min⁻¹, and the column temperature was ramped from 90°C to 190°C at 5°C min⁻¹, held at 190°C for 1 min, and then ramped to 280°C at 10°C min⁻¹. Products were identified by comparison of retention times and mass spectra to authentic standards.

RESULTS

Construction of a new sMMO-deleted methanotroph expression host for recombinant sMMO enzymes. Previous mutants of the hydroxylase component of sMMO were expressed in the sMMO-negative mutant of *M. trichosporium* known as mutant F (38). The chromosomal copy of the sMMO operon in mutant F (26) has a deletion of a 1.2-kb fragment that encompasses the portion of *mnoX* coding for amino acids Val 112-Thr 508. This limits the region of the sMMO operon that can be mutated to the portion of *mnoX* (encoding the α subunit of the hydroxylase) that is deleted from mutant F, because mutations outside this region could be repaired by homologous recombination between the plasmid carrying the mutant sMMO operon and the remainder of the chromosomal copy. The mutagenesis target during this study, the portion encoding Leu 110, lies just outside this region, so it was in principle possible that mutations could be repaired by homologous recombination with the chromosome. Furthermore, for future studies we wished to produce an expression host for recombinant sMMO that would allow mutagenesis anywhere within the hydroxylase component (encoded by *mnoX*, *-Y*, and *-Z*). The new expression host, *M. trichosporium* SMDM (for soluble-methane-monoxygenase-deleted mutant), in which the first five genes of the sMMO operon (*mnoXYBZD*, including all the structural genes for the hydroxylase and protein B) had been fully deleted by marker exchange mutagenesis, was therefore constructed (Fig. 1). The deletion of the intended portion of the sMMO-encoding operon and double recombination into the chromosome were confirmed by restriction digestion of chromosomal DNA and digestion with ClaI and SphI, followed by Southern blotting and probing with probes specific to *mnoR*, *mnoX*, and *mnoY* (data not shown). Strain SMDM exhibited the expected sMMO-negative phenotype, as judged by a negative naphthalene oxidation test result under low-copper conditions, which induced sMMO expression and under which a parallel control with wild-type *M. trichosporium* OB3b showed strong naphthalene oxidation activity.

The suitability of strain SMDM as a host for expression of recombinant sMMOs was established by introducing pTJS175, containing the wild-type sMMO operon, into SMDM to give strain SMDM-sMMO (Table 1). Growth on NMS agar medium containing a low level of copper(II) (0.4 μ M) to induce sMMO yielded colonies that gave strong positive results in the naphthalene oxidation test, confirming the expression of the recombinant sMMO.

Mutagenesis of the leucine gate residue produced mutants that gave unusual naphthalene oxidation test results. Four mutants of the proposed gating residue Leu 110 that gave a range of amino acid bulk and functionality results at this position were constructed. Mutations to Gly (less bulky; more flexible), Cys (less bulky), Arg (slightly more bulky; positively charged), and Tyr (more bulky; hydroxylated) were constructed, confirmed by DNA sequencing, and expressed in the *M. trichosporium* SMDM homologous expression system, as described in Materials and Methods. When the four mutant strains were grown in liquid culture at a low copper-to-biomass ratio, which induces expression of sMMO, all four gave positive naphthalene test results, confirming that all the mutant clones produced mutant enzymes that were active with naph-



Chromosome of *Ms. trichosporium* SMDM with *mmoXYBZD* deleted

FIG. 1. Construction of the plasmid pMD-Mdel3 and its use for marker exchange deletion of the first five genes of the sMMO operon. In addition to the sMMO-encoding *mmoXYBZD* operon, the upstream *mmoR* and *mmoG* genes are also indicated. These encode, respectively, a putative σ^{54} -dependent transcriptional regulator and molecular chaperon that (while not part of the mature sMMO complex) are needed for expression of active sMMO in vivo (39). PCR primers for amplification of '*mmoC*' were mmodel-1 (5'-ATA ATA GGA TCC ATC GTC ATC GAG ACC GAG GAC G-3'; *Bam*HI site underlined) and the M13 universal sequencing primer (3'-GTA AAA CGA CGG CCA GT-5'). Deletion of *mmoXYBZD* and the upstream region of the *mmoC* gene was effected by introducing pMD-Mdel3 into *M. trichosporium* by conjugation (25) and selecting exconjugants by using gentamicin. *M. trichosporium* SMDM, the exconjugant in which the sMMO-encoding operon had been deleted via double homologous recombination, was selected on the basis of its sMMO-negative phenotype as determined by the naphthalene oxidation test (1, 2), together with its *Gm*^R *Kn*^S phenotype. The image is not drawn to scale.

TABLE 2. Primers used for site-directed mutagenesis

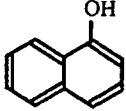
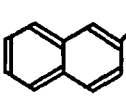
Mutation	Oligonucleotide sequence (5'-3') ^a	Altered amino acid
L110G	GTG ATC TCG AAC TTC GGC GAG GTC GGC GAA TAT A	Gly 110
L110C	GTG ATC TCG AAC TTC TGC GAG GTC GGC GAA TAT A	Cys 110
L110R	GTG ATC TCG AAC TTC CGC GAG GTC GGC GAA TAT A	Arg 110
L110Y	GTG ATC TCG AAC TTC TAT GAG GTC GGC GAA TAT A	Tyr 110

^a Mutations are shown in bold type. Codons encoding altered amino acids are underlined. The pairs of mutagenic primers used to create each mutation were complementary, so only the forward primer is shown.

thalene as the substrate. The L110G and L110C mutants gave positive naphthalene test results where the purple diazo dye product was, like that from the wild type, stable for more than 10 min. The colors produced by the L110R and L110Y mutants, however, were stable for less than 1 min and appeared pink compared to the purple seen with the wild type (data not shown). Although we had previously observed mutants of sMMO where the naphthalene test gave a very weak color change, indicating a low-activity or unstable enzyme (38), this was the first time that we had observed a mutant where the stability (and color) of the naphthalene test result was markedly changed.

The L110R and L110Y mutants of sMMO show inverted regioselectivity with naphthalene compared to the wild type. It was reasoned that the qualitative difference in the stabilities of the naphthalene test colors of the mutant and wild-type enzymes was most likely due to an alteration in the position(s) of oxygenation in the products of naphthalene oxidation by the L110R and L110Y mutants. GC-MS analysis (Table 3) confirmed that there were significant alterations in the distribution of monohydroxylated products from the mutant enzymes. Whereas the wild-type enzyme and the L110C mutant gave a slight excess of 2-naphthol over 1-naphthol, this regioselectivity was reversed in the other three mutants, and the two mutants that gave the unstable naphthalene test color (L110R and L110Y) yielded the smallest relative amounts of 2-naphthol. Other possible products, such as dihydroxylated moieties, were not detected. A separate experiment using 10 μ M solutions of

TABLE 3. Products of naphthalene oxidation by the mutants

Enzyme	Amt (mol%) of indicated product ^a	
	1-Naphthol 	2-Naphthol 
Wild type	43.0 \pm 0.4	57.0 \pm 0.4
L110G	64.0 \pm 0.5	36.0 \pm 0.5
L110C	46.2 \pm 6.3	53.8 \pm 6.3
L110Y	74.8 \pm 0.7	25.2 \pm 0.7
L110R	70.6 \pm 6.6	29.4 \pm 6.6

^a Data are derived from three independent experiments and are shown in the form of means \pm standard deviations.

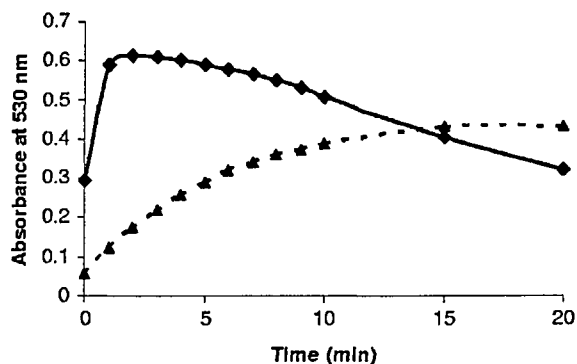
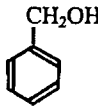
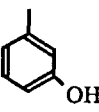
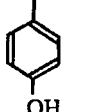


FIG. 2. Stabilities of the colored diazo compounds formed by reaction of tetrazotised *o*-dianisidine with 1-naphthol (solid line) or 2-naphthol (dotted line).

the two isomers of naphthol and the same concentration of tetrazotised *o*-dianisidine as used in the naphthalene test for sMMO activity revealed that the diazo dye produced by 1-naphthol forms more quickly and decays more quickly than that produced by 2-naphthol (Fig. 2). Thus, the difference in the regioselectivity of the mutants accounts for the visual differences in the results of their naphthalene tests.

The L110 mutants showed a relaxed regioselectivity and generated novel products with substituted monoaromatic substrates and biphenyl. With the substituted monoaromatic substrates toluene and ethylbenzene, the wild-type sMMO exhibits a mixture of side chain hydroxylation and ring hydroxylation at the *p* position, with ring hydroxylation predominating with toluene and side chain hydroxylation with ethyl benzene. With toluene as the substrate, all the mutations at position 110 showed relaxed regioselectivity (Table 4), with the appearance of significant amounts of *m*-cresol, which is not seen with the wild type. Interestingly, when Leu 110 was replaced by the smaller glycyl and cysteinyl residues, with toluene as the substrate, more benzyl alcohol was produced than *p*-cresol. When ethylbenzene was the substrate, all the mutants showed very large shifts from side chain to ring hydroxylation and at least

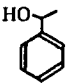
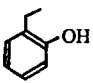
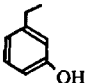
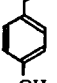
TABLE 4. Products of toluene oxidation by the mutants

Enzyme	Amt (mol%) of indicated product ^a			Molar ratio for aromatic/benzylic hydroxylation	Relative total activity (%) ^b
	Benzyl alcohol 	<i>m</i> -Cresol 	<i>p</i> -Cresol 		
Wild type	36.5 \pm 8.7 ^b	0.0	63.5 \pm 8.7	1.7	100
L110G	53.7 \pm 12.5	14.6 \pm 6.7	31.7 \pm 9.7	0.86	12
L110C	59.4 \pm 12.1	11.2 \pm 7.7	29.4 \pm 5.4	0.68	7.4
L110Y	34.9 \pm 8.2	17.8 \pm 7.4	47.3 \pm 0.8	1.9	2.8
L110R	28.0 \pm 6.5	14.0 \pm 3.1	58.0 \pm 9.7	2.6	2.5

^a Data are derived from three independent experiments and are shown in the form of means \pm standard deviations.

^b Relative total activities with toluene as the substrate, which were corrected for differences in culture OD₆₀₀, are given as percentages of the increase in total product concentration with wild-type *M. trichosporium* OB3b, which was 12 μ M h⁻¹.

TABLE 5. Products of ethyl benzene oxidation by the mutants

Enzyme	Amt (mol%) of indicated product ^a				Molar ratio for aromatic/ side chain hydroxylation	Relative total activity (%) ^f
	1-Phenylethanol 	2-Ethylphenol 	3-Ethylphenol ^b 	4-Ethylphenol ^b 		
Wild type	95.4 ± 1.4	0.0	4.6 ± 1.4	4.6 ± 1.4	0.048	100
L110G	9.2 ± 3.1	8.8 ± 0.4	82.1 ± 2.7	82.1 ± 2.7	9.9	32
L110C	23.6 ± 6.2	3.1 ± 2.1	73.3 ± 4.4	73.3 ± 4.4	3.2	48
L110Y	40.2 ± 10.5	3.1 ± 0.6	56.8 ± 10.0	56.8 ± 10.0	1.5	8.7
L110R	22.1 ± 1.6	1.3 ± 0.1	76.6 ± 1.5	76.6 ± 1.5	3.5	63

^a Data are derived from three independent experiments and are shown in the form of means ± standard deviations.

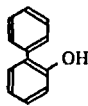
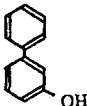
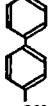
^b 3- and 4-ethylphenol were not resolved in these experiments, so the molar fractions stated are the sums of both.

^c Relative total activities with ethyl benzene as the substrate, which were corrected for differences in culture OD₆₀₀, are given as percentages of the rate of increase in total product concentrations obtained with wild-type *M. trichosporium* OB3b, which was 0.52 μM h⁻¹.

one new product (2-ethylphenol) was observed with each mutant (Table 5). 3- and 4-ethylphenol were not resolved in these experiments, so it is not clear whether the product 3-ethylphenol was produced. With biphenyl as the substrate, the wild type produced predominantly 4-hydroxybiphenyl. Mutants with the larger tyrosine or arginine residue at position 110 produced substantially more 2-hydroxybiphenyl than the wild type. The mutants with the smaller residues (glycine and cysteine) at this position yielded the new product 3-hydroxybiphenyl (Table 6).

Neither the mutants nor the wild type oxidized triaromatic hydrocarbons. Cells expressing wild-type sMMO and all four mutations at position 110 were initially screened for oxidation of the triaromatic compounds phenanthrene and anthracene in the same manner used for the semiquantitative naphthalene assay, by addition of tetrazotised *o*-dianisidine, which gave colored diazo dyes after reaction with the hydroxylated products. No visible color changes were seen from the mutants or the wild type, although a 9-phenanthrol control gave a colored product with a detection threshold of 5 μM. GC-MS was used to analyze the assay reaction mixtures that had been incubated for 30°C for 48 h, as described in Materials and Methods, but no hydroxylated products could be found from either of the triaromatic substrates with wild-type *M. trichosporium* OB3b or any of the mutant strains. Presuming that phenanthrene and anthracene are able to diffuse into the cells, these results strongly suggest that neither wild-type sMMO nor the mutants are able to oxidize these bulky aromatic substrates.

TABLE 6. Products of biphenyl oxidation by the mutants

Enzyme	Amt (mol%) of indicated product		
	2-Hydroxybiphenyl 	3-Hydroxybiphenyl 	4-Hydroxybiphenyl 
Wild type	12.2 ± 3.6	0.0	87.8 ± 3.6
L110G	8.4 ± 3.8	13.0 ± 1.8	78.6 ± 2.0
L110C	11.3 ± 4.2	20.3 ± 3.5	68.3 ± 0.7
L110Y	47.2 ± 0.01	0.0	52.7 ± 0.01
L110R	59.2 ± 3.2	0.0	40.8 ± 3.2

DISCUSSION

Further development of the expression and mutagenesis system. Mutagenesis of the hydroxylase component of sMMO requires the use of an especially developed expression system because attempts to date to obtain expression of active hydroxylase in *E. coli* have been unsuccessful (44). Expression of active sMMO has been reported to occur in various heterologous systems (16, 17, 24) as well as the homologous system used here. The previous work that we performed using the homologous expression system for sMMO, which enabled the first mutagenesis of the active site of the enzyme (38), utilized a homologous expression host (*M. trichosporium* mutant F [26]) from which only part of the *mmoX* gene was deleted, thus limiting the region of the hydroxylase that could be mutagenized. The new strain developed here, *M. trichosporium* SMDM, like mutant F, is a homologous expression host that gives expression of recombinant wild-type sMMO comparable to that from the parental strain *M. trichosporium* OB3b. Moreover, strain SMDM not only allows mutagenesis anywhere within the active site-containing α subunit, including Leu 110, but also allows mutagenesis of all components of the sMMO-encoding operon except the *mmoC* reductase, i.e., the hydroxylase (*mmoXYZ*), protein B (*mmoB*), and *mmoD* genes, whose product may have a role in sMMO complex assembly (27).

Regioselectivity of the wild-type sMMO with aromatic substrates. Our results with *M. trichosporium* expressing recombinant wild-type sMMO confirmed previous results concerning the regioselectivity of sMMO with aromatic substrates. If the substrates are considered to be roughly rectangular, the wild-type enzyme shows a strong preference for hydroxylation nearest to the two short sides of the rectangle. Thus, naphthalene gives primarily 2-naphthol, biphenyl gives predominantly 4-hydroxybiphenyl, and toluene and ethyl benzene undergo a mixture of side chain and 4-position hydroxylation on the benzene ring (2, 3, 14).

Mutations at Leu 110 in sMMO relax regioselectivity but do not extend activity to triaromatic hydrocarbons. The mutant strains showed lower rates of total product accumulation than the wild type, ranging from 2.5 to 63% of the wild-type activities (Tables 4 and 5). Examining the data from ethyl benzene and toluene as substrates, we did not find a clear correlation

between the property of the amino acid and the reduction in activity, and these results may also reflect differences in expression and stability between the mutants. Analysis of the proportions of products formed from the aromatic substrates, however, yielded information that is not biased by the level of expression.

As detailed in the introduction, previous work on homologous monooxygenases that naturally oxidize aromatic substrates has variously indicated effects of mutations at the position equivalent to Leu 110 of the hydroxylase α subunit of sMMO on regioselectivity and substrate range. In the case of sMMO, none of the mutants, including those with substantially smaller residues at position 110, had measurable activity toward the triaromatic substrates phenanthrene and anthracene. However, all had substantial changes in regioselectivity, showing a shift away from "terminal" oxidation of aromatic substrates, with increasing proportions of 1-naphthol from naphthalene and 2- and 3-hydroxy products from substituted monoaromatics and biphenyl. This result was to some extent unexpected, since a "gating role" for Leu 110 suggested that mutations to smaller residues would be likely to let larger substrates into the active site. There was some correlation between the changes in product distribution and the size of the residue at position 110. The shift in regioselectivity of naphthalene oxidation was greatest in the mutants with the largest residues (Tyr and Arg) at position 110. Conversely, the novel product from biphenyl oxidation, 3-hydroxybiphenyl, is seen only in the mutants with the smaller residues (Gly and Cys) at this position. The shift from side chain to ring hydroxylation of toluene was greatest in the mutants with smaller residues (Gly and Cys) at position 110, and the corresponding shift in regioselectivity in oxygenation of ethyl benzene was almost 2 orders of magnitude greater than that seen with any of the other mutants. In the homologous soluble butane monooxygenase, the mutation G113N, which is near the "leucine gate" (Leu 109 in butane monooxygenase), also led to a shift in regioselectivity away from the ends of the substrate molecules, in this case giving rise in the regiospecificities of oxygenation of butane and propane from predominantly terminal to predominantly subterminal (13).

In monooxygenases of the naphthalene dioxygenase family, a residue at the narrowest part of the active-site pocket (Phe 352 in naphthalene dioxygenase from *Pseudomonas* sp. NCIB 9816-4) (18) has also been shown, via mutagenesis studies (19, 29), to influence substrate range and regioselectivity. X-ray crystallography of an enzyme-product complex indicated that the product (and presumably also the substrate) contacts Phe 352 when bound in the active site (6). Unfortunately, there are currently to our knowledge no structural data for sMMO or its homologues complexed with aromatic substrates, but the situation with Leu 110 in these enzymes seems likely to be different, since this residue is on the edge of the active site and less likely to contact the substrate at the moment of oxygenation.

Our data indicate that Leu 110 is an important residue in determining the precision of regioselectivity of sMMO with aromatic substrates. The various mutations that we have made at this position relax the regioselectivity for aromatic substrates, which could be advantageous in activating polyaromatic pollutants for biological breakdown by consortia of microorganisms. While our results do not allow us to judge

whether Leu 110 functions as a substrate gate, they strongly suggest that Leu 110 is not the limiting factor for the size of an aromatic substrate that can enter the active site. It may be that the important role that Leu 110 has in determining the catalytic specificity of the enzyme may be mediated via conformational changes of the type already shown to affect this residue in various crystal forms of the enzyme (30). In the future, we propose to undertake detailed kinetic and structural analysis of the mutants to determine how their effect on the regioselectivity of the enzyme is mediated.

ACKNOWLEDGMENTS

We are grateful to Joan Hague and Keith Richards (Sheffield Hallam University) for advice and technical assistance with GC and GC-MS. We thank Julie Scanlan (Warwick) for technical support.

This work was supported by the Biotechnology and Biological Sciences Research Council through a research grant (reference no. BB/C003276/1 and BB/C00339X/1) to J.C.M. and T.J.S.

REFERENCES

- Bodrossy, L., J. C. Murrell, H. Dalton, M. Kalman, L. G. Puskas, and K. L. Kovacs. 1995. Heat-tolerant methanotrophic bacteria from the hot-water effluent of a natural-gas field. *Appl. Environ. Microbiol.* **61**:3549-3555.
- Brusseau, G. A., H.-C. Tsien, R. S. Hanson, and L. P. Wackett. 1990. Optimization of trichloroethylene oxidation by methanotrophs and the use of a colorimetric assay to detect soluble methane mono-oxygenase activity. *Biodegradation* **1**:19-29.
- Burrows, K. J., A. Cornish, D. Scott, and I. J. Higgins. 1984. Substrate specificity of the soluble and particulate methane mono-oxygenase of *Methylosinus trichosporium* OB3b. *J. Gen. Microbiol.* **130**:3327-3333.
- Canada, K. A., S. Iwashita, H. Shim, and T. K. Wood. 2002. Directed evolution of toluene *ortho*-monooxygenase for enhanced naphthol synthesis and chlorinated ethene degradation. *J. Bacteriol.* **184**:344-349.
- Cardy, D. L. N., V. Laidler, G. P. C. Salmond, and J. C. Murrell. 1991. Molecular analysis of the methane monooxygenase (MMO) gene-cluster of *Methylosinus trichosporium* OB3b. *Mol. Microbiol.* **5**:335-342.
- Carredano, E., A. Karlsson, B. Knappi, D. Choudhury, R. E. Parales, J. V. Parales, K. Lee, D. T. Gibson, H. Eklund, and S. Ramaswamy. 2000. Substrate binding site of naphthalene 1,2-dioxygenase: functional implications of indole binding. *J. Mol. Biol.* **296**:701-712.
- Dennis, J. J., and G. J. Zylstra. 1998. Plasmids: modular self-cloning minitransposon derivatives for rapid genetic analysis of gram-negative bacterial genomes. *Appl. Environ. Microbiol.* **64**:2710-2715.
- DeWitt, J. G., J. G. Bentsen, A. C. Rosenzweig, B. Hedman, J. Green, S. Pilkington, G. C. Papaefthymiou, H. Dalton, K. O. Hodgson, and S. J. Lippard. 1991. X-ray absorption, Mossbauer, and EPR studies of the dinuclear iron center in the hydroxylase component of methane monooxygenase. *J. Am. Chem. Soc.* **113**:9219-9235.
- Elango, N., R. Radmakrishnan, W. A. Froland, B. J. Wallar, C. A. Earhart, J. D. Lipscomb, and D. H. Ohlendorf. 1997. Crystal structure of the hydroxylase component of methane monooxygenase from *Methylosinus trichosporium* OB3b. *Protein Sci.* **6**:556-568.
- Feinberg, A. P., and B. Vogelstein. 1983. A technique for radiolabeling DNA restriction endonuclease fragments to high specific activity. *Anal. Biochem.* **132**:6-13.
- Feinberg, A. P., and B. Vogelstein. 1984. "A technique for radiolabeling DNA restriction endonuclease fragments to high specific activity". *Addendum. Anal. Biochem.* **137**:266-267.
- George, A. R., P. C. Wilkins, and H. Dalton. 1996. A computational investigation of the possible substrate binding sites in the hydroxylase of soluble methane monooxygenase. *J. Mol. Catal. B* **2**:103-113.
- Halsey, K. H., L. A. Sayavedra-Soto, P. J. Bottomley, and D. J. Arp. 2006. Site-directed amino acid substitutions in the hydroxylase subunit of butane monooxygenase from *Pseudomonas butanovora*: implications for substrate knocking at the gate. *J. Bacteriol.* **188**:4962-4969.
- Higgins, I. J., D. J. Best, and R. C. Hammond. 1980. New findings in methane-utilizing bacteria highlight their importance in the biosphere and their commercial potential. *Nature* **286**:561-564.
- Ho, S. N., H. D. Hunt, R. M. Horton, J. K. Pullen, and R. L. Pease. 1989. Site-directed mutagenesis by overlap extension using the polymerase chain reaction. *Gene* **77**:51-59.
- Jahng, D., K. S. Kim, R. S. Hanson, and T. K. Wood. 1996. Optimization of trichloroethylene degradation using soluble methane monooxygenase of *Methylosinus trichosporium* OB3b expressed in recombinant bacteria. *Biotechnol. Bioeng.* **51**:349-359.
- Jahng, D., and T. K. Wood. 1994. Trichloroethylene and chloroform deg-

- radiation by a recombinant pseudomonad expressing soluble methane monooxygenase from *Methylosinus trichosporium* OB3b. *Appl. Environ. Microbiol.* **60**:2473–2482.
18. Kauppi, B., K. Lee, E. Carredano, R. E. Parales, D. T. Gibson, H. Eklund, and S. Ramaswamy. 1998. Structure of an aromatic-ring-hydroxylating dioxygenase-naphthalene 1,2-dioxygenase. *Structure* **6**:571–586.
 19. Keenan, B. G., T. Leungskul, B. F. Smets, and T. K. Wood. 2004. Saturation mutagenesis of *Burkholderia cepacia* R34 2,4-dinitrotoluene dioxygenase at DntAC valine 350 for synthesizing nitrohydroquinone, methylhydroquinone, and methoxyhydroquinone. *Appl. Environ. Microbiol.* **70**:3222–3231.
 20. Kovach, M. E., P. H. Elzera, D. S. Hill, G. T. Robertson, M. A. Farris, R. M. Roop, and K. M. Peterson. 1995. Four new derivatives of the broad-host-range cloning vector pBBR1MCS, carrying different antibiotic-resistance cassettes. *Gene* **166**:175–176.
 21. Leahy, J. G., P. J. Batchelor, and S. M. Morecomb. 2003. Evolution of the soluble diiron monooxygenases. *FEMS Microbiol. Rev.* **27**:449–479.
 22. Lee, S.-K., J. C. Nesheim, and J. D. Lipscomb. 1993. Transient intermediates in the methane monooxygenase catalytic cycle. *J. Biol. Chem.* **268**:21569–21577.
 23. Lindner, A. S., P. Adriaens, and J. D. Semrau. 2000. Transformation of *ortho*-substituted biphenyls by *Methylosinus trichosporium* OB3b: substituent effects on oxidation kinetics and product formation. *Arch. Microbiol.* **174**:35–41.
 24. Lloyd, J. S., P. De Marco, H. Dalton, and J. C. Murrell. 1999. Heterologous expression of soluble methane monooxygenase genes in methanotrophs containing only particulate methane monooxygenase. *Arch. Microbiol.* **171**:364–370.
 25. Lloyd, J. S., R. Finch, H. Dalton, and J. C. Murrell. 1999. Homologous expression of soluble methane monooxygenase genes in *Methylosinus trichosporium* OB3b. *Microbiology* **145**:461–470.
 26. Martin, H., and J. C. Murrell. 1995. Methane monooxygenase mutants from *Methylosinus trichosporium* constructed by marker-exchange mutagenesis. *FEMS Microbiol. Lett.* **127**:243–248.
 27. Merks, M., and S. J. Lippard. 2002. Why OrfY? Characterization of MmoD, a long overlooked component of the soluble methane monooxygenase from *Methylococcus capsulatus* (Bath). *J. Biol. Chem.* **277**:5858–5865.
 28. Murrell, J. C., B. Gilbert, and I. R. McDonald. 2000. Molecular biology and regulation of methane monooxygenase. *Arch. Microbiol.* **173**:325–332.
 29. Parales, R. E., K. Lee, S. M. Resnick, H. Jiang, D. J. Lessner, and D. T. Gibson. 2000. Substrate specificity of naphthalene dioxygenase: effect of specific amino acids at the active site of the enzyme. *J. Bacteriol.* **182**:1641–1649.
 30. Rosenzweig, A. C., H. Brandstetter, D. A. Whittington, P. Nordlund, S. J. Lippard, and C. A. Frederick. 1997. Crystal structure of the methane monooxygenase hydroxylase from *Methylococcus capsulatus* (Bath): implications for substrate gating and component interactions. *Proteins* **29**:141–152.
 31. Rosenzweig, A. C., C. A. Frederick, S. J. Lippard, and P. Nordlund. 1993. Crystal structure of a bacterial nonheme iron hydroxylase that catalyzes the biological oxidation of methane. *Nature* **366**:537–543.
 32. Sambrook, J., E. F. Fritsch, and T. Maniatis. 1989. *Molecular cloning: a laboratory manual*, 2nd ed. Cold Spring Harbor Laboratory, Cold Spring Harbor, NY.
 33. Sazinsky, M. H., J. Bard, A. Di Donato, and S. J. Lippard. 2004. Crystal structure of the toluene/o-xylene monooxygenase hydroxylase from *Pseudomonas stutzeri* OX1. *J. Biol. Chem.* **279**:30600–30610.
 34. Schäfer, A., A. Tauch, W. Jäger, J. Kalinowski, G. Thierbach, and A. Pühler. 1994. Small mobilizable multi-purpose cloning vectors derived from the *Escherichia coli* plasmids pK18 and pK19: selection of defined deletions in the chromosome of *Corynebacterium glutamicum*. *Gene* **145**:69–73.
 35. Shu, L., J. C. Nesheim, K. Kauffmann, E. Münck, J. D. Lipscomb, and L. Que. 1997. An Fe^{IV}O₂ diamond core structure for the key intermediate Q of methane monooxygenase. *Science* **275**:515–517.
 36. Simon, R., U. Priefer, and A. Pühler. 1983. A broad host range mobilization system for *in vivo* genetic engineering—transposon mutagenesis in Gram-negative bacteria. *Bio/Technology* **1**:784–791.
 37. Smith, T. J., and H. Dalton. 2004. Biocatalysis by methane monooxygenase and its implications for the petroleum industry, p. 177–192. *In* R. Vazquez-Duhalt and R. Quintero-Ramirez (ed.), *Petroleum biotechnology, developments and perspectives*. Elsevier, Amsterdam, The Netherlands.
 38. Smith, T. J., S. E. Slade, N. P. Burton, J. C. Murrell, and H. Dalton. 2002. Improved system for protein engineering of the hydroxylase component of soluble methane monooxygenase. *Appl. Environ. Microbiol.* **68**:5265–5273.
 39. Stafford, G. P., J. Scanlan, I. R. McDonald, and J. C. Murrell. 2003. *rpoN*, *mmoR* and *mmoG*, genes involved in regulating the expression of soluble methane monooxygenase in *Methylosinus trichosporium* OB3b. *Microbiology* **149**:1771–1784.
 40. Steffan, R. J., and K. R. McClay. December 2000. Preparation of enantio-specific epoxides. International patent no. WO 00/73425.
 41. Tao, Y., A. Fishman, W. E. Bentley, and T. K. Wood. 2004. Altering toluene 4-monooxygenase by active-site engineering for the synthesis of 3-methoxy-catechol, methoxyhydroquinone, and methylhydroquinone. *J. Bacteriol.* **186**:4705–4713.
 42. Vardar, G., and T. K. Wood. 2004. Protein engineering of toluene-o-xylene monooxygenase from *Pseudomonas stutzeri* OX1 for synthesizing 4-methyl-resorcinol, methylhydroquinone, and pyrogallol. *Appl. Environ. Microbiol.* **70**:3253–3262.
 43. Vieira, J., and J. Messing. 1982. The pUC plasmids, an M13mp7-derived system for insertion mutagenesis and sequencing with synthetic universal primers. *Gene* **19**:259–268.
 44. West, C. A., G. P. C. Salmond, H. Dalton, and J. C. Murrell. 1992. Functional expression in *Escherichia coli* of protein B and protein C from soluble methane monooxygenase of *Methylococcus capsulatus* (Bath). *J. Gen. Microbiol.* **138**:1301–1307.
 45. Woodland, M. P., D. S. Patil, R. Cammack, and H. Dalton. 1986. Electron-spin-resonance studies of protein A of the soluble methane monooxygenase from *Methylococcus capsulatus* (Bath). *Biochim. Biophys. Acta* **873**:237–242.